

3-23-2021

## Experimental Investigations of the Aerodynamics and Wind Loading of Buildings with Balconies

Lisette Ludena

*Florida International University*, llude001@fiu.edu

Follow this and additional works at: <https://digitalcommons.fiu.edu/etd>



Part of the [Civil Engineering Commons](#)

---

### Recommended Citation

Ludena, Lisette, "Experimental Investigations of the Aerodynamics and Wind Loading of Buildings with Balconies" (2021). *FIU Electronic Theses and Dissertations*. 4644.

<https://digitalcommons.fiu.edu/etd/4644>

This work is brought to you for free and open access by the University Graduate School at FIU Digital Commons. It has been accepted for inclusion in FIU Electronic Theses and Dissertations by an authorized administrator of FIU Digital Commons. For more information, please contact [dcc@fiu.edu](mailto:dcc@fiu.edu).

FLORIDA INTERNATIONAL UNIVERSITY  
Miami, Florida

EXPERIMENTAL INVESTIGATIONS OF THE AERODYNAMICS AND WIND  
LOADING OF BUILDINGS WITH BALCONIES

A dissertation submitted in partial fulfillment of  
the requirements for the degree of  
DOCTOR OF PHILOSOPHY  
in  
CIVIL ENGINEERING  
by  
Lisette Ludena

2021

To: Dean John Volakis  
College of Engineering and Computing

This dissertation, written by Lisette Ludena, and entitled Experimental Investigations of the Aerodynamics and Wind Loading of Buildings with Balconies, having been approved in respect to style and intellectual content, is referred to you for judgment.

We have read this dissertation and recommend that it be approved.

---

Peter Irwin

---

Maryam Asghari Mooneghi

---

Atorod Azizinamini

---

Ioannis Zisis

---

Arif Mohaimin Sadri

---

Arindam Gan Chowdhury, Major Professor

Date of Defense: March 23, 2021

The dissertation of Lisette Ludena is approved.

---

Dean John Volakis  
College of Engineering and Computing

---

Andrés G. Gil  
Vice President for Research and Economic Development  
and Dean of the University Graduate School

Florida International University, 2021

© Copyright 2021 by Lisette Ludena

All rights reserved.

## DEDICATION

Foremost, I want to dedicate this dissertation to God Almighty for the wisdom He gave to me and the professors and mentors He put on my path.

To my lovely mother Nancy Navarro, for all her love and sacrifice. Regardless of her journey battling cancer, she filled me strength and encouragement during the complete Ph.D. program.

To my dear father, Virgilio Ludena, for his wisdom and life advice during my existence.

To my husband, Jeffrey Gropper, for all his unconditional love and support in everything I do.

To my 100-year-old grandmother Luisa Espinosa de Navarro and my aunt Helma Navarro for all their love, kind words, and encouragement during my whole life.

To my siblings Alexis Ludena and Tessi Ludena, for all the support and joy they bring to my life.

To my dear FIU Engineering School that gave me the foundation of engineering and created in me the seed to give back to my industry. Special thanks to my advisor and mentor's Dr. Chowdhury, Dr. Peter Irwin, and Dr. Maryam Asghari Mooneghi who are examples for me and have inspired me in my career.

To all the women and men who have dedicated their time and energy towards the advancement of engineering and who continue inspiring others to continue their legacy and impacting different industries with their work.

## ACKNOWLEDGMENTS

I would like to express my greatest gratitude and appreciation to my major advisor Dr. Arindam Chowdhury for his trust, support, and valuable mentorship during my doctoral studies and research. Additionally, I would like to thank all my mentors and doctoral committee Dr. Peter Irwin, Dr. Maryam Asghari Mooneghi, Dr. Atorod Aziznamini, Dr. Arif Mohaimin Sandri, Dr. Mohammad Moravej, Dr. Erdin, Hediye, Gigi Caviedes, and Cristina Caviedes, for their accessibility and valuable discussions. Special thanks to Dr. Peter Irwin, one of the most respectable and knowledgeable engineers in the industry who I admire, and I have been privileged of working with during my Ph.D. Program. Similarly, I would like to thank Dr. Maryam Asghari Mooneghi for her valuable guidance and advice through all my Ph.D. Program; Dr. Maryam Asghari Mooneghi is an example for me and all the women contributing back to engineering.

I have been very fortunate to be part of Florida International University whose resources and labs such as the FIU Wall of Wind Facility were vital contributions towards the fulfillment of my experimental work of my Dissertation.

ABSTRACT OF THE DISSERTATION  
EXPERIMENTAL INVESTIGATIONS OF THE AERODYNAMICS AND WIND  
LOADING OF BUILDINGS WITH BALCONIES

by

Lisette Ludena

Florida International University, 2021

Miami, Florida

Professor Arindam Gan Chowdhury, Major Professor

Balconies constitute an important element of the building design, especially in areas with a mild climate where they represent a characteristic component of the local architecture and provide the occupants an easy access to the environment. Nevertheless, in parallel with aesthetics and functionality, balconies have an effect on the wind loading of buildings. If balconies are poorly designed, they could cause catastrophic accidents. Failure of balcony glass handrail panels has been a frequent occurrence during past windstorms. Such failure poses safety concerns for the building residents and generates wind-borne debris affecting other structures. The current methodology for establishing wind effects on building facades involves determining the design load using the wind provisions of codes and standards (e.g., ASCE 7-16). However, the current methodology does not provide adequate guidance on the wind loading affecting the balcony glass hand railings in residential mid-rise and high-rise buildings.

Large-scale testing of balcony handrail panels is essential as it provides more representative information about the realistic wind effects than the typical small-scale

studies. However, as the model scale increases, the limited dimensions of wind tunnels do not allow simulating the low frequency end of the turbulence spectrum.

To address these limitations, the Partial Turbulence Simulation (PTS) method compensates analytically for the effects of the missing low-frequency content of the spectrum. In this method, the turbulence spectrum is divided into two processes. The high frequencies are simulated in the wind tunnel, and the low frequencies are treated in a quasi-steady manner.

This PTS methodology is based on the assumption of equilibrium of small-scale turbulence; however, this assumption is not applicable for high-rise buildings. The current study is an extension of the PTS to include balcony handrail panels in high-rise buildings. Three scale experiments at 1:180, 1:67, and 1:25 scales were carried out to investigate the wind loading on balconies and the effect of balconies on wind loads on high-rise buildings. Analysis was compared among model scales and existing codes and standards on pressure coefficients on components and cladding.

The area average PTS results on the balconies' corners show higher magnitude values compared to the C&C external coefficients provided by ASCE 7-16. Additionally, overall PTS results show that when increasing the model scale, higher net pressure coefficients are obtained in the balcony handrail panels compared to smaller scale, and such accurate estimation is imperative for reliable wind design of handrail systems. This shows the scale effects and justifies the need for large-scale models and PTS.

## TABLE OF CONTENTS

CHAPTER	PAGE
CHAPTER I.....	1
INTRODUCTION .....	1
1.1 Scaling Effects for Building Cladding.....	2
1.2 Research Objectives.....	4
1.3 Dissertation Structure.....	6
1.4 References.....	7
 CHAPTER II.....	 9
PARTIAL TURBULENCE SIMULATION (PTS) FOR CLADDING COMPONENTS IN TALL BUILDINGS .....	 9
2.1 Background.....	10
2.2 PTS Assumptions and Requirements.....	12
2.2.1 Equilibrium of Small-Scale Turbulence .....	12
2.2.2 Determination of Dividing Frequency between Low & High Frequencies ( $n_c$ ).....	13
2.2.3 Wind Simulation – Requirements for Partial Turbulence Simulations in Wind Tunnels.....	 13
2.3 PTS for Building Components in High-Rise Buildings .....	14
2.3.1 Method Definition .....	14
2.3.2 Data Analysis .....	17
2.4 References.....	19
 CHAPTER III .....	 21
EXPERIMENTAL SETUP AND PROTOCOLS.....	21
3.1 Test Models and Instrumentation.....	22
3.1.1 Test Models Setup and Instrumentation .....	23
3.1.2 Measuring Devices .....	28
3.2 Test Protocol .....	40
3.3 References .....	43
 CHAPTER IV .....	 44
THE EFFECT OF BALCONIES ON THE WIND LOADING ON BUILDINGS.....	44
4.1 Abstract.....	45
4.2 Introduction.....	46
4.3 Description of the Experiments .....	49
4.3.1 Wall of Wind (WOW) Facility .....	49
4.3.2 Test Building.....	51
4.4 Data Analysis .....	53
4.5 Results and Discussion .....	56
4.5.1 Mean Pressure Coefficients on Building Walls .....	56

4.5.2 Mean Pressure Coefficients on Balcony Handrail Panels .....	59
4.5.3 Peak Pressure Coefficients on Building Walls .....	62
4.5.4 Peak Pressure Coefficients on Balcony Handrail Panels .....	69
4.5.5 Comparison with Codes and Standards .....	72
4.6 Major Findings .....	77
4.7 Acknowledgments .....	79
4.8 References .....	79
CHAPTER V .....	82
EXPERIMENTAL INVESTIGATION OF THE AERODYNAMICS OF BALCONIES AND SCALING EFFECTS .....	82
5.1 Abstract .....	83
5.2 Introduction .....	84
5.3 Data Analysis .....	86
5.4 Results and Discussion .....	87
5.4.1 Envelope External Pressure and Envelope Net Pressures Results .....	87
5.4.2 Net Peak Pressure Coefficients at Main Wind Directions .....	92
5.4.3 Comparison with Codes and Standards .....	95
5.4.4 Major Findings on Balcony Handrail Panels .....	102
5.4.5 Scaling and Reynolds Number Effects .....	103
5.4.6 Effect of Pressure Tap Resolution .....	108
5.4.7 Area Average Pressure .....	111
5.5 References .....	115
CHAPTER VI .....	116
CONCLUSIONS .....	116
6.1 Conclusions and Future Work .....	117
6.1.1 Summary .....	117
6.1.2 Effects of Balconies on the Wind Loading on Buildings .....	118
6.1.3 Experimental Investigations of Aerodynamics & Wind Loading on Balconies .....	118
6.1.4 Limitations and Future Work .....	120
VITA .....	122

LIST OF TABLES

TABLE	PAGE
CHAPTER II	
Table 1 – Prototype and Model Dimensions .....	16
Table 2 – Model Scale Parameters Considered for the Analysis .....	19
Table 3 – Full-Scale Parameters Considered for the Analysis .....	19
CHAPTER III	
Table 1 – Building dimensions at different scales.....	23
Table 2 – Building types and wind directions .....	40
CHAPTER IV	
Table 1 – Building wind tunnel models (scale 1:180) .....	52
Table 2 – Parameters considered for the analysis .....	56
Table 3 – External pressure coefficients from ASCE 7-16.....	73
Table 4 – Area-averaged net maximum and minimum pressure coefficients on the balcony handrail panels from the envelope of all wind directions .....	74
Table 5 – C&C external pressure coefficients from ASCE 7-16 and the area-averaged net maximum and minimum pressure coefficients on the balcony handrail panels from the experiments .....	78
CHAPTER V	
Table 1 – External pressure coefficients from ASCE 7-16.....	96
Table 2 – Area-averaged net maximum and minimum pressure coefficients on the balcony handrail panels from the envelope of all wind directions .....	97
Table 3 – ASCE and area-averaged net maximum and minimum pressure coefficients from the envelope of all wind directions across all floors .....	100
Table 4 – ASCE and area-averaged exterior maximum and minimum pressure coefficients from the envelope of all wind directions across all floors .....	100

Table 5 – Area covered by tap combinations in the 15<sup>th</sup> floor.....112

Table 6 – Area covered by tap combinations in the 12<sup>th</sup> floor.....114

LIST OF FIGURES

FIGURE	PAGE
CHAPTER II	
Figure 1 – Mean flow velocity, Low frequency, and High frequency fluctuations.....	15
CHAPTER III	
Figure 1 – (a) NHERI Wall of Wind Experimental Facility (WOW EF), FIU; (b) Spires and floor roughness elements .....	22
Figure 2 – Building Elevation.....	23
Figure 3 – (a) Base building model (b) Building-Balcony model .....	24
Figure 4 – Scale 1:180 a) Base building model (b) Building-Balcony model .....	24
Figure 5 – Printed 3D Balconies (a) Top View (b) Side View .....	25
Figure 6 – Balcony Dimensions .....	25
Figure 7 – Model Scale 1:67 (a) Base Building (b) Building with Balconies .....	26
Figure 8 – Model Scale 1:25 (a) Base Building (b) Building with Balconies .....	26
Figure 9 – Wood Framing 1:67 Scale – Assembly Details .....	27
Figure 10 – Wood Framing 1:25 Scale – Assembly Details .....	27
Figure 11 – All Model Scales – Height Comparison (a) Scale 1:180, (b) Scale 1:67, (c) Scale 1:25 .....	28
Figure 12 – Transducer – Channel Layout .....	29
Figure 13 – Model Scale 1:25 – TCU located above the ground .....	30
Figure 14 – Building with Balconies Plan View .....	30
Figure 15 – Building with Balconies Elevation View – Full Scale .....	31
Figure 16 – Model Scale 1:180 and 1:67 – Pressure Tap Layout Side A .....	32
Figure 17 – Model Scale 1:180 and 1:67 – Pressure Tap Layout Side B .....	33

Figure 18 – Model Scale 1:180 and 1:67 – Pressure Tap Layout Side C .....	34
Figure 19 – Model Scale 1:180 and 1:67 – Pressure Tap Layout Side D .....	35
Figure 20 – Model Scale 1:25 – Pressure Tap Layout Side A .....	36
Figure 21 – Model Scale 1:25 – Pressure Tap Layout Side B .....	37
Figure 22 – Model Scale 1:25 – Pressure Tap Layout Side C .....	38
Figure 23 – Model Scale 1:25 – Pressure Tap Layout Side D .....	39
Figure 24 – Wind Direction .....	41
Figure 25 – Wind Speed Profile and Turbulence Intensity Scale 1:180.....	41
Figure 26 – Wind Speed Profile and Turbulence Intensity Scale 1:67.....	42
Figure 27 – Wind Speed Profile and Turbulence Intensity Scale 1:25.....	42
 CHAPTER IV	
Figure 1 – (a) NHERI Wall of Wind Experimental Facility (WOW EF), FIU; (b) Spires and floor roughness elements .....	50
Figure 2 – (a) Wind speed and turbulence intensity profiles; (b) Turbulence power spectra .....	51
Figure 3 – Wind direction convention .....	52
Figure 4 – Building model without balconies (scale: 1:180).....	53
Figure 5 – Building model with balcony handrail systems (scale: 1:180).....	53
Figure 6 – Mean pressure coefficients for wind direction 0 degrees .....	58
Figure 7 – Mean pressure coefficients for wind direction 45 degrees .....	59
Figure 8 – Net mean pressure coefficients on the balconies for 0 degrees wind direction .....	61
Figure 9 – Net mean pressure coefficients on the balconies for 45 degrees wind direction .....	62
Figure 10 – Maximum peak pressure coefficients for wind direction 0 degrees .....	63

Figure 11 – Maximum peak pressure coefficients for 45 degrees wind direction.....	64
Figure 12 – Minimum peak pressure coefficients for 45 degrees wind direction .....	65
Figure 13 – Minimum peak pressure coefficients for 90 degrees wind direction .....	66
Figure 14 – Envelope of maximum peak pressure coefficients among all wind directions .....	68
Figure 15 – Envelope of the minimum peak pressure coefficients among all wind directions.....	69
Figure 16 – Envelope of peak pressure coefficients on the balconies among all wind directions (figure shows the plan view of the building and the balconies).....	71
Figure 17 – Definition of Zone 4 and Zone 5 in ASCE 7-16 .....	73
Figure 18 – Zones defined for area averaging of pressures on the balconies (figure shows the plan view of the building and balconies) .....	74
Figure 19 – Area-averaged net maximum and minimum pressure coefficients on the balconies’ handrail panels from the envelope of all wind directions; Discontinuous Balcony (Maximum of Sides A and D) .....	77
Figure 20 – Area-averaged net maximum and minimum pressure coefficients on the balconies’ handrail panels from the envelope of all wind directions; Continuous Balcony (Maximum of Sides B and C).....	77
 CHAPTER V	
Figure 1 – External Maximum and Minimum Peak Pressures on the Building .....	88
Figure 2A – Envelope Net Min Peak Pressures (Net $C_{p_{min}}$ ) – Scale 1:180.....	90
Figure 2B – Envelope Net Min Peak Pressures (Net $C_{p_{min}}$ ) – Scale 1:67 .....	90
Figure 2C – Envelope Net Min Peak Pressures (Net $C_{p_{min}}$ ) – Scale 1:25 .....	90
Figure 3A – Envelope Net Max Peak Pressures (Net $C_{p_{max}}$ ) – Scale 1:180.....	91
Figure 3B – Envelope Net Max Peak Pressures (Net $C_{p_{max}}$ ) – Scale 1:67.....	92
Figure 3C – Envelope Net Max Peak Pressures (Net $C_{p_{max}}$ ) – Scale 1:25.....	92

Figure 4 – Convention for the Wind Direction at 0 Degrees. Side walls corners are numbered from 1 to 4.....	93
Figure 5 – Net Min Peak Pressures (Net $C_{p_{min}}$ ) for 0 degrees – Scale 1:67.....	93
Figure 6 – External Min Peak Pressures for 0 degrees – Scale 1:67 .....	94
Figure 7 – Convention for the Wind Direction at 180 Degrees. Side walls corners are numbered from 1 to 4.....	95
Figure 8 – Net Max Peak Pressures for 180 degrees (Net $C_{p_{max}}$ ) – Scale 1:25.....	95
Figure 9 – External Max Peak Pressures for 180 degrees – Scale 1:25.....	95
Figure 10 – Definition of Zone 4 and Zone 5 in ASCE 7-16 .....	96
Figure 11 – Zones defined for area-averaging of pressures on the balconies (figure shows the plan view of the building and balconies) .....	97
Figure 12 – Area-averaged net maximum and minimum pressure coefficients on the balconies’ handrail panels from the envelope of all wind directions; Discontinuous Balcony .....	101
Figure 13 – Area-averaged net maximum and minimum pressure coefficients on the balconies’ handrail panels from the envelope of all wind directions; Continuous Balcony .....	101
Figure 14 – Building Elevation View and Wind Direction at 0 Degrees .....	104
Figure 15A – Reynolds number effect, Net $C_{p_{max}}$ at 0 Degrees.....	104
Figure 15B – Reynolds number effect, Net $C_{p_{max}}$ at 0 Degrees .....	105
Figure 15C – Reynolds number effect, Net $C_{p_{max}}$ at 90 Degrees.....	105
Figure 15D – Reynolds number effect, Net $C_{p_{max}}$ at 90 Degrees.....	105
Figure 16A – Reynolds number effect, Net $C_{p_{min}}$ at 0 Degrees .....	106
Figure 16B – Reynolds number effect, Net $C_{p_{min}}$ at 0 Degrees .....	107
Figure 16C – Reynolds number effect, Net $C_{p_{min}}$ at 0 Degrees .....	107
Figure 16D – Reynolds number effect, Net $C_{p_{min}}$ at 0 Degrees .....	107

Figure 17 – Building Elevation of Side B and Side C .....	109
Figure 18A – Effect of pressure tap layout on Net $C_{p_{min}}$ at the 15 <sup>th</sup> floor, 72 degrees wind direction – Side B.....	109
Figure 18B – Effect of pressure tap layout on Net $C_{p_{min}}$ at the 12 <sup>th</sup> floor, 0 degrees wind direction – Side C.....	110
Figure 19A – Effect of pressure tap layout on Net $C_{p_{max}}$ at the 15 <sup>th</sup> floor, 0 degrees wind direction – Side B.....	110
Figure 19B – Effect of pressure tap layout on Net $C_{p_{max}}$ at the 12 <sup>th</sup> floor, 135 degrees wind direction – Side C .....	111
Figure 20 – Tributary Areas.....	112
Figure 21 – Notation of tap combinations considered in the study .....	112
Figure 22 – Net $C_{p_{min}}$ and Net $C_{p_{max}}$ for tap combination cases at the 15 <sup>th</sup> floor .....	113
Figure 23 – Notation of tap combinations considered in the study .....	114
Figure 24 – Net $C_{p_{min}}$ and Net $C_{p_{max}}$ for tap combination cases at the 12 <sup>th</sup> floor .....	114

**CHAPTER I**  
**INTRODUCTION**

# CHAPTER 1

## INTRODUCTION

### 1.1 Scaling Effects for Building Cladding

Failure of balcony glass railings has been a frequent occurrence during past windstorms. The current methodology for establishing the wind effects on building facades involves determining the design load using the wind provisions of codes and standards (e.g., ASCE 7-16). However, the current methodology does not provide adequate guidance on the wind loading affecting the balcony glass hand railings in residential mid-rise and high-rise buildings. The knowledge gap pertaining to wind effects on balcony handrails can lead to inadequate designs which may pose significant safety issues for residents and incur economic losses. Accordingly, there is an urgent need to develop a means of reliable wind design of such systems. Not meeting this need represents an important problem because without new knowledge, inadequately designed building systems will continue to be built. Also, existing, deficient buildings would unlikely be retrofitted appropriately.

Research on wind loading on balcony handrail systems in high-rise buildings and their effects on the wind loads on the building's façade has been limited. Cochran and Peterka [1] studied the cladding external pressure for two mid-rise building configurations: (i) building with an open balcony with no hurricane shutters, and (ii) building with slab-edge shutters. The second configuration changed the shape of the building from a structure with balconies to a cleaner rectilinear structure, similar to a building with no balconies. The external negative pressures on the buildings with shutters demonstrated greater outward loads along building's edges compared to the building with no shutters (building with open balconies). The wind-tunnel derived, corner-zone peak-negative loads for the

building with open balconies (un-shuttered case) were about 40% lower (in magnitude) as compared to the building with shutters. The balconies had minimal or zero impact on the peak-positive cladding pressures. Browne and Kumar [2] studied the impact of corner and continuous balconies on the wind loads on tall buildings. Several wind tunnel tests were performed on rectangular towers with and without balconies of various sizes in order to quantify wind-induced loads on the building. The results showed that corner balconies significantly reduce the crosswind sway response and torsional response of the structure. Continuous balconies had similar but less pronounced influence as compared to the corner balconies. Montazeri and Blocken performed a balcony study [3] using Computational Fluid Dynamics (CFD), where it was concluded that balconies could cause significant changes to the wind pressure distribution on windward walls, due to flow separation, recirculation, and reattachment generated by the presence of balconies. In addition, corner balconies could help reduce the crosswind response of tall buildings.

Building codes and standards such as the International Building Code (IBC), the Florida Building Code (FBC), and the American Society of Civil Engineers (ASCE 7-16) do not provide information on the influence of balcony handrail systems on cladding or structural wind loads. For the building, the designer decides how to approach the additional surface area from the vertical facades of the balconies (such as in glass panel balcony railing systems). This decision could be complicated for the cases where there are many balconies in line sheltering the building. Wind testing that fully captures the aerodynamics of flows over balconies provides information for designing more reliable and safer balconies and façade elements.

For tall buildings, wind tunnel tests have become the norm as they take into account the effect of the building shape and surrounding terrain and other nearby structures. Wind tunnels testing of these large structures is typically done on models with scales in the range 1:200 to 1:500 [4]. At this range of scales, boundary layer wind tunnels can produce an adequate simulation of the turbulent planetary boundary layer, including the correct scaling of the large turbulent eddies and the integral length scales of turbulence. For smaller structures and for building components (i.e. balconies), the use of model scales of 1:200 to 1:500 becomes impractical. The models become too small for (i) adequate instrumentation of pressure taps, (ii) modeling of the finer details that may affect the aerodynamics, and (iii) simulating high enough Reynolds number to avoid scale effects that make the test results no longer fully representative of the full scale [4]. All these reasons support the need for large-scale testing as this impacts the accuracy of the test results.

## **1.2 Research Objectives**

To address the knowledge gaps the objectives of this research is to develop better ways of quantifying balcony wind loads by: 1) doing a scale model testing study; 2) studying model tests at large scale for better accuracy; and 3) overcoming problems of simulating turbulence at large scale using the Partially Turbulence Method (PTS).

The wind actions on glass handrails are affected by: 1) aerodynamics pertaining to the glass railings in the presence of the building; 2) the large variation of wind pressures on glass railings depending on their locations on the building, e.g. corners versus central areas; and 3) dynamic and buffeting effects that may lead to vibrations and fatigue failures of elements and connections. This dissertation focuses on the first two issues and investigates wind loads on balcony glass hand railings of residential mid-rise and high-rise

buildings under simulated hurricane wind effects. The research is important as it addresses the knowledge gap by providing new data to facilitate efficient wind design of glass hand railings. This will reduce the risk of failure of balcony glass railing components during hurricanes and prevent generation of flying debris. The implication of this research is mitigation of economic impacts and enhancement of public safety.

Large-scale experiments were performed in the NHERI Wall of Wind (WOW) Experimental Facility (EF) at Florida International University (FIU). A 15-story building was selected for the study. In order to study the wind-induced pressures on balconies and handrails of the building, and to evaluate the effect of the presence of such systems on wind loading on the building itself, two sets of experiments were performed using building models without and with balconies and handrail systems. Wind effects on both continuous and discontinuous balconies were studied. To study the scaling and Reynolds number effects, in each set of experiments, detailed pressure measurements were performed on three models with scales 1:180, 1:67, and 1:25. Pressure taps were installed on the vertical panels of the balcony handrail systems as well as on the building walls. The resolution of pressure taps on the balcony panels was higher in the critical corner areas for the largest (1:25) model. Partial Turbulence Simulation (PTS) methodology [5], described later, was used to improve the accuracy of the results obtained using large-scale model testing associated with missing low frequency turbulence. Results showed that the balconies can change the flow pattern around the building and consequently the pressure distribution on the walls. This is a major finding since the current wind loads on the building given in the codes and standards do not consider the effect of balconies on the wind loading. Considering the scaling effects, pressure coefficients obtained from larger models were

higher than those from the smaller scales. This difference was more significant on the balcony handrail structure which indicates the importance of large-scale studies of building components such as balconies. The pressure coefficients on the balcony structures determined by this research provide useful information for more reliable design guidance for balcony glass railings that will improve residents' safety and preclude generation of windborne debris during hurricanes. The findings are expected to inform codes and enhance wind design provisions for glass handrail systems. The expected benefits are safer designs of building systems, which would ensure reduction of economic losses, human injuries, and fatalities caused by handrail failures in coastal buildings and impacts from flying debris.

### **1.3 Dissertation Structure**

The dissertation contains two manuscripts for scholarly journals. One is under review (Chapter 4), and the second one will be submitted shortly (Chapter 5). Additionally, a general introduction chapter is provided at the beginning, followed by chapters of the research methodology proposed to estimate wind loading on balcony handrail panels, description of the experimental setup, and finally a summary conclusion chapter at the end of the dissertation.

Chapter 1 presents the introduction to the effects of balconies on the wind loads on a building where the latest research in this topic is provided and the importance of large-scale testing is highlighted. Furthermore, the knowledge gap in the design of the balcony handrail panels and its impact on the wind load on a building are identified. Chapter 2 introduces the advancement of the Partial Turbulence Simulation (PTS) method for balcony handrail panels in high-rise buildings. The existing PTS method addresses the

issues of missing low-frequency turbulence in large-scale testing; however, it is based on the quasi-steady assumption applicable only for low-rise buildings. The challenges of PTS application to high-rise buildings and the advancement of the PTS for estimating wind loads on balcony handrail panels and building cladding components in tall buildings are discussed. Chapter 3 discusses the experimental setup including the instrumentation, tap layout details, and test protocol. Chapter 4 embodies the first paper, under review in the “Engineering Structures Journal” in which the effects of balcony handrail on wind loads of buildings are presented for the 1:180 model. The study uses data from two types of buildings (i.e., building with balconies and building without balconies) for different wind directions at 3-degree increments. Chapter 5 shows the second paper, to be submitted for journal publication, which focuses on analyzing and comparing the experimental results for balcony handrail panels at different scales (i.e. 1:180, 1:67, and 1:25) to investigate the Reynolds number and scaling effects. Furthermore, the study of resolution of pressure taps was presented. The conclusions and recommendations for future work are provided in Chapter 6.

#### 1.4 References

- [1] Cochran, L., Jon, P., (2000). Cladding Loads: The Influence of Balconies and Slab-Edge Storm Shutters. Structures Congress 2000, May 8-10, 2000, Pennsylvania, United States.
- [2] Browne, M., Kumar, S., (2005). Effect of corner balconies on wind-induced response of tall buildings. 10th Americas Conference on Wind Engineering, Baton Rouge, Louisiana, USA.
- [3] Montazeri, H., Blocken, B., (2013). CFD simulation of wind-induced pressure coefficients on buildings with and without balconies: validation and sensitivity analysis. *Building and Environment*, 60, 137-149.

- [4] Moravej, M. (2018). Investigating Scale Effects on Analytical Methods of Predicting Peak Wind Loads on Buildings. Florida International University.
- [5] Asghari Mooneghi, M. (2014). Experimental and Analytical Methodologies for Predicting Peak Loads on Building Envelopes and Roofing Systems Dissertation. FIU Electronic Theses and Dissertations. Florida International University.

**CHAPTER II**  
**PARTIAL TURBULENCE SIMULATION (PTS) FOR CLADDING**  
**COMPONENTS IN TALL BUILDINGS**

## CHAPTER 2

### PARTIAL TURBULENCE SIMULATION (PTS) FOR CLADDING

#### COMPONENTS IN TALL BUILDINGS

##### 2.1 Background

Wind tunnel testing is one of the most reliable tools when investigating the wind effects on structures [1]. During these tests, the simulated wind flows should have similar wind profile and turbulence spectrum as the actual full-scale atmospheric boundary layer (ABL) that is being investigated.

Large-scale testing better replicates the effects of wind on building components as it allows the ability to install more pressure taps that impact the resolution of the data, better replicates the effect of architectural features, and avoids adverse scaling effect due to inadequate Reynolds number simulation. The challenge of simulating the wind flow using a large-scale model is to replicate the low frequency large-scale eddies in testing as it is dependent on the wind tunnel dimensions. So for large-scale testing, the turbulence spectrum is missing low frequency turbulence components in the simulation [2].

Large-scale eddies associated with low frequency fluctuation and small-scale eddies associated with high frequency fluctuations are crucial when simulating the wind flow during testing and can impact the peak wind pressure results obtained. The high frequency turbulence is required to accurately model the flow reattachment and separation which affect the strength and configuration of shear layer and vortices; and the low frequency fluctuations are similar to slow changes in wind speed and wind direction and can also impact the peak loading [3].

Research has been performed in the past to simulate correctly the high frequency turbulence and analytically compensate for the missing low frequency turbulence by the use of Partial Turbulence Simulation (PTS) theory. For example, Davenport and King (1984) studied the partial simulation of a bridge test model, where the missing low frequency of the turbulence was compensated analytically using quasi-steady assumptions [4].

Asghari Mooneghi (2014) proposed a theoretical partial turbulence simulation approach and the corresponding analytical procedures to account for the effects of the missing low frequency in wind flows with partial turbulence simulation. In the Partial Turbulence Simulation (PTS) methodology proposed by Asghari Mooneghi et al. [5,6], the analysis for a large-scale model is performed in two processes: (1) the high frequency turbulence spectrum is simulated during testing, and (2) the effect of the missing low frequency fluctuations is included in a post-test analysis using quasi-steady theory. The current PTS proposed by Asghari Mooneghi et al (2015) is developed for low-rise buildings and small structural appurtenances. This PTS methodology is based on the assumption of “equilibrium of small-scale turbulence” which assumes that the small scales of turbulence rapidly reach an equilibrium state when changes are imposed by large-scale turbulence. However, the current PTS approach is not directly applicable to taller buildings and their cladding elements such as balcony handrail systems. In this chapter, the PTS approach proposed by Asghari Mooneghi et al (2015) is advanced to include the estimation of peak wind loads for components and cladding (e.g., balconies) of tall buildings.

## 2.2 PTS Assumptions and Requirements

### 2.2.1 *Equilibrium of Small-Scale Turbulence*

For low-rise buildings, Asghari Mooneghi et al [5,6] used the assumption that high frequency turbulence rapidly attains a new equilibrium with increased energy, with the turbulence intensity from high frequency fluctuations  $I_{uH}$  remaining constant. In other words, during testing, where only the high frequency end of the turbulence spectrum is included in testing, it is assumed that the small scales of the turbulence rapidly reach an equilibrium state when changes are imposed by large scale turbulences. This new equilibrium is assumed to happen particularly near solid surfaces such as the ground where the Reynolds stresses and mean velocity profile converge to universal values consistent with the universal law of the wall [Irwin, 1981], provided that the average time over which they are determined corresponds to a wavelength large compared to the height of interest above the ground (e.g., roof height of a low-rise building).

Since the high frequency fluctuations are assumed to be uncorrelated with the low frequency fluctuations, the turbulence intensity of the missing low frequency component is calculated in equation (1) [5, 6].

$$I_{uL} = \sqrt{I_u^2 - I_{uH}^2} \quad (1)$$

where  $I_u$  is the full-spectrum longitudinal turbulence intensity, and  $I_{uH}$  is the turbulence intensity measured in the partial turbulence simulation.

The wind speed scaling is set as the ratio of the mean speed in partial turbulence simulation (in wind experiments) to the full-scale gust due to missing low frequency turbulences which can be estimated using the peak factor of 3.4 used in ASCE 7-16 for background turbulence as shown in equation (2) [5,6].

$$U_{LP} = U_p *(1 + 3.4 I_{uL}) \quad (2)$$

Where  $I_{uL}$  is the intensity of the missing low frequency component,  $U_{LP}$  is the full scale gust, and  $U_p$  is the mean wind speed at full scale.

### 2.2.2 Determination of Dividing Frequency between Low & High frequencies ( $n_c$ )

The cut-off frequency is calculated in equation (3) which is used to estimate the cut-off frequency between the high frequency and low frequency turbulence.

$$n_c = 0.0716 \left( \frac{U}{xL_u} \right) \left( \frac{I_u}{I_{uH}} \right)^3 \quad (3)$$

### 2.2.3 Wind Simulation – Requirements for Partial Turbulence Simulations in Wind Tunnels

In the Partial Turbulence Simulation (PTS) method, the following requirements must be met in the wind tunnel testing:

As stated by Asghari Mooneghi et al [5,6], in order to simulate correctly the wind in the wind tunnels, the goal is to have the kinetic energy of the high frequency turbulence per unit frequency in the right ratio to the kinetic energy of the mean wind. This can be achieved if, at high frequencies in the scale-model tests, the non-dimensional power spectrum  $fS/U^2$  where  $f$  = frequency and  $S$  = average power spectrum, is the same in the full scale and simulated wind. This implies that at high frequencies, there is a ratio of model turbulence intensity to prototype turbulence intensity governed by Equation (4).

- 1) The non-dimensional spectrum at high frequency,  $fS/U^2$ , on the model at the critical height of the structure, such as roof height, shall be the same as the target spectrum at full scale. This implies that the ratio of model to full scale turbulence intensity at the critical height is as shown in equation (4).

$$\frac{I_{um}}{I_{up}} = \left( \frac{x_{Lum}}{x_{Lup}} \right)^{1/3} \left( \frac{b_p}{b_m} \right)^{1/3} \quad (4)$$

In this relationship, m and p denote model and prototype (full) scale quantities respectively, and  $x_{Lu}$  denotes the turbulence integral length.

- 2) The ratio of the model turbulence integral scale to the model critical dimension,  $b_m$ , which in most low-rise cases will be roof height, shall satisfy:

$$\frac{x_{Lum}}{b_m} > 0.7 \quad (5)$$

### 2.3 PTS for Building Components in High-Rise Buildings

The PTS method proposed by Asghari Mooneghi et al [5,6] for low rise buildings assumes that near the ground the flow has a high gradient  $dU/dz$ . In such conditions, the high frequency turbulence responds quickly to low frequency gusts. Therefore, the intensity of the high frequency turbulence,  $I_{uH}$ , stays approximately constant even though the fluctuating velocity of the low frequency gusts varies. However, for tall buildings, the rapid equilibrium of the high frequency turbulence can no longer be assumed across the building height because  $dU/dz$  reduces with height, and the turbulence intensity  $I_H$  is not constant. On the other hand, for small components on tall buildings, the large-scale eddies should remain reasonably well-correlated over their much smaller dimensions which allows the possibility to use the PTS method with the changes proposed in this section.

#### 2.3.1 Method Definition

In the FIU Wall of Wind (WOW), the measured mean velocity ( $U_{ps}$ ), is effectively the mean speed  $U$  corresponding to an atmospheric flow (with full spectrum) plus whatever

the low frequency gust component  $u_L$  is at the time, as illustrated in Figure 1 and shown in equation 6. Also, it was assumed that the high frequency turbulence  $I_{uH}$  is fixed due to the rapid equilibrium assumption. The missing low frequency turbulence is adjusted using the quasi-steady assumption which is acceptable provided that the eddies simulated in the WOW cover wave lengths up to about an order of magnitude greater than the building dimension  $H$ . This method is acceptable for small structures because during the wind tunnel testing this range of wave lengths is covered since  $H$  being small. However, the quasi-steady assumption is not applicable for overall loading of a tall building due to the large magnitude of  $H$ .

$$U_{ps} = U + u_L \tag{6}$$

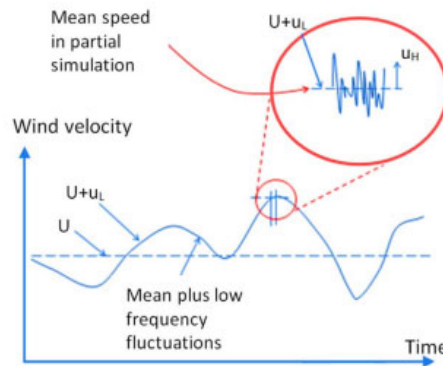


Figure 1 – Mean flow velocity, Low frequency, and High frequency fluctuations

For tall buildings, it is important to take into consideration that the gradient  $dU/dz$  reduces with height, and the rapid equilibrium of the high frequency turbulence can no longer be assumed across the building height and therefore the turbulence intensity  $I_H$  is not constant. However, for small components on a tall building, the larger scale eddies

should remain reasonably well-correlated over their much smaller dimensions. Therefore, PTS is still applicable as an approximate method with the modification proposed in this section.

To address the methodology of PTS on small components, this research proposes the following:

- At higher levels above ground, the overall turbulence intensity is less than that at near ground level.
- For the balconies of study located in the 9<sup>th</sup>, 12<sup>th</sup>, and 15<sup>th</sup> floors of a tall building, the fluctuations in  $I_H$  will not be significant, and this brings up the possibility of using a single representative value of  $I_H$  for the level in where the component (i.e. balcony) is located.
- After measuring the load/pressure coefficients at this representative value of  $I_H$ , the missing low frequency fluctuations are compensated using the quasi-steady assumption, by following the PTS methodology.

**Table 1 – Prototype and Model Dimensions**

<b>Parameters</b>	<b>Scale 1:180</b>	<b>Scale 1:67</b>	<b>Scale 1:25</b>
<b>H (m)</b>	0.31	0.82	2.21
<b>b<sub>m</sub> (m)</b>	0.14	0.36	0.98
<b>*L<sub>u</sub> (m)</b>	0.40	0.47	0.50
<b>*L<sub>u</sub>/b<sub>m</sub></b>	2.95	1.29	0.51

For PTS to be applicable, at each balcony elevation, the minimum ratio of  $^xL_{um}/b_m$  needs to be met at which the use of the quasi-steady assumption remains valid (ratio of the model turbulence integral scale to the model critical dimension). The minimum ratio  $^xL_{um}/b_m$  at which use of the quasi-steady assumption remains valid is suggested by Asghari, Wu and Kopp to be in the range of 0.7 to 1.5 [3,7]. In the proposed

methodology, the balcony width is considered as the critical dimension ( $b_m$ ) for balconies in a high-rise building. Table 1 shows the magnitude of the applicable minimum ratio  $\lambda_{um}/b_m$  for the model scales considered in this study (1:180, 1:67, and 1:25 scales). Results show that scales 1:180 and 1:67 meet this minimum ratio requirement. Scale 1:25 is close to the minimum ratio range, and it is considered on the borderline of applicability. With scale 1:180 being a small scale, the wind tunnel covers the wavelength in the testing; therefore, there is no concern on the high ratio range.

### 2.3.2 *Data Analysis*

In the current model test, the mean wind speeds and turbulence intensities for scales 1:180, 1:67, and 1:25 are given in Table 2. A summary of the steps to calculate the WOW scaling parameters used for determining the required probability level at which peak pressures were estimated is shown in this section.

1. The missing low frequency turbulence is calculated using Equation (1). This value is calculated corresponding to the balconies' elevation at the 15<sup>th</sup>, 12<sup>th</sup>, and 9<sup>th</sup> floors.
2. The full-scale gust due to the missing low frequency turbulence was estimated using Equation (2) at each balcony height.
3. The speed scaling for the present study was set such that the mean speed of the PTS tests corresponded to the low frequency gust speeds at each balcony height calculated from the Equation (7).

$$\lambda_U = \frac{U_m}{U_{LP}} \quad (7)$$

where  $U_{LP}$  corresponds to the low frequency gust speed calculated using Equation (2), and  $U_m$  corresponds to the mean speed.

4. The time scale is calculated in Equation (8)

$$\lambda_t = \frac{\lambda_L}{\lambda_U} \quad (8)$$

where  $\lambda_L$  is the length scale based on the model scale.

5. The pressure coefficients calculated from the above analysis are representative of the most probable peak (mode of the distribution) which has about 37% probability of not being exceeded in the selected full sample period.
6. Peak pressure coefficients are calculated corresponding to the Probability of Exceedance  $G$  given in Equation (9)

$$G = \frac{t_{subinterval, Full\ scale}}{Full\ Scale\ time\ (i.e.1\ hour)} \quad (9)$$

Where  $t_{subinterval, Full\ Scale}$  is calculated from Equation (10)

$$t_{subinterval, Full\ scale} = \frac{t_{subinterval, PS}}{Full\ Scale\ time\ (i.e.1\ hour)} \quad (10)$$

$$t_{subinterval, PS} = \frac{test\ duration}{N_{test}} \quad (11)$$

And where  $t_{subinterval, PS}$  is the test duration divided by subintervals  $N_{test}$ , and

$t_{subinterval, Full\ scale}$  is the equivalent gust-duration at full scale.

Please refer to Table 2 on the next page for the parameters used in the PTS analysis for each of the model scales of this study.

**Table 2 – Model Scale Parameters Considered for the Analysis**

Test Characteristics	Model Scale 1:180	Model Scale 1:67	Model Scale 1:25
<b>High Turbulence Intensity</b>	9 <sup>th</sup> Floor $I_{uH} = 0.153$ 12 <sup>th</sup> Floor $I_{uH} = 0.152$ 15 <sup>th</sup> Floor $I_{uH} = 0.144$	9 <sup>th</sup> Floor $I_{uH} = 0.150$ 12 <sup>th</sup> Floor $I_{uH} = 0.148$ 15 <sup>th</sup> Floor $I_{uH} = 0.138$	9 <sup>th</sup> Floor $I_{uH} = 0.131$ 12 <sup>th</sup> Floor $I_{uH} = 0.128$ 15 <sup>th</sup> Floor $I_{uH} = 0.120$
<b>Reference Height (m)</b>	9 <sup>th</sup> Floor $Z_{ref} = 0.17$ 12 <sup>th</sup> Floor $Z_{ref} = 0.23$ 15 <sup>th</sup> Floor $Z_{ref} = 0.29$	9 <sup>th</sup> Floor $Z_{ref} = 0.46$ 12 <sup>th</sup> Floor $Z_{ref} = 0.61$ 9 <sup>th</sup> Floor $Z_{ref} = 0.77$	9 <sup>th</sup> Floor $Z_{ref} = 1.23$ 12 <sup>th</sup> Floor $Z_{ref} = 1.65$ 15 <sup>th</sup> Floor $Z_{ref} = 2.07$
<b>Mean Wind speed (m/s)</b>	9 <sup>th</sup> Floor $U = 17.59$ 12 <sup>th</sup> Floor $U = 17.73$ 15 <sup>th</sup> Floor $U = 18.74$	9 <sup>th</sup> Floor $U = 19.17$ 12 <sup>th</sup> Floor $U = 19.53$ 15 <sup>th</sup> Floor $U = 20.82$	9 <sup>th</sup> Floor $U = 21.44$ 12 <sup>th</sup> Floor $U = 22.72$ 15 <sup>th</sup> Floor $U = 23.67$
<b>Test Duration (s)</b>	9 <sup>th</sup> Floor $T_s = 60$ 12 <sup>th</sup> Floor $T_s = 60$ 15 <sup>th</sup> Floor $T_s = 60$	9 <sup>th</sup> Floor $T_s = 60$ 12 <sup>th</sup> Floor $T_s = 60$ 15 <sup>th</sup> Floor $T_s = 60$	9 <sup>th</sup> Floor $T_s = 60$ 12 <sup>th</sup> Floor $T_s = 60$ 15 <sup>th</sup> Floor $T_s = 60$
<b>Low Turbulence Intensity</b>	9 <sup>th</sup> Floor $I_{uL} = 0.152$ 12 <sup>th</sup> Floor $I_{uL} = 0.149$ 15 <sup>th</sup> Floor $I_{uL} = 0.135$	9 <sup>th</sup> Floor $I_{uL} = 0.233$ 12 <sup>th</sup> Floor $I_{uL} = 0.225$ 15 <sup>th</sup> Floor $I_{uL} = 0.209$	9 <sup>th</sup> Floor $I_{uL} = 0.282$ 12 <sup>th</sup> Floor $I_{uL} = 0.280$ 15 <sup>th</sup> Floor $I_{uL} = 0.270$
<b>Probability of Exceedance G</b>	9 <sup>th</sup> Floor $G = 0.0052$ 12 <sup>th</sup> Floor $G = 0.0051$ 15 <sup>th</sup> Floor $G = 0.0053$	9 <sup>th</sup> Floor $G = 0.0018$ 12 <sup>th</sup> Floor $G = 0.0017$ 15 <sup>th</sup> Floor $G = 0.0019$	9 <sup>th</sup> Floor $G = 0.00069$ 12 <sup>th</sup> Floor $G = 0.00069$ 15 <sup>th</sup> Floor $G = 0.00071$

**Table 3 – Full-Scale Parameters Considered for the Analysis**

Test Characteristics	Full Scale	Full Scale	Full Scale
<b>Surface Roughness <math>Z_0</math></b>	9 <sup>th</sup> Floor $Z_0 = 0.1$ to $0.3$ 12 <sup>th</sup> Floor $Z_0 = 0.1$ to $0.3$ 15 <sup>th</sup> Floor $I_{uH} = 0.3$ to $0.7$	9 <sup>th</sup> Floor $Z_0 = 0.3$ to $0.7$ 12 <sup>th</sup> Floor $Z_0 = 0.3$ to $0.7$ 15 <sup>th</sup> Floor $I_{uH} = 1$	9 <sup>th</sup> Floor $Z_0 > 1$ 12 <sup>th</sup> Floor $Z_0 > 1$ 15 <sup>th</sup> Floor $I_{uH} > 1$
<b>Turbulence Intensity</b>	9 <sup>th</sup> Floor $I_{uH} = 0.22$ 12 <sup>th</sup> Floor $I_{uH} = 0.21$ 15 <sup>th</sup> Floor $I_{uH} = 0.20$	9 <sup>th</sup> Floor $I_{uH} = 0.28$ 12 <sup>th</sup> Floor $I_{uH} = 0.27$ 15 <sup>th</sup> Floor $I_{uH} = 0.25$	9 <sup>th</sup> Floor $I_{uH} = 0.31$ 12 <sup>th</sup> Floor $I_{uH} = 0.31$ 15 <sup>th</sup> Floor $I_{uH} = 0.30$
<b>Reference Height (m)</b>	9 <sup>th</sup> Floor $Z_{ref} = 30.63$ 12 <sup>th</sup> Floor $Z_{ref} = 41.15$ 15 <sup>th</sup> Floor $Z_{ref} = 51.66$	9 <sup>th</sup> Floor $Z_{ref} = 30.63$ 12 <sup>th</sup> Floor $Z_{ref} = 41.15$ 9 <sup>th</sup> Floor $Z_{ref} = 51.66$	9 <sup>th</sup> Floor $Z_{ref} = 30.63$ 12 <sup>th</sup> Floor $Z_{ref} = 41.15$ 15 <sup>th</sup> Floor $Z_{ref} = 51.66$
<b>Mean Wind speed (m/s)</b>	9 <sup>th</sup> Floor $U = 65.70$ 12 <sup>th</sup> Floor $U = 69.61$ 15 <sup>th</sup> Floor $U = 72.63$	9 <sup>th</sup> Floor $U = 65.70$ 12 <sup>th</sup> Floor $U = 69.61$ 15 <sup>th</sup> Floor $U = 72.63$	9 <sup>th</sup> Floor $U = 65.70$ 12 <sup>th</sup> Floor $U = 69.61$ 15 <sup>th</sup> Floor $U = 72.63$
<b>Test Duration (minutes)</b>	9 <sup>th</sup> Floor $T_s = 60$ 12 <sup>th</sup> Floor $T_s = 60$ 15 <sup>th</sup> Floor $T_s = 60$	9 <sup>th</sup> Floor $T_s = 60$ 12 <sup>th</sup> Floor $T_s = 60$ 15 <sup>th</sup> Floor $T_s = 60$	9 <sup>th</sup> Floor $T_s = 60$ 12 <sup>th</sup> Floor $T_s = 60$ 15 <sup>th</sup> Floor $T_s = 60$

## 2.4 References

- [1] Cermak, J.E., (1975). Applications of Fluid Mechanics to Wind Engineering-A Freeman Scholar Lecture. Journal of Fluids Engineering 97, 9-38.
- [2] Irwin, P.A., (1998). The role of wind tunnel modeling in the prediction of wind effects on bridges; in: Esdahl, A.L.S. (Ed.), The International symposium on advances in bridge aerodynamics. Copenhagen, Denmark, pp. 99-117.

- [3] Asghari Mooneghi, M., Irwin, P., Chowdhury, A.G. (2016). Partial turbulence simulation method for predicting peak wind loads on small structures and building appurtenance. *Journal of Wind Engineering and Industrial Aerodynamics*. 157- 46-62.
- [4] Davenport, A.G., King, J.P.C., (1984). *Dynamic Forces on Long Span Bridges*, 12th Congress of the International Association of Bridge and Structural Engineers (IABSE), Vancouver.
- [5] Asghari Mooneghi, M. (2014). *Experimental and Analytical Methodologies for Predicting Peak Loads on Building Envelopes and Roofing Systems* Dissertation. FIU Electronic Theses and Dissertations. Florida International University.
- [6] Asghari Mooneghi, M., Chowdhury, A.G., Irwin, P., (2015). *Partial Turbulence Simulation Method for Small Structures*. Conference Paper.
- [7] Wu, C.H., Kopp, G.A., (2018). A quasi-steady model to account for the effects of upstream turbulence characteristics on pressure fluctuations on a low-rise building. *J. Wind Eng. Ind. Aerod.* 179, 338–357.

**CHAPTER III**  
**EXPERIMENTAL SETUP AND PROTOCOLS**

## CHAPTER 3

### EXPERIMENTAL SETUP AND PROTOCOLS

#### 3.1 Test Models and Instrumentation

Testing was performed in the 12-fan Wall of Wind (WOW). This facility can generate a 6 m wide and 4.3 m high wind field and speeds as high as 70 m/s [1]. The WOW Experimental Facility (EF) at FIU is assigned by the National Science Foundation (NSF) as a shared-use, national facility under the Natural Hazards Engineering Research Infrastructure (NHERI) [1]. Figure 1a shows the WOW open jet facility that was used to conduct the testing.



Figure 1 - (a) NHERI Wall of Wind Experimental Facility (WOW EF), FIU; (b) Spires and floor roughness elements.

The mean wind speed profile and turbulence parameters within the atmospheric boundary layer (ABL) were simulated at the WOW using floor roughness elements and triangular spires as shown in Figure 1b. All three directional components of the velocity and static pressure were measured at different elevations using the Cobra probes.

### 3.1.1 Test Models Setup and Instrumentation

The prototype (full-scale) building selected for this study was a 15-story mid-rise building. The dimensions of the full-scale building were height (H) = 55.2 m and width (L) = 24.5 m as shown in Figure 2. The balconies were assumed to be glass panel handrail systems, one of the most common types of handrails used in balconies. Such systems also provided more vertical surface area for the wind to act upon in comparison to partially open systems using balustrade or picket type handrails.

Two types of models, building with balconies and building with no balconies (as shown in Figures 3a and 3b), were tested using scales 1:180, 1:67, and 1:25. Table 1 shows the building dimensions of these tested scales. For the test of the building with balconies, two types of balconies were considered: continuous balcony handrail panels and discontinuous balcony handrail panels. In this research, only balcony handrail panels at the 15<sup>th</sup>, 12<sup>th</sup>, and 9<sup>th</sup> floors were tested for all model scales.

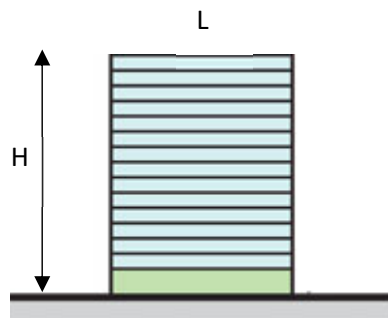


Figure 2 – Building Elevation

Table 1 – Building dimensions at different scales

Scale	H (m)	L (m)
1:25	2.21	0.98
1:67	0.82	0.37
1:180	0.31	0.14

The balcony dimensions were obtained from approved Miami-Dade County Notice of Approval (NOA) reference plans.

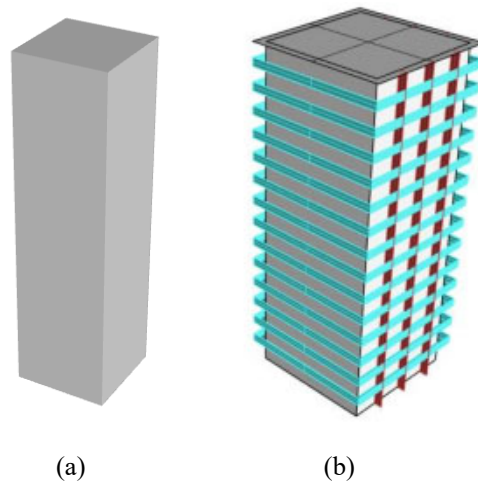


Figure 3 – (a) Base building model (b) Building-Balcony model

3D printing technology is becoming more frequently used in test model construction due to its advantage of time efficiency and accuracy. In this study, 3D printed technology was used to build the smallest test model. For the 1:180 model scale, all the building and balcony members were printed using this technology as shown in Figures 4a and 4b. No internal wood frame was used for model stability.

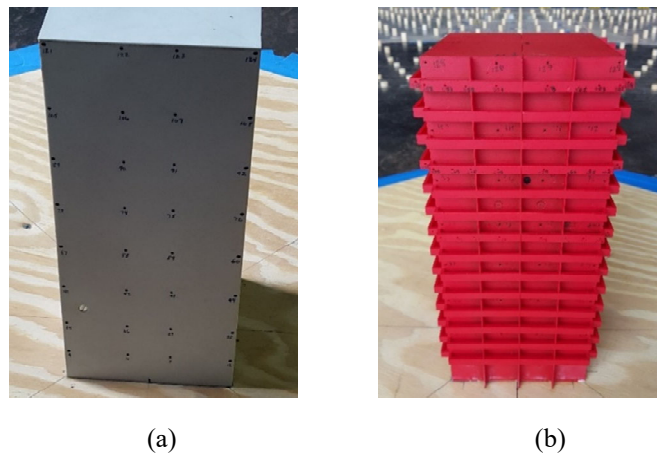


Figure 4 – Scale 1:180 a) Base building model (b) Building-Balcony model

For the model scales 1:67 and 1:25, a plexiglass material was used to construct the building models. For these scales, the balcony handrail panels (tested at the 15<sup>th</sup>, 12<sup>th</sup>, and 9<sup>th</sup> floors) were 3D printed as shown in Figure 5. Other floors' balcony handrail panels (dummy balconies) were constructed from a thin wood material. Figure 6 shows the balcony dimensions of the scaled models. An internal wood frame was used for the stability and rigidity of the 1:67 and 1:25 models as shown in Figures 7 and 8, respectively. Figures 9 and 10 show the internal wood frame assembly for scales 1:67 and 1:25, respectively.

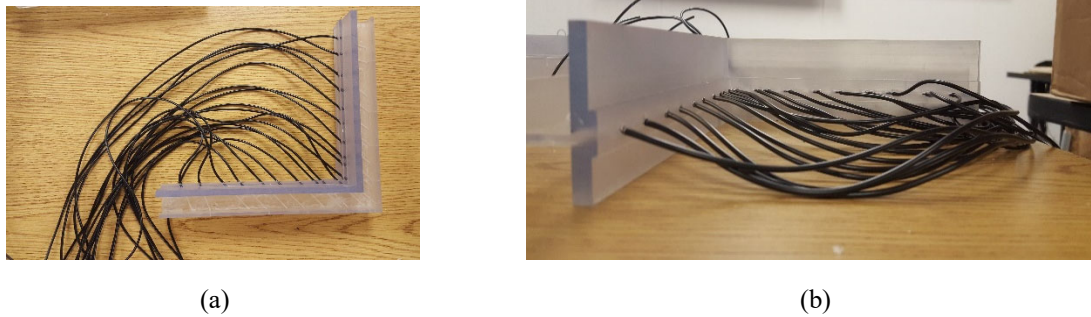


Figure 5 – Printed 3D Balconies (a) Top View (b) Side View

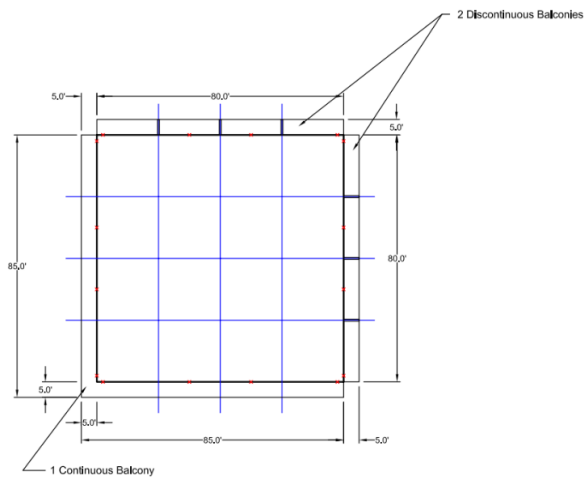


Figure 6 – Balcony Dimensions



(a)



(b)

Figure 7 – Model Scale 1:67 (a) Base Building (b) Building with Balconies



(a)



(b)

Figure 8 – Model Scale 1:25 (a) Base Building (b) Building with Balconies

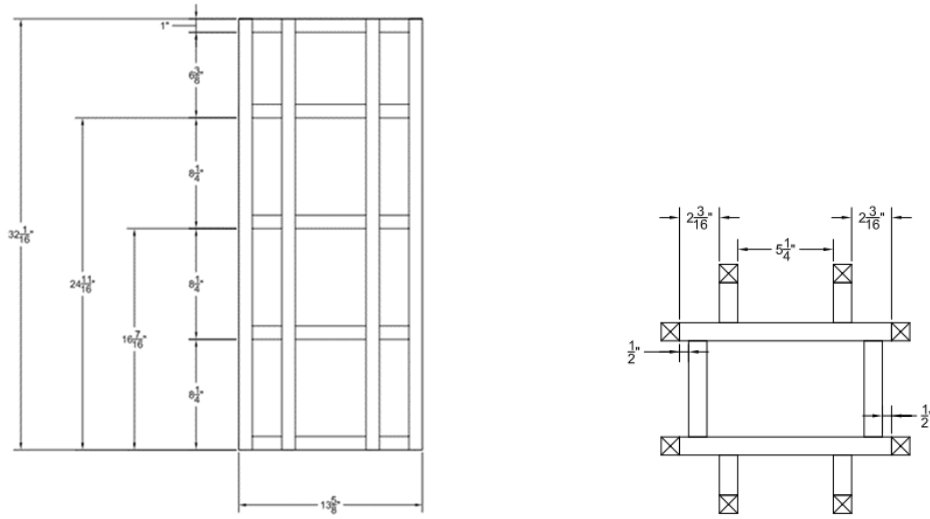


Figure 9 – Wood Framing 1:67 Scale – Assembly Details

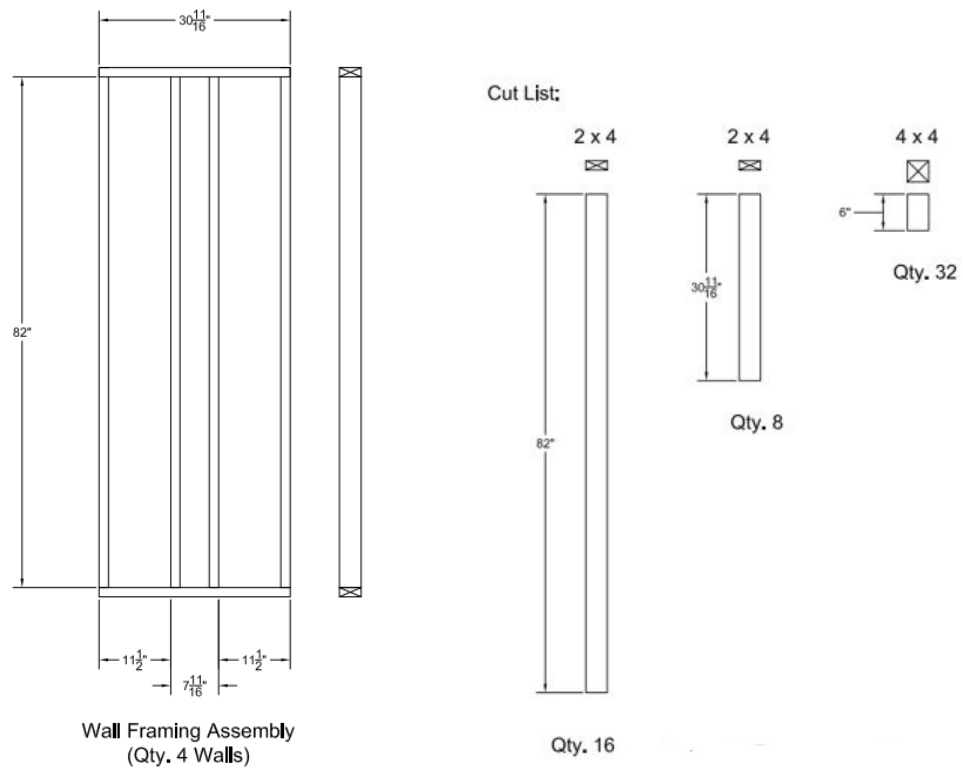


Figure 10 – Wood Framing 1:25 Scale – Assembly Details

Figure 11 shows the comparison of the different model scales tested at the WOW.

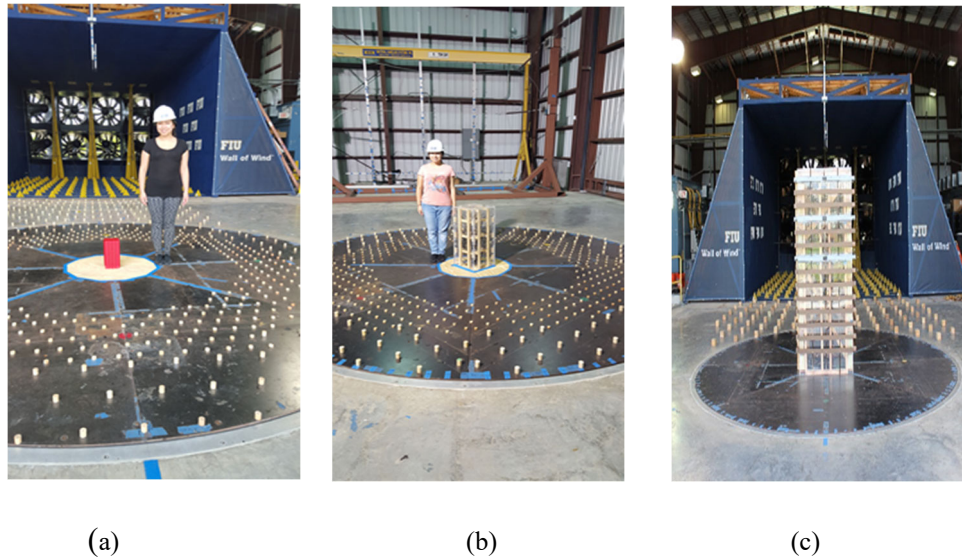


Figure 11 – All Model Scales – Height Comparison (a) Scale 1:180, (b) Scale 1:67, (c) Scale 1:25

### 3.1.2 Measuring Devices

The surface pressure distribution in the buildings and balcony handrail panels was measured with pressure taps. A similar pressure tap layout was chosen for all the model scales. This was done to compare the pressure distributions on the three models.

All base models (buildings with no balconies) had 128 pressure taps. All models with balcony handrail panels, except scale 1:25, had a total of 368 pressure taps. For the 1:25 scale building with balcony handrail panels, the pressure tap 49 was the first wall tap used for the tests. The wall taps 1-48 were not used in the 1:25 model in order to accommodate the additional taps on the continuous balcony handrail panels' corners for Reynolds number effects studies.

A 5/64-inch diameter hole was drilled at each tap location, and a piece of 5/64 inch outside diameter (O.D.) tubing was glued into each tap. The pressure taps were glued in

the surface of the building and balcony handrail panels scale models, and each tap was connected to a pressure transducer. Each transducer had 64 channels. Building walls had only external pressure taps, and balcony handrail panels had pressure taps on both sides to measure net pressures for all model scales.

The channel tube lengths connected to the pressure taps varied between the models. Figure 12 shows the channel layout used as reference for this study. For the smallest model scale 1:180, the total length was 4 ft (2 ft and 2 ft), and for the models 1:67 and 1:25, the length was 5 ft (2 ft and 3 ft). A transfer function designed for the tubing was used to correct for tubing effects. Pressure data were acquired at a sampling frequency of 512 Hz for a period of 60 seconds.

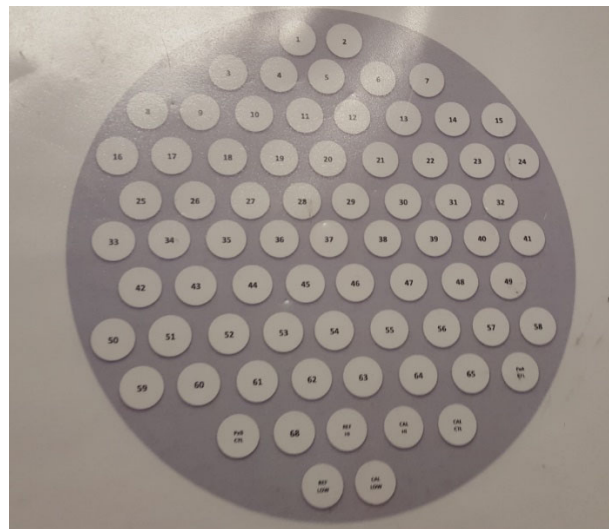


Figure 12 – Transducer – Channel Layout

The 512 Channel Scanivalve Corporation pressure scanning system was used to measure the pressure time histories on the building models' walls and balcony handrail panels according to the tap layout. The pressure transducers were connected to a

temperature control unit (TCU). There were 3 TCU's used in the experiments. For the 1:180 and 1:67 models, the TCU's were at the top level. However, for the 1:25 model as shown in Figure 13, the TCU was located above ground, because the total tube length of 5 ft. was short compared to the height of the model. The TCU was connected to a Digital Service Module DSM 4000 that transferred the information to the Data Acquisition.

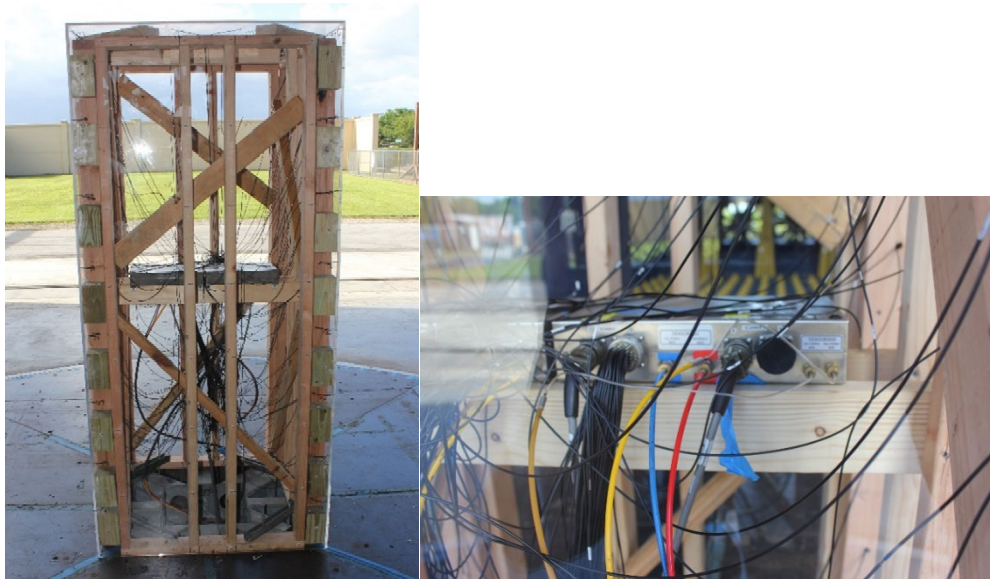


Figure 13 – Model Scale 1:25 – TCU located above the ground

Figures 14 and 15 show the balcony plan view and elevation view, respectively.

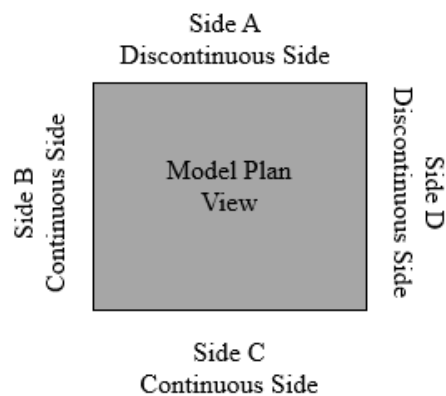


Figure 14 – Building with Balconies Plan View

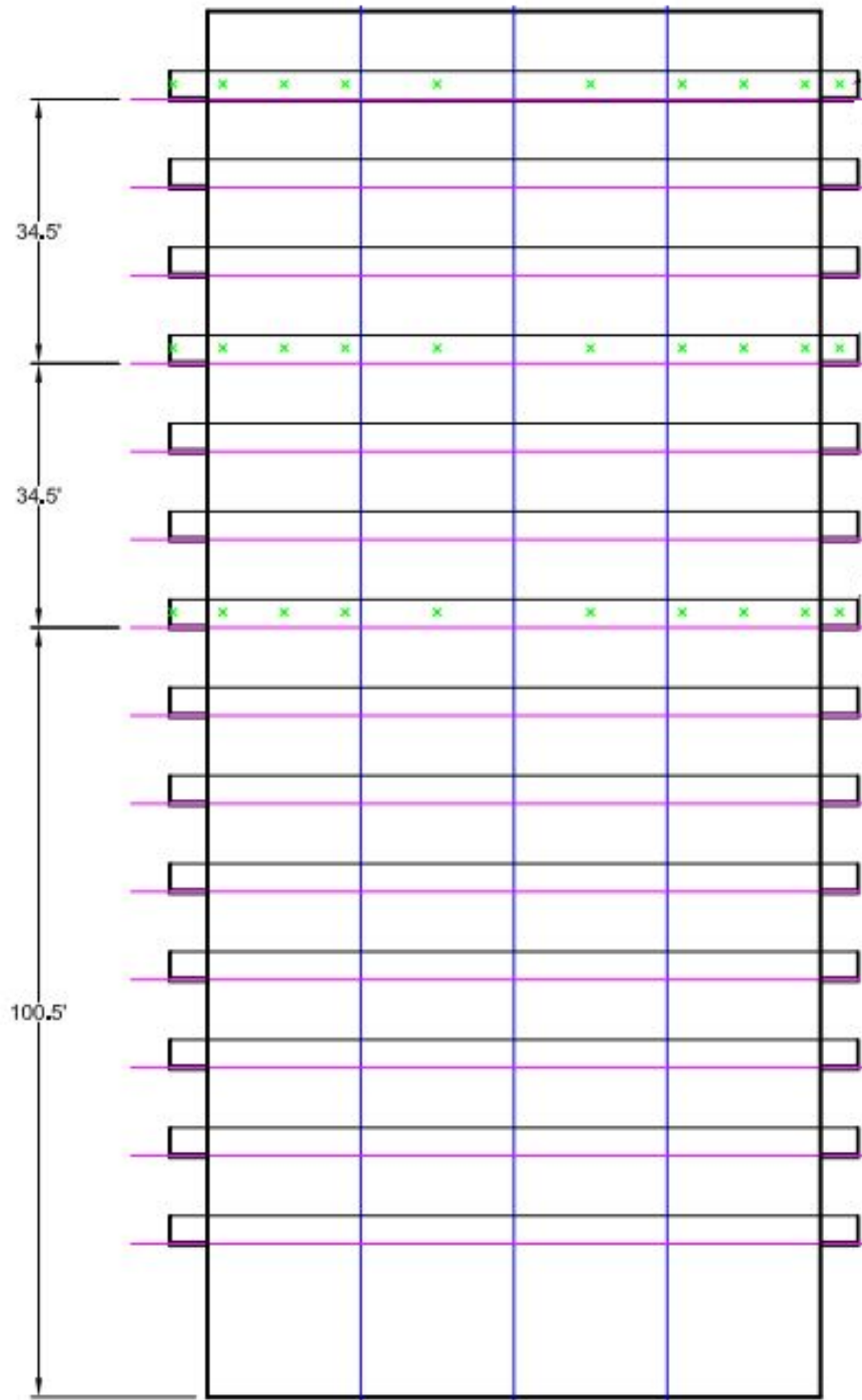


Figure 15 – Building with Balconies Elevation View – Full Scale

Figures 16 to 23 show the pressure taps of 1:180, 1:67, and 1:25 models.

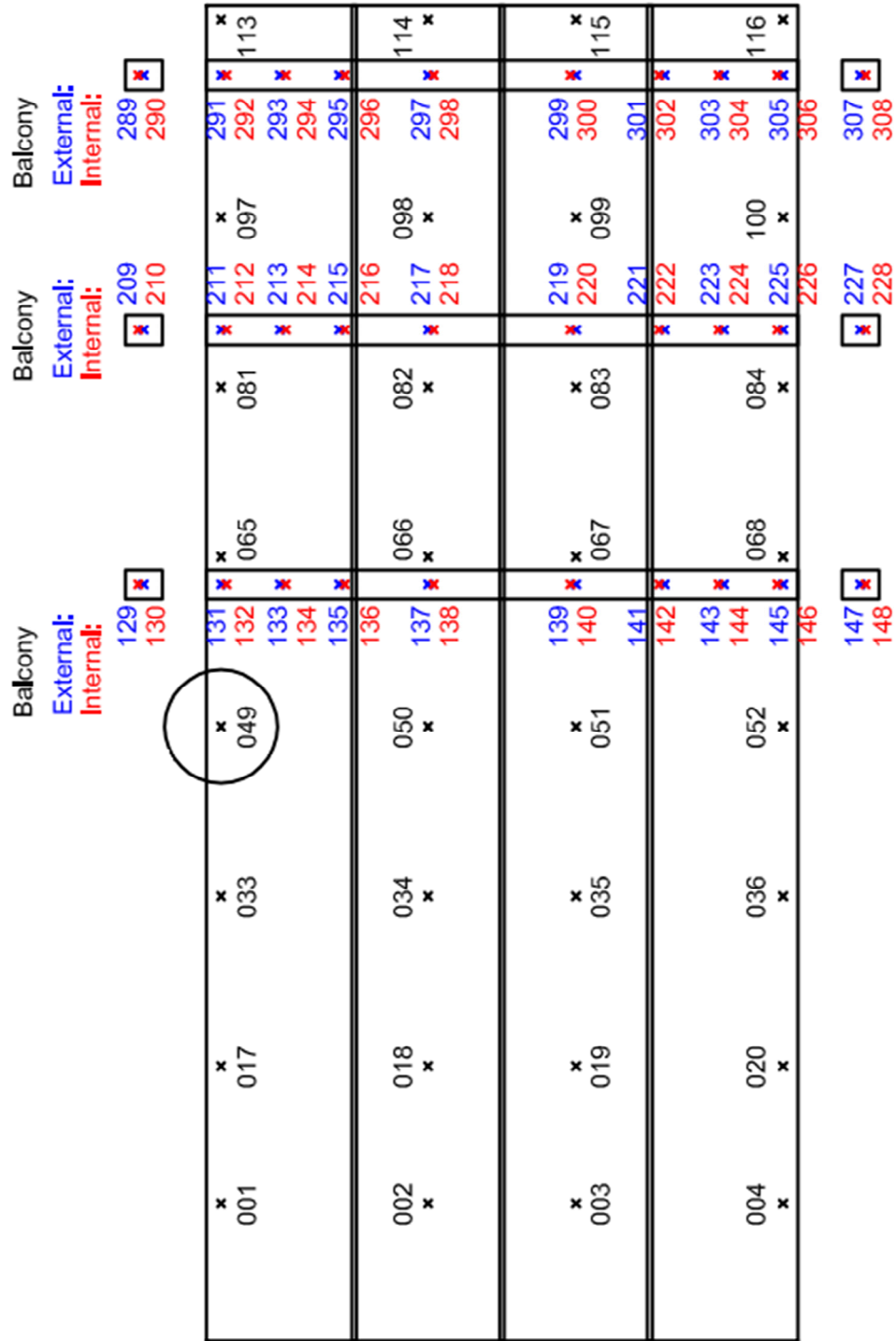


Figure 16 – Model Scale 1:180 and 1:67 – Pressure Tap Layout Side A

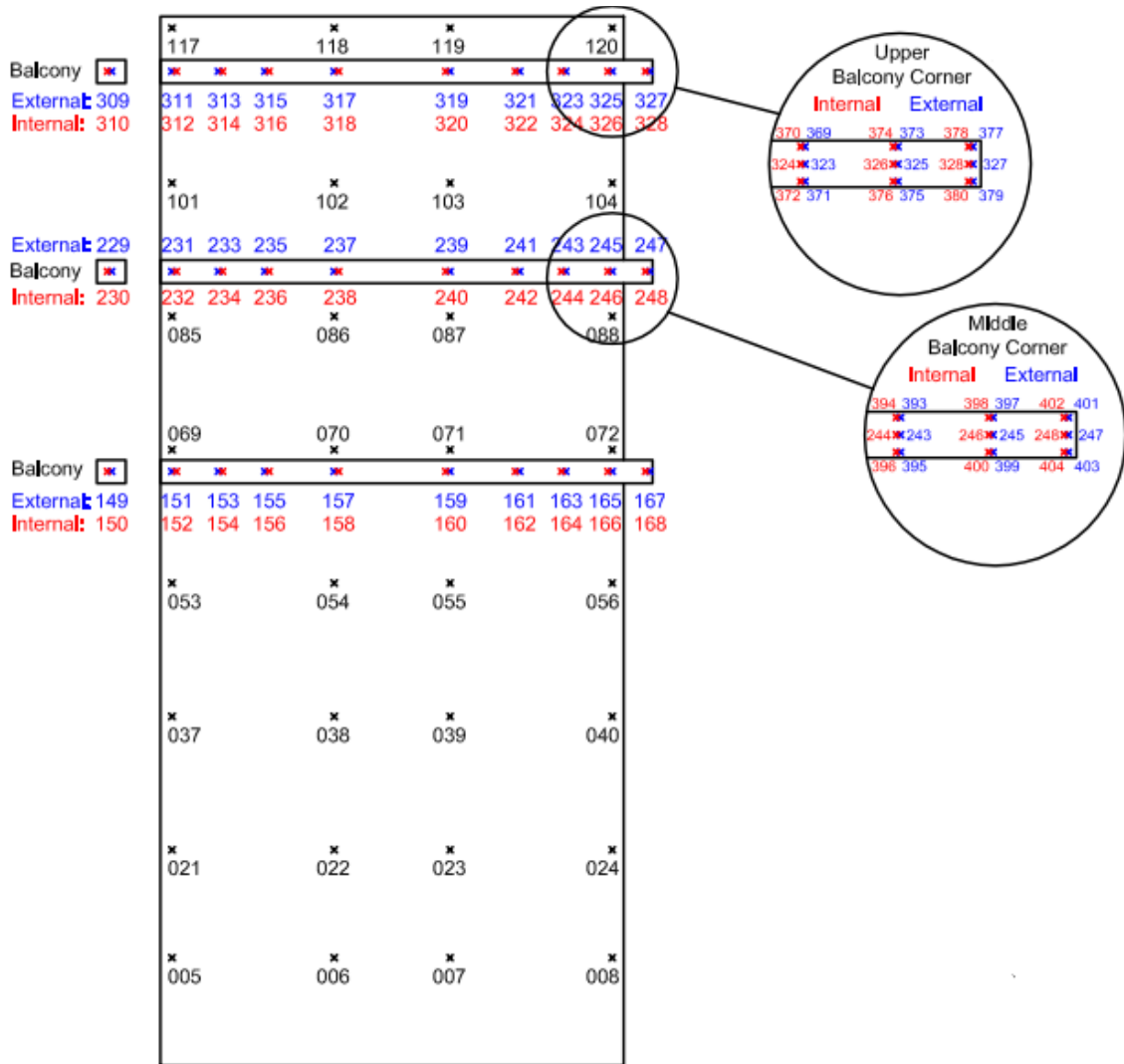


Figure 17 – Model Scale 1:180 and 1:67 – Pressure Tap Layout Side B

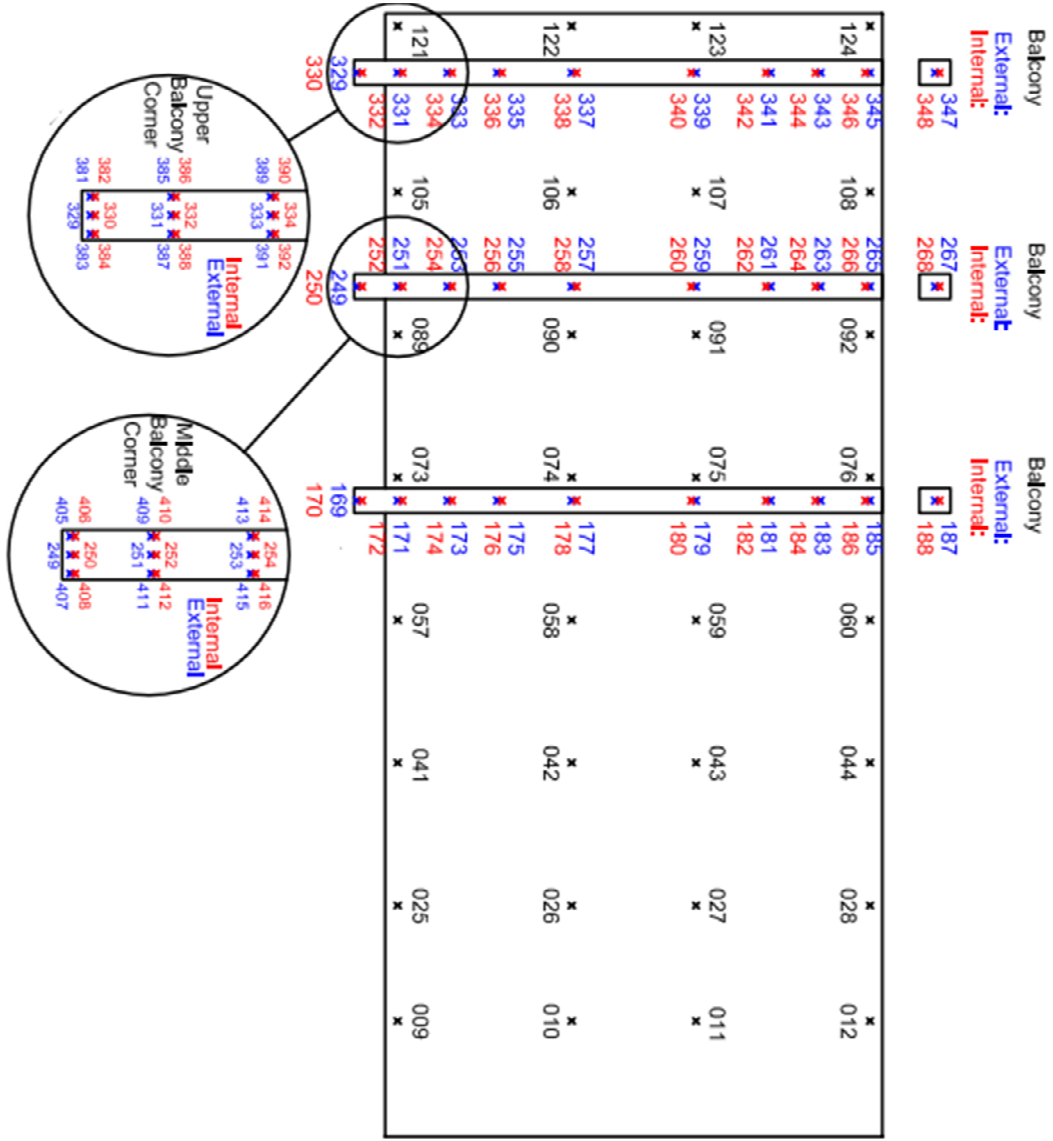


Figure 18 – Model Scale 1:180 and 1:67 – Pressure Tap Layout Side C

	x 125	x 126	x 127	x 128	
349	x x x	x	x	x x x	External: 367
350	x x x	x	x	x x x	Internal: 368
	351 353 958 352 354 958	357 358	359 360	361 363 365 362 364 366	Balcony
	x 109	x 110	x 111	x 112	
269	x x x	x	x	x x x	External: 367
	272 274 276	278	280	282 284 286	Internal: 368
270	x x x	x	x	x x x	Balcony
	271 273 275 093	277 094	279 095	281 283 285 096	
	x 077	x 078	x 079	x 080	
189	x x x	x	x	x x x	External: 367
190	x x x	x	x	x x x	Internal: 368
	191 193 195 192 194 196	197 198	199 200	201 203 205 202 204 206	Balcony
	x 061	x 062	x 063	x 064	
	x 045	x 046	x 047	x 048	
	x 029	x 030	x 031	x 032	
	x 013	x 014	x 015	x 016	

Figure 19 – Model Scale 1:180 and 1:67 – Pressure Tap Layout Side D

	Balcony		Balcony		Balcony		Balcony	
	External:	Internal:	External:	Internal:	External:	Internal:	External:	Internal:
x 001	x 017	x 033	x 049	x 065	x 081	x 211	x 291	x 113
			131	132	133	212	292	113
			134	135	136	213	293	
			137	138	139	214	294	
			140	141	142	215	295	
			143	144	145	216	296	
x 002	x 018	x 034	x 050	x 066	x 082	217	297	x 114
			146	147	148	218	298	x 114
			149	150	151			
x 003	x 019	x 035	x 051	x 067	x 083	219	299	x 115
			152	153	154	220	300	x 115
			155	156	157	221	301	
			158	159	160	222	302	
			161	162	163	223	303	
x 004	x 020	x 036	x 052	x 068	x 084	224	304	x 116
			164	165	166	225	305	x 116
			167	168	169	226	306	
			170	171	172			
			173	174	175	227	307	
			176	177	178	228	308	

Figure 20 – Model Scale 1:25 – Pressure Tap Layout Side A



Figure 21 – Model Scale 1:25 – Pressure Tap Layout Side B

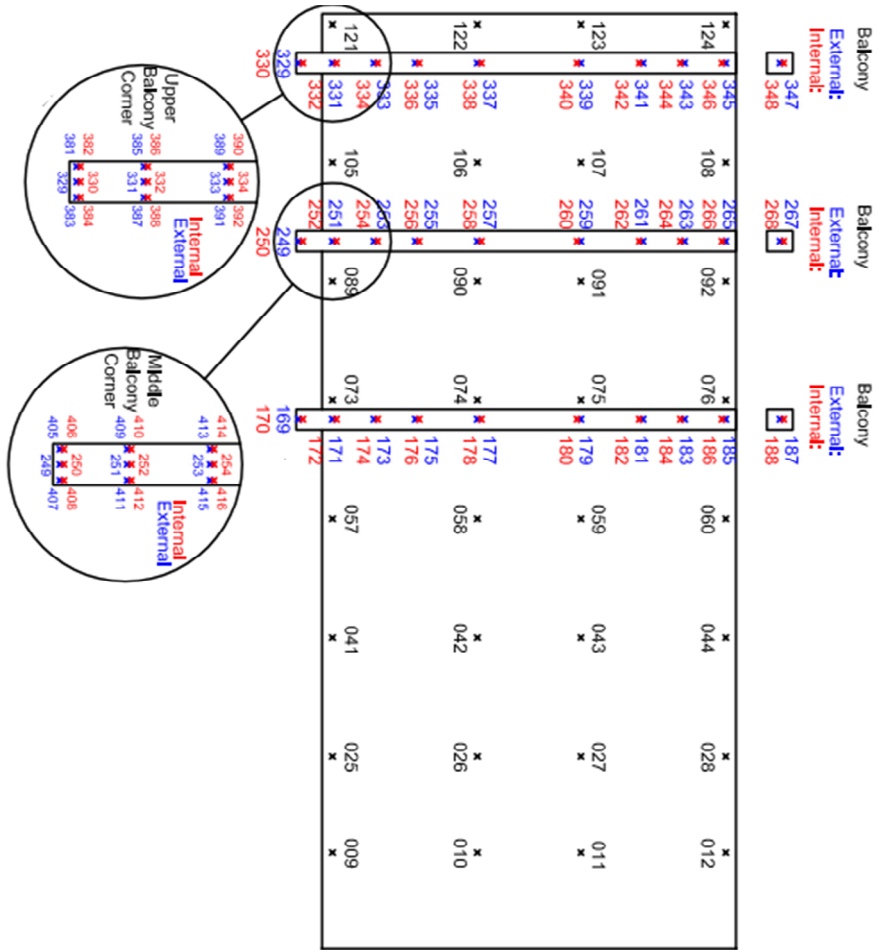


Figure 22 – Model Scale 1:25 – Pressure Tap Layout Side C

	x 125	x 126	x 127	x 128	
349 350	x x x	x x	x x	x x x	External: 367 Internal: 368
<input type="checkbox"/>	351 353 998 352 354 998	357 358	359 360	361 363 365 362 364 366	Balcony <input type="checkbox"/>
	x 109	x 110	x 111	x 112	
269	272 274 276	278	280	282 284 286	External: 367 Internal: 368
<input type="checkbox"/>	x x x	x	x	x x x	Balcony <input type="checkbox"/>
270	271 273 275	277	279	281 283 285	
	x 093	x 094	x 095	x 096	
	077	078	079	080	
	x x x	x	x	x	
189 190	x x x	x	x	x x x	External: 367 Internal: 368
<input type="checkbox"/>	191 193 195 192 194 196	197 198	199 200	201 203 205 202 204 206	Balcony <input type="checkbox"/>
	x 061	x 062	x 063	x 064	
	x 045	x 046	x 047	x 048	
	x 029	x 030	x 031	x 032	
	x 013	x 014	x 015	x 016	

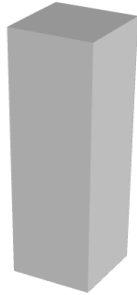
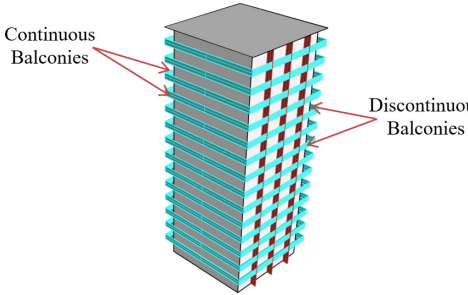
Figure 23 – Model Scale 1:25 – Pressure Tap Layout Side D

### 3.2 Test Protocol

The wind directions considered for testing were 0° to 360° at 3° intervals for the building with balconies and the building without balconies as shown in Table 2. Prior studies [2] showed that this small increment in the wind direction during testing provided the resolution required to capture enough lateral turbulence fluctuations in the upcoming wind [3]. Figure 24 shows the convention for wind directions and the model placement. Models were tested at 40% of the WOW fan throttle.

To study the pressure distribution resolution, the largest scale model (1:25) had three-layer taps at the continuous balcony handrail panel corners of the 15<sup>th</sup> and 12<sup>th</sup> floors. Additionally, to study the Reynolds number (Re) effects, the 1:25 scale model was tested at 70% and 40% fan throttle.

Table 2 – Building types and wind directions

	Building Type	Wind Directions
 <p data-bbox="342 1438 607 1465">Building without Balconies</p>	 <p data-bbox="657 1159 748 1205">Continuous Balconies</p> <p data-bbox="1024 1230 1122 1276">Discontinuous Balconies</p> <p data-bbox="657 1438 1101 1516">Building with Balconies Two-sides with continuous balconies and two-sides with discontinuous balconies</p>	<p data-bbox="1154 1312 1370 1367">0 to 180 degrees in 3-degree intervals</p>

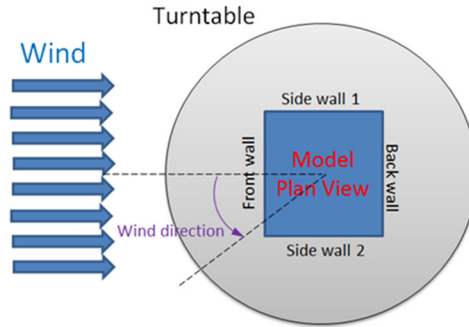


Figure 24 – Wind Direction

To obtain the free flow wind profile, the 512 channel Scanivalve Corporation pressure scanning system was used. The pressures obtained were converted into mean wind speed. Wind speeds were collected at two fan throttles of 40% and 70%. Figures 25, 26, and 27 show the along wind component of the mean wind speed at 40% throttle and turbulence intensity. These profiles were derived from the free stream wind speed measurements of each terrain at each corresponding scale. The mean wind speed profile at 40% throttle for WOW open terrain is shown below.

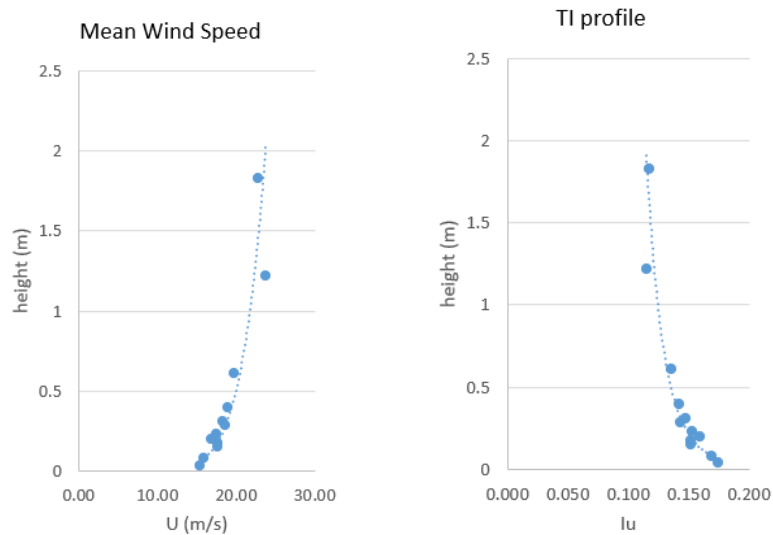


Figure 25 – Wind Speed and Turbulence Intensity Profiles (Scale 1:180)

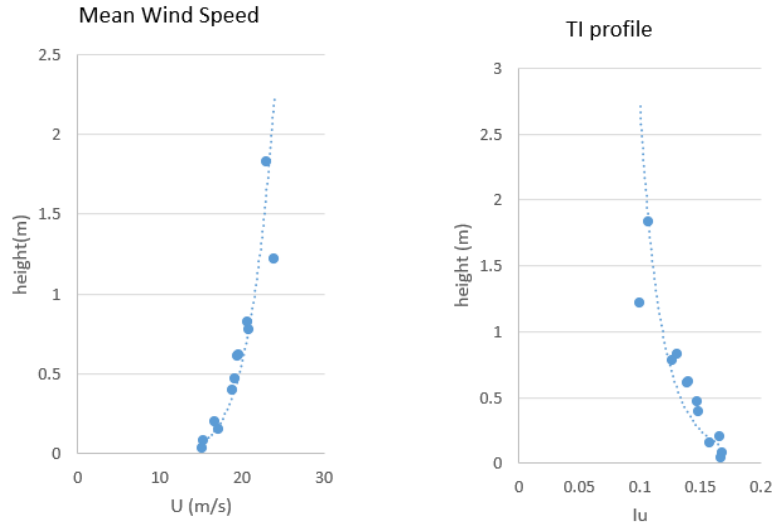


Figure 26 – Wind Speed and Turbulence Intensity Profiles (Scale 1:67)

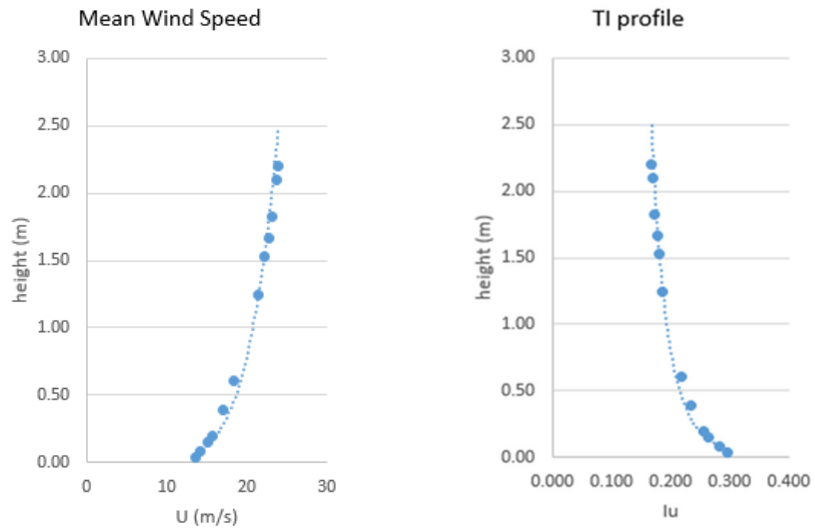


Figure 27 – Wind Speed and Turbulence Intensity Profiles (Scale 1:25)

### 3.3 References

- [1] Chowdhury, A.G., Zisis, I., Irwin, P., Bitsuamlak, G., Pinelli, J., Hajra, B., and Moravej, M., (2017). Large-Scale Experimentation Using the 12-Fan Wall of Wind to Assess and Mitigate Hurricane Wind and Rain Impacts on Buildings and Infrastructure Systems. *Journal of Structural Engineering*, 143(7): 04017053.
- [2] Asghari Mooneghi, M., Irwin, P., and Chowdhury, A.G. (2016). Partial turbulence simulation method for predicting peak wind loads on small structures and building appurtenances. *J. Wind Eng. Ind. Aerodyn.*, vol. 157, pp. 47–62.
- [3] Moravej, M. (2018). *Investigating Scale Effects on Analytical Methods of Predicting Peak Wind Loads on Buildings*. Florida International University.

## **CHAPTER IV**

### **THE EFFECT OF BALCONIES ON THE WIND LOADING ON BUILDINGS**

## CHAPTER 4

### THE EFFECT OF BALCONIES ON THE WIND LOADING ON BUILDINGS

#### 4.1 Abstract

Balcony handrail systems are used for aesthetics and safety reasons and should be designed for wind loading. Also, their effects should be taken into consideration when calculating wind loads on a building. The majority of the existing building codes do not provide an accurate approach for estimating the effect of balconies on the wind loading on buildings. To address this need, experiments were undertaken at the NHERI Wall of Wind (WOW) Experimental Facility (EF) at Florida International University (FIU) to investigate wind loads on glass panel handrail systems and the effect of such systems on the wind loading on buildings. A prototype fifteen-story mid-rise building was chosen for this study. Two series of tests were conducted: 1) one on the model building with no balconies and then 2) one on the model building with continuous balconies on two adjacent sides and discontinuous balconies on the remaining two sides. Detailed pressure measurements were performed on the handrail systems as well as on the building walls. Experiments showed that in most cases, balcony handrail systems reduced the external negative peak pressure coefficients on the building walls, while they slightly increased the positive peak pressure coefficients. The net pressure coefficients on the balcony handrail panels were compared with values provided in the National Building Code of Canada (NBCC) [1] for balcony handrails and ASCE 7-16 [2] components and cladding external pressure coefficients on walls. The results show that generally pressure equalization leads to reduced net pressures on the balcony handrail panels. However, close to the building's roof, the pressure

equalization is less effective, and the net pressure coefficients obtained were higher than those predicted using the standards. Future testing is recommended to cover the study of wider range of building heights and the wind effects on buildings with balconies to achieve reliable guidance for design of balcony handrail systems that will enhance the safety of the building's occupants.

**Keywords:** Wind Loading, Pressure Coefficient, Component and Cladding, Balcony Handrail Systems, Wind Tunnel Testing, Mid-rise Buildings, Wall of Wind.

## 4.2 Introduction

It is important to understand the pressure distribution on the building walls when analyzing wind loads on walls and components of the building. The pressure distribution on the building is affected by various factors such as the structure's geometry, approach-flow conditions, surroundings, and wind orientation. Also, it is important to note that balconies and other non-structural elements can impact the surface pressure distributions on a building's roof and walls [3,4,5,6,7].

Balconies with glass panel, balustrade or picket type handrail systems are regularly found on residential mid- and high-rise buildings. Balconies can change the flow and pressure distribution on the building. Research on wind loading mechanism on balcony handrail systems in mid-rise and high-rise buildings and their effects on the wind loads on the building's façade has been limited. Chand et al. [8] studied the effects of balconies on surface pressures on a mid-rise building using a 1:30 scale model in a wind tunnel. It was shown in the results that balconies can modify the peak and mean surface pressure distributions on buildings walls and roofs. Cochran and Peterka [9] studied the cladding external pressure for two mid-rise building configurations: (i) building with an open

balcony with no hurricane shutters, and (ii) building with slab-edge shutters. The second configuration changed the shape of the building from a structure with balconies to a cleaner rectilinear structure, similar to a building with no balconies. The external negative pressures on the buildings with shutters demonstrated greater outward loads along building's edges compared to the building with no shutters (building with open balconies). The wind-tunnel derived, corner-zone peak-negative loads for the building with open balconies (un-shuttered case) were about 40% lower (in magnitude) as compared to the building with shutters. The balconies had minimal or zero impact on the peak-positive cladding pressures. Rofail and Mans [10] studied the wind loading on an isolated balcony situated on a low-rise and on a high-rise building using wind tunnel testing on 1:50 scale models. Various balustrade types and building configurations were studied. Results were compared to the design provisions for balustrades provided in the Australian Building Code which states that balustrades in private residences should withstand the highest magnitude loading from either the wind loading or a uniform loading of  $1 \text{ kN/m}^2$  [11]. Also, the British Standard [12] and Hong Kong Building Regulations [13] provide similar suggestions. The results suggested that balconies should be designed for wind loading if the 3-sec gust wind speed exceeds  $30 \text{ m/s}$ ; otherwise, they should be designed for a live load of  $1 \text{ kN/m}^2$ . Kotani and Yamanaka [14] investigated the influence of the building façade elements on the wind pressure coefficients and the wind velocities along the building wall. Five-story building models with/without balconies were assessed in a wind tunnel using 1:60 scale models. Their results showed that the wind pressure on the wall was mainly generated by the building, and the existence of balconies had little effect on the wind pressure distribution. At a wind direction normal to a wall (0 degrees), the local wind velocity along the façade

wall was much affected by the type of balcony. A partition on the balcony caused a large velocity reduction to about one fifth compared to the wall without balconies and made the vertical velocity distribution more uniform. Browne and Kumar [15] studied the impact of corner and continuous balconies on the wind loads on tall buildings. The corner balconies are cantilevered balconies which are a slab extension from the building's interior slab surface. Several wind tunnel tests were performed on rectangular towers with and without corner/continuous balconies of various sizes in order to quantify wind-induced loads on the building. The results showed that corner balconies significantly reduce the crosswind sway response and torsional response of the structure. Continuous balconies had similar but less pronounced influence as compared to the corner balconies. As shown in the balcony study of Montazeri and Blocken [16] using Computational Fluid Dynamics (CFD), balconies could cause significant changes to the wind pressure distribution on windward walls, due to flow separation, recirculation, and reattachment generated by the presence of balconies. In addition, corner balconies could help reduce the crosswind response of tall buildings. This is mainly because they can act as general roughness and disrupt the formation of vortices shedding from the building. For instance, in the research by Kumar et al., the corner balconies that extended out of the building caused 10-30% reduction in the crosswind base loads [17]. Morton and Mara [18] investigated the impact of balconies on the overall wind response a building. Results of the wind tunnel testing showed that balconies located near a sharp-edged corner reduced the peak suctions experienced by the leeward wall. Also, results showed a minimal impact in the peak positive cladding pressure for the case of wind normal to the balconies.

Building codes and standards such as the International Building Code (IBC), the Florida Building Code (FBC), and the American Society of Civil Engineers (ASCE 7-16) do not provide information on the influence of balcony handrail systems on cladding or structural wind loads. Therefore, the design decision is up to the engineer's interpretation. For cladding, this means that, without a wind tunnel test, the "hot spots" prescribed in the codes (zones with positive or negative pressures of high magnitudes) must be considered even though they will likely change due to the presence of the balconies. For the building, the designer decides how to approach the additional surface area from the vertical facades of the balconies (such as in glass panel balcony railing systems).

This paper presents results from an experiment performed at the Wall of Wind (WOW) at Florida International University (FIU), on a fifteen-story building using a 1:180 scale model. The paper is comprised of an experimental description section, and the discussion of results of the loads on the building and balconies. The results of the mean and peak pressure coefficients are discussed in Sections 4.1 and 4.2 in the paper, along with a comparison of results with codes and standards (such as ASCE 7-16 and NBCC 15) in Section 4.3.

### **4.3 Description of the Experiments**

#### **4.3.1 *Wall of Wind (WOW) Facility***

The WOW Experimental Facility (EF) at FIU is assigned by the National Science Foundation (NSF) as a shared-use, national facility under the Natural Hazards Engineering Research Infrastructure (NHERI) [19]. The 12-fan WOW open jet facility (Figure 1a) was used to conduct the testing for this study. WOW can simulate mean wind speed and turbulence characteristics of those of hurricane winds.



Figure 1 - (a) NHERI Wall of Wind Experimental Facility (WOW EF), FIU; (b) Spires and floor roughness elements

The mean wind speed profile and turbulence effects within the atmospheric boundary layer (ABL) were simulated at the WOW using floor roughness elements and triangular spires as shown in Figure 1b. All the three directional components of velocity and static pressure were measured at different elevations using the Cobra probes.

Figure 2a shows the mean wind speed and turbulence intensity profiles simulated for the tests. The turbulence intensity power spectrum is shown in Figure 2b where it is compared to a full-scale spectrum obtained from ESDU [20]. The comparison of the spectra shows that the measured wind speed spectrum is missing some of the turbulence fluctuations at low frequencies as compared to the full-scale spectrum. The effect of this discrepancy on the estimated peak wind loads is discussed in the subsequent sections of the paper.

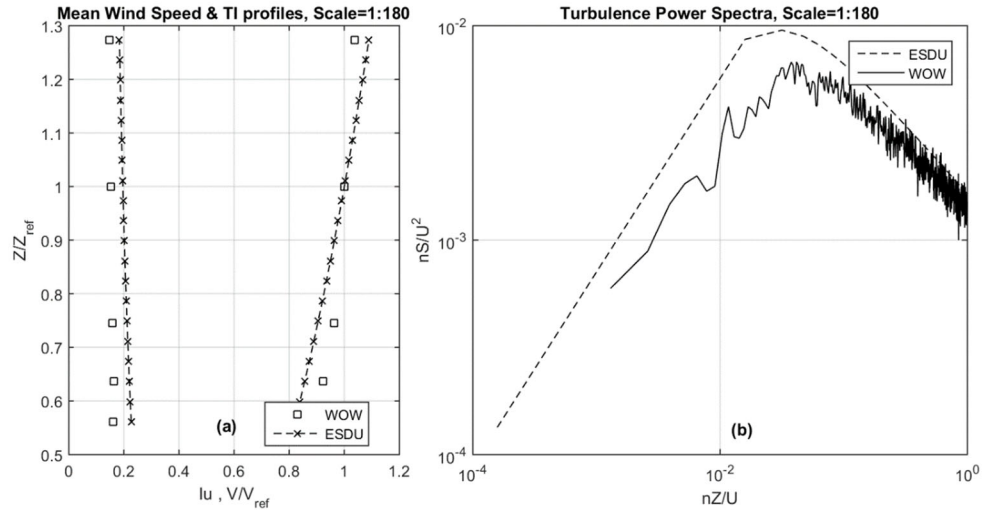


Figure 2 – (a) Wind speed and turbulence intensity profiles; (b) Turbulence power spectra

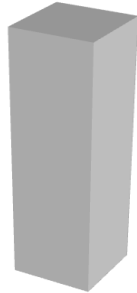
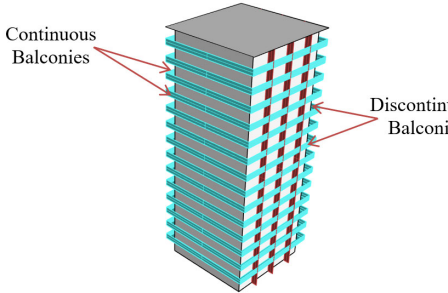
#### 4.3.2 Test Building

The test building selected for this study was a 15-story mid-rise building [21]. The dimensions of the full-scale building were the following: height = 55.2 m and width = 24.5 m. The balconies were assumed to be glass panel handrail systems, which are one of the most common types of handrails used in balconies. Such system also provides more vertical surface area for the wind to act upon in comparison to partially open systems that use balustrade or picket type handrails.

Two series of tests were conducted by using building models with and without balconies. Wind effects pertaining to both continuous and discontinuous balconies were studied. Continuous balconies run along the building from one side to the other side of the building. Discontinuous balconies have partitions in between. The balcony handrail vertical panels (representing the glass panels) were instrumented (using pressure taps) for the 15<sup>th</sup>, 12<sup>th</sup>, and 9<sup>th</sup> floors; for the remaining floors, the balconies were modeled using vertical panels without sensors (termed as ‘dummy’ balconies). The Table below presents

the schematics of the building models used for the experiments. The wind direction convention is shown in Figure 3.

Table 1 – Building wind tunnel models (scale 1:180)

	Building Type	Wind Directions
 <p data-bbox="342 800 607 825">Building without Balconies</p>	 <p data-bbox="656 800 1101 869">Building with Balconies Two-sides with continuous balconies and two-sides with discontinuous balconies</p>	<p data-bbox="1154 674 1370 726">0 to 180 degrees in 3-degree intervals</p>

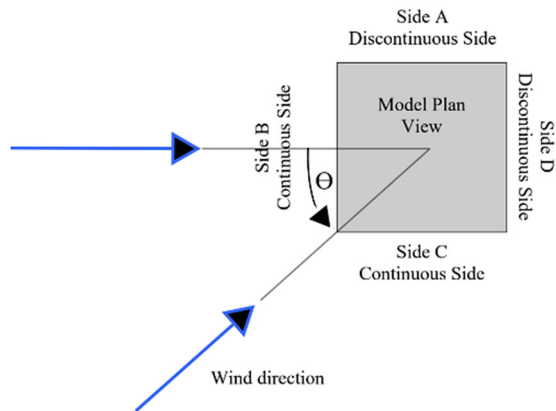


Figure 3 – Wind direction convention

The exterior side of the building walls as well as the inner and outer faces of the balcony handrail vertical panels had pressure taps installed. A Scanivalve Corporation pressure measuring system with 512 channels was used to measure the pressures for a period of one minute. The sampling rate for pressure measurements was 520 Hz. Pressure data were low pass filtered at 250 Hz. The tubing effects were corrected using a transfer function designed for the tubing [22]. Figures 4 and 5 show the models used in this study.



Figure 4 – Building model without balconies (scale: 1:180)

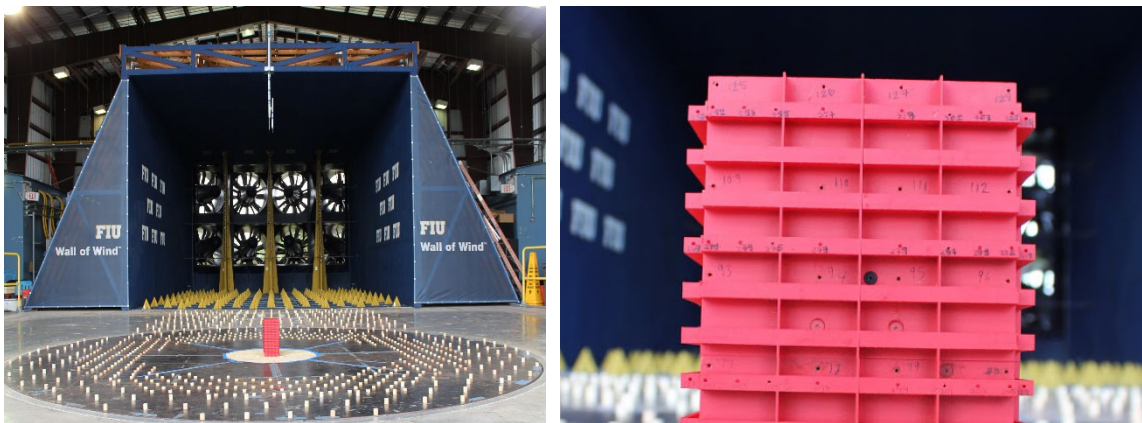


Figure 5 – Building model with balcony handrail systems (scale: 1:180)

#### 4.4 Data Analysis

Results from the tests are shown as mean and peak surface pressure coefficients which were obtained based on equations proposed by Richards et al. [23]. They suggested expressing (1) the mean pressure coefficient as the ratio of the mean surface pressures to the mean dynamic pressure, and (2) the peak pressure coefficient as the ratio of the extreme surface pressures to the peak dynamic pressure, recorded during the tests, as shown below in Equation 1:

$$C_{p \text{ mean}} = \frac{P_{\text{mean}}}{\frac{1}{2}\rho U_{\text{mean}}^2} \quad (1)$$

where  $P_{\text{mean}}$  is the mean pressure,  $\rho$  is the density of air at the time of the test ( $1.225 \text{ kg/m}^3$ ) and  $U_{\text{mean}}$  is the mean wind speed measured at the top of the building.

The peak pressure coefficient based on 3-second gust dynamic pressure is calculated as shown in Equation 2.

$$C_{p \text{ peak}} = \frac{P_{\text{peak}}}{\frac{1}{2}\rho U_{3 \text{ sec}}^2} \quad (2)$$

where  $P_{\text{peak}}$  is the peak pressure, and  $U_{3 \text{ sec}}$  is the peak 3-s gust at the top of the building.

In large-scale wind tunnel testing, the dimension limitations of the test section usually compromise the ability of obtaining a large enough turbulence integral scale inside the wind tunnels. Hence, the turbulence intensity in the experiments will be lower than that of ABL which contains full spectrum of the turbulence. Since the large turbulence eddies fluctuate at lower frequencies, also a shortage at the low-frequency content of the turbulence is observed in a power spectrum comparison between the simulated and full-scale flow. As the model scale (1:180) used was not too large, the amount of missing low-frequency turbulence content was not considerable (Figures 2a and 2b). However, this can affect the obtained peak pressures from the experiments and to incorporate the effect of missing low- frequency turbulence in the peak estimation process, the method of Partial Turbulence Simulation (PTS) was used [24, 25, 26]. This method assumes that the turbulence can be divided into two distinct statistical processes; one at high frequencies and one at low frequencies. The high frequency part of the turbulence can be correctly simulated in wind tunnels and the low frequency part of the turbulence can be treated using

the quasi-steady assumptions. The joint probability of load from these two distinct processes is then derived, with the high frequency part coming from the wind tunnel data and the low frequency part coming from the Gaussian behavior of the missing low frequency component.

In the current experiments, the model scale was 1:180. The mean wind speeds, turbulence intensities, and the integral scales are given in Table 2. A summary of the steps followed, based on the PTS methodology is given below [25].

1. The intensity of the missing low frequency turbulence is calculated using Equation 3:

$$I_L = (I^2 - I_H^2)^{1/2} \quad (3)$$

where  $I$  is the turbulence intensity at full-scale and  $I_H$  is the turbulence intensity measured in the PTS.

2. Equation 4 is used to estimate the full-scale gust due to the missing low frequency turbulence:

$$U_{LP} = U_P(1 + 3.4I_L) \quad (4)$$

where  $U_P$  is the full-scale mean wind speed.

3. The velocity scaling was set such that the mean speeds at relevant floor heights in the tests (using PTS) correspond to the low frequency gust speeds at each height calculated using Equation 4.
4. The pressure coefficients represent the most probable peak which has almost 37% probability of non-exceedance in the selected full sample period.

The input parameters needed for the PTS are provided in Table 2.

Table 2 – Parameters considered for the analysis

Characteristics	Full-Scale	1:180 model scale
Turbulence intensity	0.19	0.154
Integral length scale	275.5 m	0.4 m
Reference height	56 m	0.311 m
Mean wind speed	73.5 m/s	18.29 m/s
Test duration	60 min	1 min

The net pressure coefficient for the balcony handrail panel is the delta between the external and the internal pressure coefficients as defined in Equation 5. The outward force on the panel is considered negative and the inward force is considered as positive.

$$C_{p_{net}} = C_{p_{external}} - C_{p_{internal}} \quad (5)$$

## 4.5 Results and Discussion

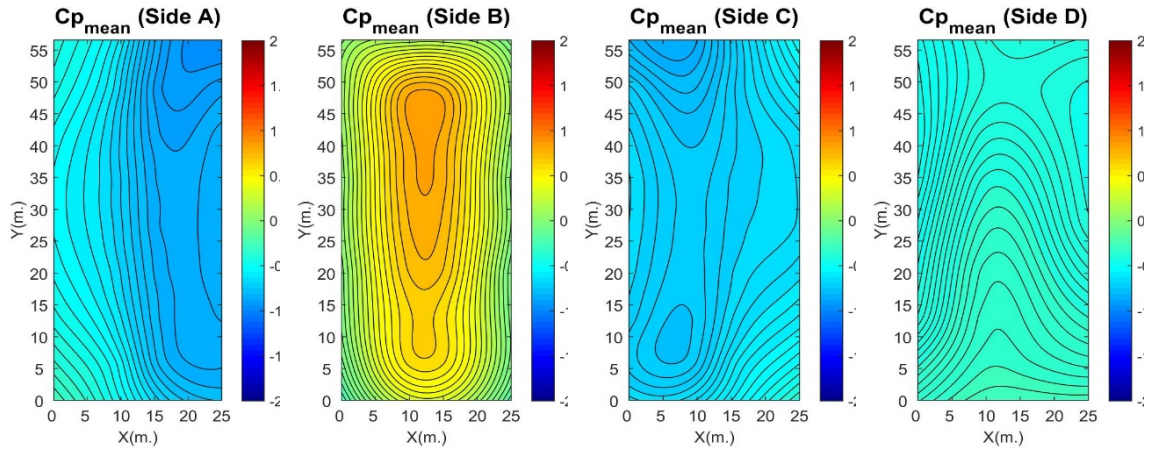
### 4.5.1 Mean Pressure Coefficients on Building Walls

Figure 6 and Figure 7 show the surface contour plots of the mean pressure coefficients ( $C_{p_{mean}}$ ) for the buildings with and without balconies for 0 degrees and 45 degrees wind directions, respectively. From these contours, it is seen that the balcony handrail systems alter the pressure distribution. For example, for the front wall (Side B), higher positive pressure coefficients were generally observed for the building with balconies. The difference in results is dependent upon the wind direction with the highest difference observed for 0 degrees wind direction.

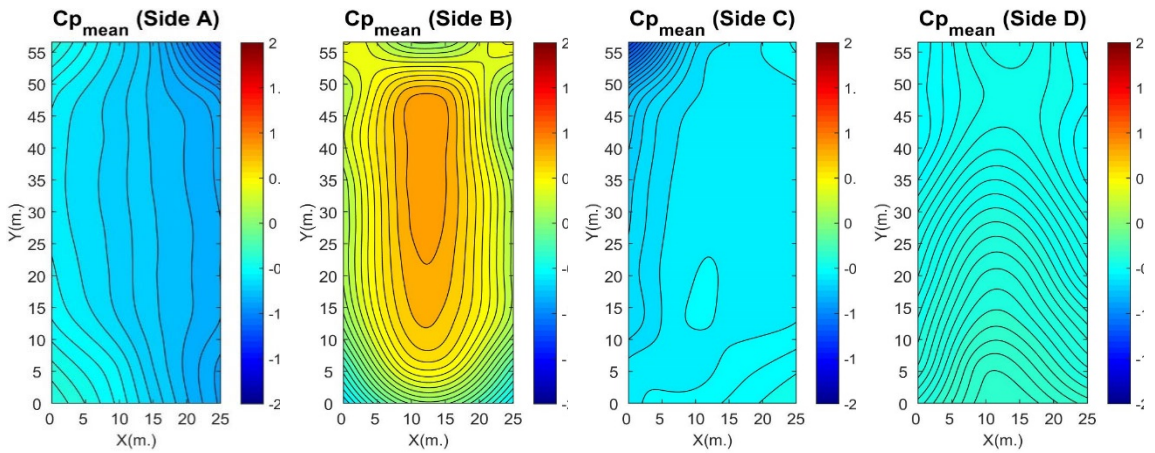
In Figure 6, the building with balconies shows primarily higher positive  $C_{p_{mean}}$  values at 0 degrees wind direction compared to the building without balconies in the top corners of the building. The highest increase in the positive  $C_{p_{mean}}$  due to balconies is 0.50 on the top corners of Side B ( $C_{p_{mean}}$  of 0 in both top corners for building without balconies versus a  $C_{p_{mean}}$  of 0.50 in both top corners for building with balconies). Additionally, for 0 degrees wind direction, the building without balconies on Side C shows

higher negative  $C_{p\ mean}$  values compared to the building with balconies across the building height except in the left corner of Side C (top floor). The largest decrease of the negative  $C_{p\ mean}$  in Side C due to balconies is 0.18 at the bottom center of the wall ( $C_{p\ mean}$  of -0.74 in the bottom center for the wall without balconies versus a  $C_{p\ mean}$  of -0.55 for the building with balconies at the same location).

In Figure 7, for the 45 degrees wind direction, the largest positive  $C_{p\ mean}$  is 0.68 in both buildings with and without balconies on Side B. The building with balconies shows the largest positive  $C_{p\ mean}$  (0.68) in the 9<sup>th</sup> floor on the right edge of Side B. For the building without balconies, the largest positive  $C_{p\ mean}$  (0.68) is observed at the 12<sup>th</sup> floor on the right edge of Side B. The largest increase in the positive  $C_{p\ mean}$  is 0.28 which is observed in the 15<sup>th</sup> floor right corner of Side B (i.e.  $C_{p\ mean}$  of 0.23 for building without balconies versus a  $C_{p\ mean}$  of 0.51 for building with balconies). For 45 degrees wind direction, Side D has the largest negative  $C_{p\ mean}$  in the 12<sup>th</sup> floor for both the building with and without balconies (i.e.  $C_{p\ mean}$  of -0.61 in the 12<sup>th</sup> floor right edge of the building without balconies versus a  $C_{p\ mean}$  of -0.55 for building with balconies in the same location). The building without balconies on Side D shows slightly larger negative  $C_{p\ mean}$  values compared to the building with balconies along the building height.

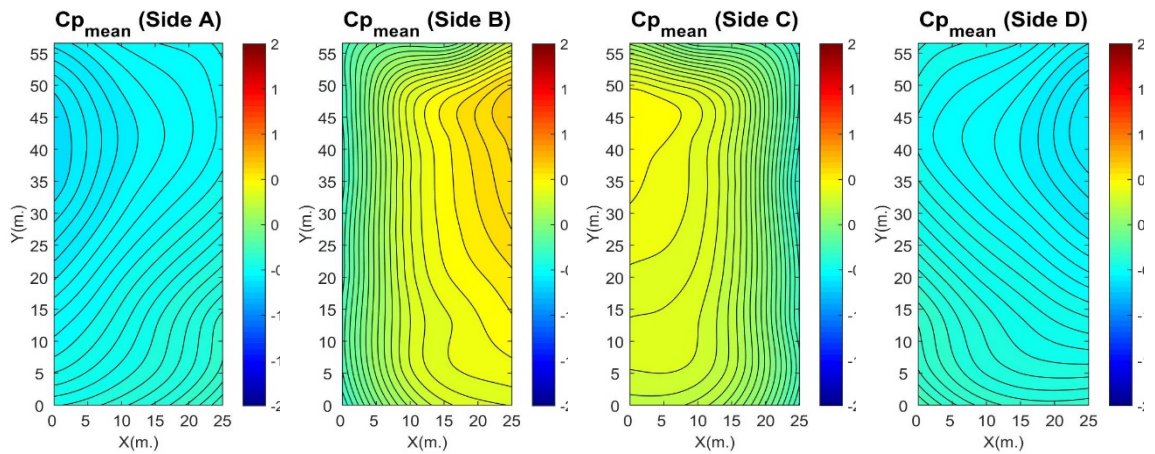


No Balconies



With Balconies

Figure 6 – Mean pressure coefficients for wind direction 0 degrees



No Balconies

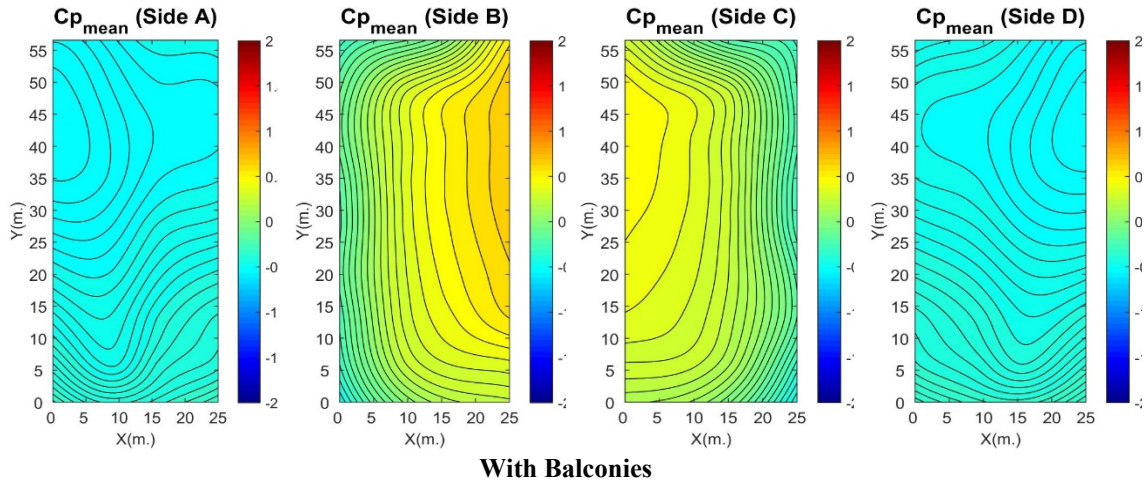


Figure 7 – Mean pressure coefficients for wind direction 45 degrees

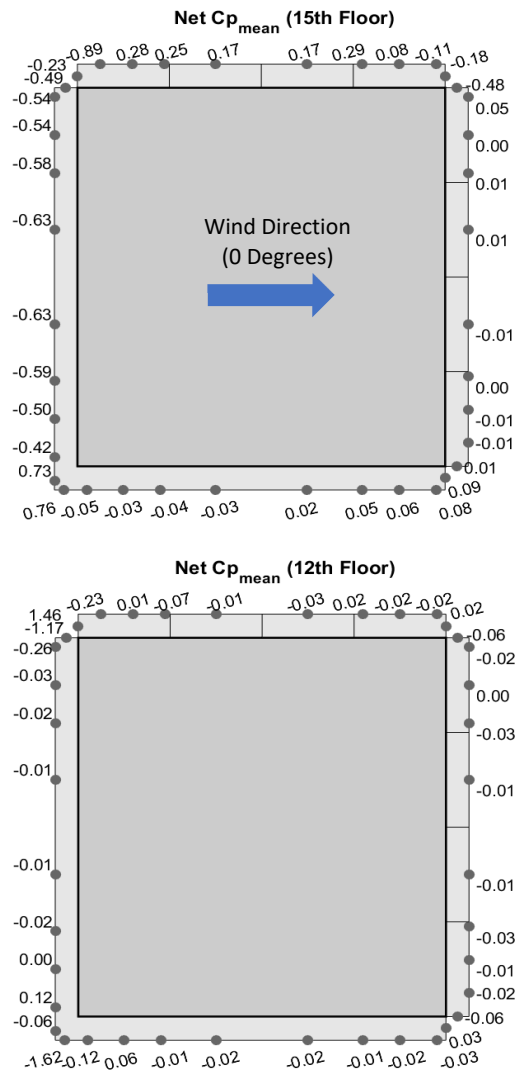
#### 4.5.2 Mean Pressure Coefficients on Balcony Handrail Panels

Figure 8 presents net values of the mean pressure coefficients ( $Net C_{p_{mean}}$ ) on balconies' vertical panels (representing the glass panels in the full-scale balcony handrail systems) for 0 degrees wind direction. Except for the windward facing balconies and parts of the discontinuous balconies on Side A (refer to Figure 3) on the 15<sup>th</sup> floor, significant pressure equalization was observed which resulted in very low net loads for most of the balconies. Higher net pressure coefficients were obtained on the handrail panels on the 15<sup>th</sup> floor, showing that close to the top of the building the windward balconies and parts of the discontinuous balconies on Side A did not have the advantage of pressure equalization to help reducing wind loads. Another important observation was that the pressure equalization was not effective for the corner balconies. Net  $C_{p_{mean}}$  values, as high as -1.62 and 1.46, were noted for the corner balconies.

Figure 9 shows  $Net C_{p_{mean}}$  for 45 degrees wind direction. Similar to the results obtained for 0 degrees wind direction, higher net mean pressure coefficients were observed

on the 15<sup>th</sup> floor handrail panels compared to lower floors, with Net  $C_{p\ mean}$  values up to -0.73 and 0.34 on the corners of the continuous balcony handrail panels. The 12<sup>th</sup> and 9<sup>th</sup> floors have Net  $C_{p\ mean}$  values close to zero due to the significant pressure equalization in most locations except for the corners where generally negative net pressure coefficients as high as -1.21 were observed.

Figures 8 and 9 show the plan view of the building and its balconies.





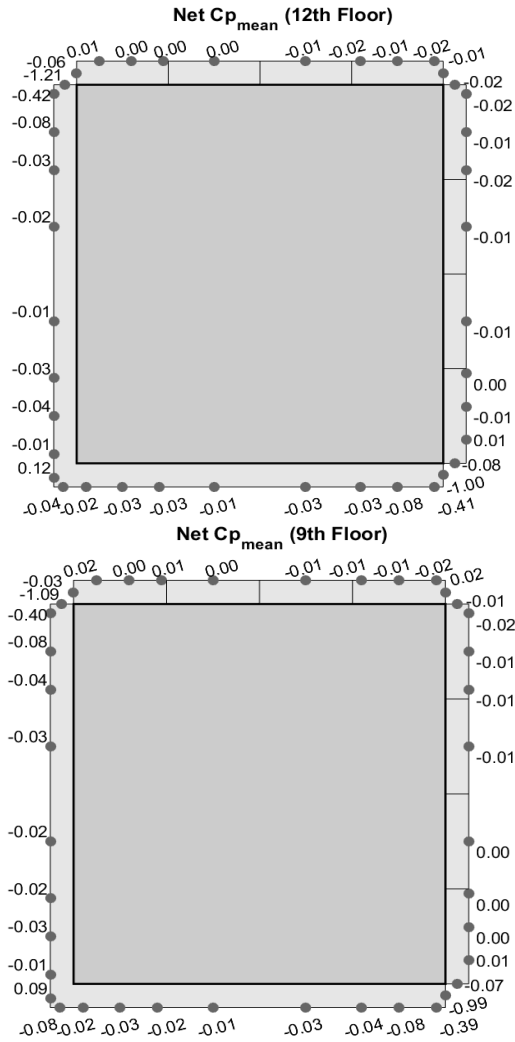


Figure 9 – Net mean pressure coefficients on the balconies for 45 degrees wind direction

#### 4.5.3 Peak Pressure Coefficients on Building Walls

Figures 10 to 13 show the surface plots of the peak pressure coefficients ( $C_{p \text{ peak}}$ ) for the building models with and without balconies at 0, 45, and 90 degrees wind directions. It is shown that the balconies affect the pressure distribution on the building walls.

Figure 10 presents the maximum peak pressure coefficients at 0 degrees wind direction. On the 15<sup>th</sup> floor, the maximum peak pressure coefficients of the building walls with continuous balconies are higher by 0.50 compared to the building walls without

balconies (e.g. at the 15<sup>th</sup> floor, the maximum  $C_{p\ peak}$  is 1.10 for the building walls with balconies whereas the maximum  $C_{p\ peak}$  is 0.60 for the building walls without balconies). Comparing Figures 10b and 10c, it is found that the walls with continuous and discontinuous balconies have generally similar values across the wall with differences in  $C_{p\ peak}$  values from 0.01 to 0.10. The biggest difference in magnitude is observed at the top floor where the maximum  $C_{p\ peak}$  for the wall with continuous balconies is 1.09, which is higher than the maximum  $C_{p\ peak}$  of 0.86 for the middle of the wall with discontinuous balconies.

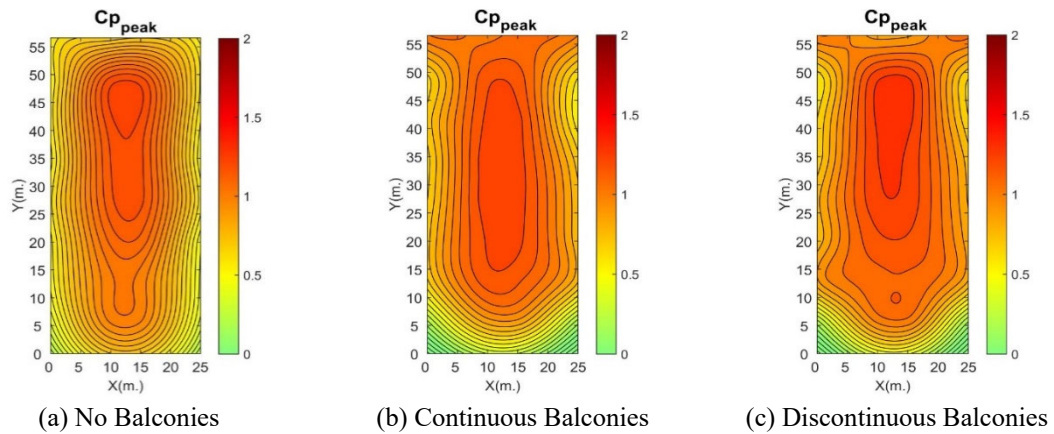


Figure 10 – Maximum peak pressure coefficients for wind direction 0 degrees

Figure 11 shows the maximum peak pressure coefficients at 45 degrees wind direction. Figure 11a and Figure 11b have generally similar maximum peak pressure coefficients except on the 15<sup>th</sup> floor. For example, on the 15<sup>th</sup> floor in the top middle of the wall away from the edges, the maximum  $C_{p\ peak}$  is 0.70 for the building walls with continuous balconies, whereas the maximum  $C_{p\ peak}$  is 0.00 for the building walls without balconies at the same location. Comparing Figures 11b and 11c, it is found that the walls with continuous and discontinuous balconies have generally similar values across the wall

height; the biggest difference is found at the top floor. For example, in the 15<sup>th</sup> floor at the middle of the wall away from the edges, the maximum  $C_{p\ peak}$  is 0.70 at the wall with continuous balconies versus the maximum  $C_{p\ peak}$  of 1.02 for the walls with discontinuous balconies in the same location.

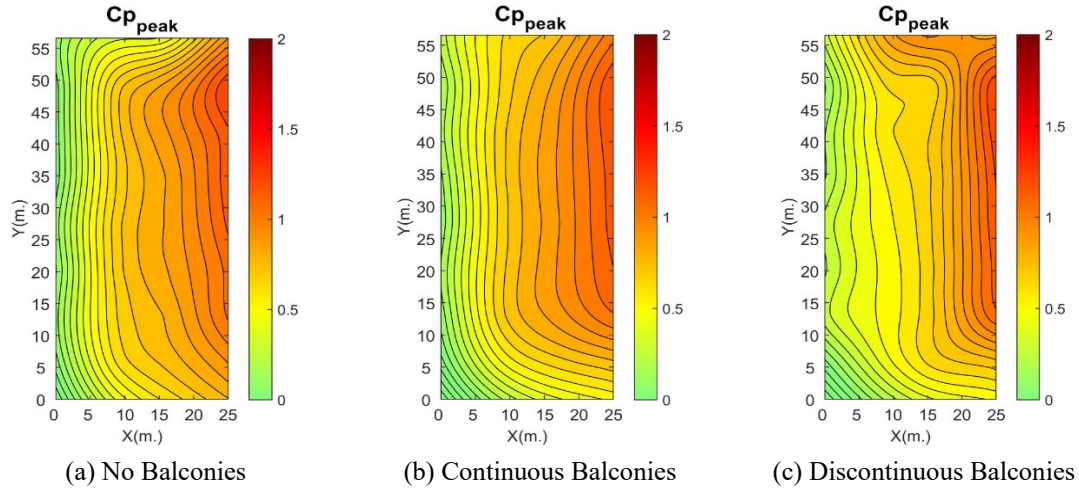


Figure 11 – Maximum peak pressure coefficients for 45 degrees wind direction

Figure 12 shows the minimum peak pressure coefficients at 45 degrees wind direction. The magnitudes of the minimum peak pressure coefficients have higher values for the building walls without balconies compared to the building walls with balconies across the wall height. Overall, balconies help reduce the external minimum peak pressure coefficients of the building, with the biggest reduction in the bottom of the building. For example, the minimum  $C_{p\ peak}$  at 45 degrees wind direction is -0.01 for the building walls with continuous balconies in the bottom middle of the building wall, while the minimum  $C_{p\ peak}$  is -0.68 for the building walls without balconies at the same location. Comparing Figures 12b and 12c, it is found that the walls with discontinuous balconies have higher values than the continuous balconies from the bottom middle wall to the 12<sup>th</sup> floor middle

wall, with an average difference of 0.25 in results. For example, in the bottom middle wall, the continuous balconies have a minimum  $C_{p\ peak}$  of -0.01 versus a minimum  $C_{p\ peak}$  of -0.28 for the discontinuous balconies at the same location.

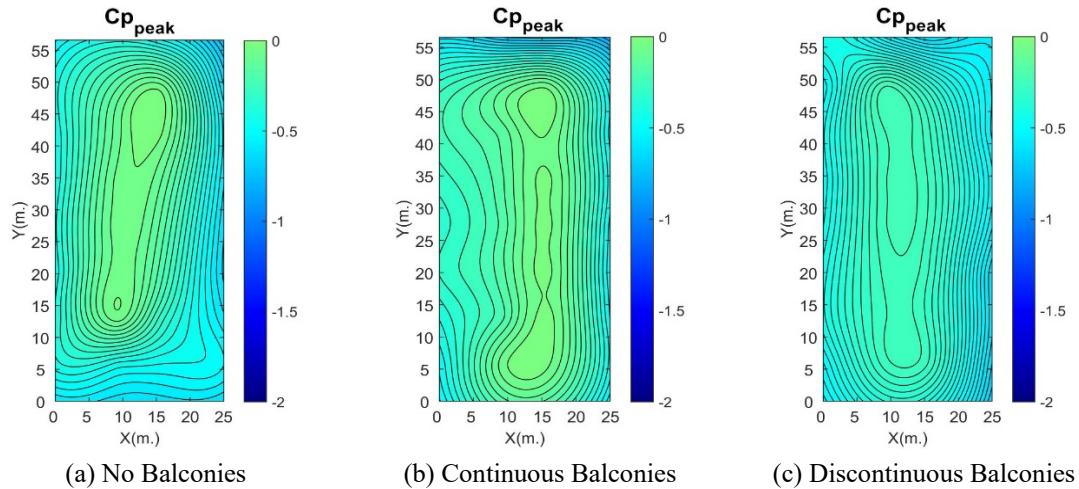


Figure 12 – Minimum peak pressure coefficients for 45 degrees wind direction

Figure 13 shows the minimum peak pressure coefficients at 90 degrees wind direction. The magnitudes of the minimum peak pressure coefficients have higher values for the building without balconies compared to the building walls with balconies across the height of the building. Overall, balconies help reduce the external minimum peak pressure coefficients for the building walls, with the biggest reduction from the 1<sup>st</sup> to the 12<sup>th</sup> floors. For example, in the 12<sup>th</sup> floor left edge of the building, the minimum  $C_{p\ peak}$  is -1.14 for the building walls with continuous balconies, while the minimum  $C_{p\ peak}$  is -1.93 for the building walls without balconies at the same location. Comparing the building walls with balconies in Figures 13b and 13c, it is found that the walls with discontinuous balconies have a higher magnitude of minimum peak pressures compared to the walls with

continuous balconies across the building height, especially in the middle wall of the building. For example, the minimum  $C_{p\ peak}$  is -1.29 at the 9<sup>th</sup> floor middle of the wall with discontinuous balconies, while the minimum  $C_{p\ peak}$  is -0.98 for the wall with continuous balconies at the same location.

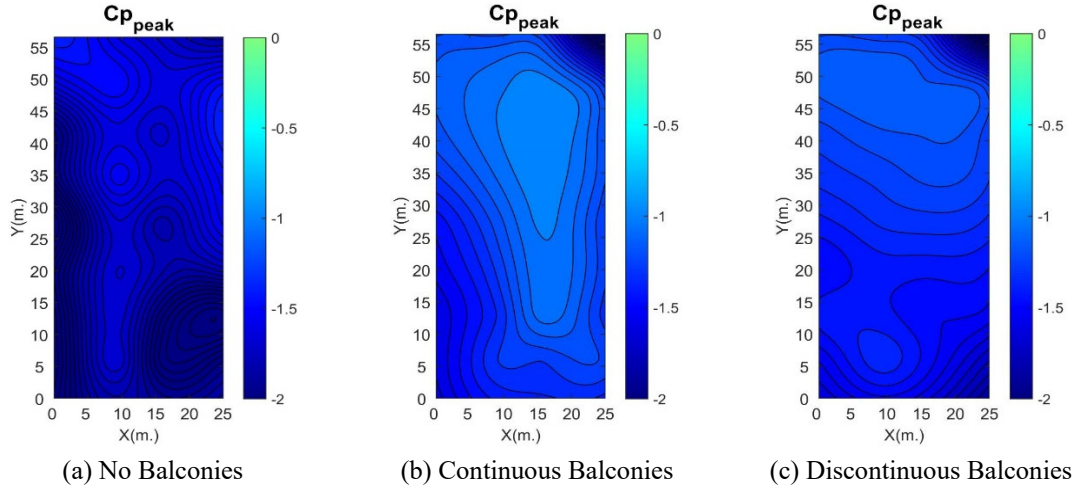


Figure 13 – Minimum peak pressure coefficients for 90 degrees wind direction

Figure 14 and Figure 15 show the maximum and minimum peak pressure coefficients, respectively, on the building walls by using the largest values (in magnitude) based on all wind directions tested. In other words, each value in the plots corresponds to the worst wind direction case. Comparing Figures 14a and 14b, it is seen that continuous balconies affect the pressure distribution on building walls with the biggest impact at the top and bottom floors. In the top floor (15<sup>th</sup> floor), continuous balconies increase the external maximum  $C_{p\ peak}$  of the building by an average increase of 0.40. For example, in the left corner of the 15<sup>th</sup> floor, the maximum  $C_{p\ peak}$  for the building with continuous balconies is 1.11 versus a maximum  $C_{p\ peak}$  of 0.58 for the building walls without balconies at the same location. In the 9<sup>th</sup> and 12<sup>th</sup> floors, the continuous balcony impact is minimal.

For example, on the 9<sup>th</sup> floor middle of the wall, the maximum  $C_{p\ peak}$  is 1.30 for the building walls with continuous balconies versus a maximum  $C_{p\ peak}$  of 1.26 for the building walls without balconies at the same location. In the bottom floor, continuous balconies decrease the external maximum  $C_{p\ peak}$  of the building with an average decrease of 0.13. For example, in the bottom left corner of the building, the maximum  $C_{p\ peak}$  for the building with continuous balconies is 0.30 versus a maximum  $C_{p\ peak}$  of 0.48 for the building walls without balconies at the same location.

Comparing the building walls with balconies in Figures 14b and 14c, it is found that the walls with continuous and discontinuous balconies have generally similar values for maximum peak pressure coefficient except on the top floor. On the top floor right corner of the walls with discontinuous balconies, maximum  $C_{p\ peak}$  is 1.35, which is higher than the walls with continuous balconies (maximum  $C_{p\ peak}$  of 1.23) at the same location. On the 9<sup>th</sup> and 12<sup>th</sup> floors, the maximum  $C_{p\ peak}$  values are very similar. For example, in the 9<sup>th</sup> floor right edge of the building walls with continuous balconies, the maximum  $C_{p\ peak}$  is 1.27, which is close to the discontinuous balconies result (maximum  $C_{p\ peak}$  of 1.29) at the same location. On the 9<sup>th</sup> floor left edge of the walls with discontinuous balconies, the maximum  $C_{p\ peak}$  is 0.74 which is close to the continuous balconies value (maximum  $C_{p\ peak}$  of 0.72) at the same location.

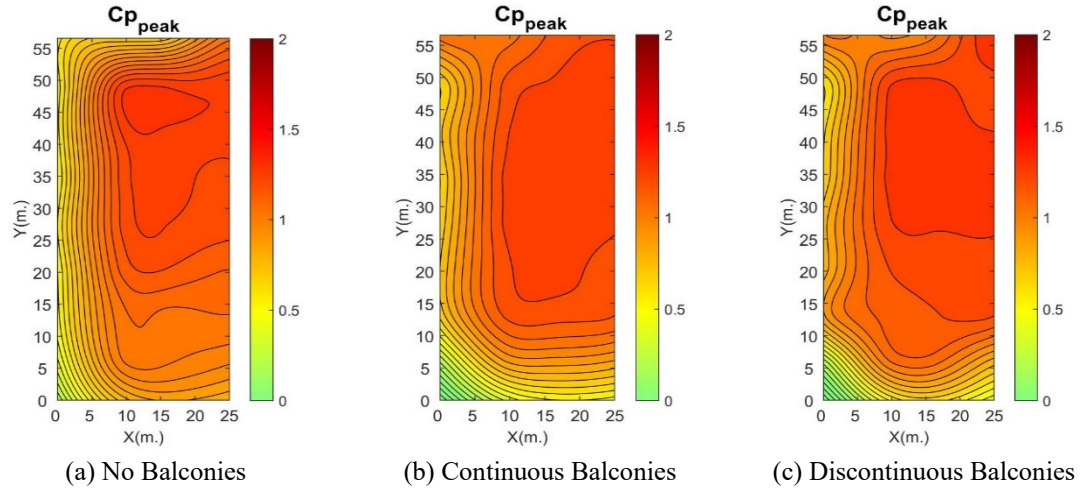


Figure 14 – Envelope of maximum peak pressure coefficients among all wind directions.

Figure 15 shows the envelope of the minimum peak pressure coefficients among all wind directions. The magnitudes of the minimum  $C_{p\ peak}$  for the building without balconies have higher values compared to the building walls with balconies across the height of the building. Balconies help reduce (in magnitude) the external minimum peak pressure coefficients for the building in all floors. Comparing Figures 15a and 15b, it is seen that continuous balconies decrease the pressure distribution on building walls throughout the building height by a decrease ranging from -0.2 to -0.9 (delta). The biggest impact of continuous balconies is from 1<sup>st</sup> to the 12<sup>th</sup> floors. For example, at the 3<sup>rd</sup> floor right edge side, the minimum  $C_{p\ peak}$  is -1.11 for building with continuous balconies versus a minimum  $C_{p\ peak}$  of -2.03 for the control case at the same location. Similarly, on the 12<sup>th</sup> floor right edge of the wall, the minimum  $C_{p\ peak}$  is -0.98 for building with continuous balconies versus a minimum  $C_{p\ peak}$  of -1.74 for the building without balconies at the same location.

Comparing the building walls with balconies in Figures 15b and 15c, it is found that walls with discontinuous balconies have generally higher magnitude results than the

building with continuous balconies across the building with the biggest magnitude difference at the bottom of the building. For example, at the bottom right corner of the building, the minimum  $C_{p\ peak}$  is -1.69 for building with discontinuous balconies versus a minimum  $C_{p\ peak}$  of -1.24 for continuous balconies at the same location. Another example is at the 12<sup>th</sup> floor middle of the wall where the minimum  $C_{p\ peak}$  is -1.20 for building with discontinuous balconies versus a minimum  $C_{p\ peak}$  of -0.94 for continuous balconies at the same location.

Please refer to the next page for Figures 15a, 15b, and 15c for the envelope of the minimum peak pressure coefficients among all wind directions for cases of no balconies, continuous balconies, and discontinuous balconies, respectively.

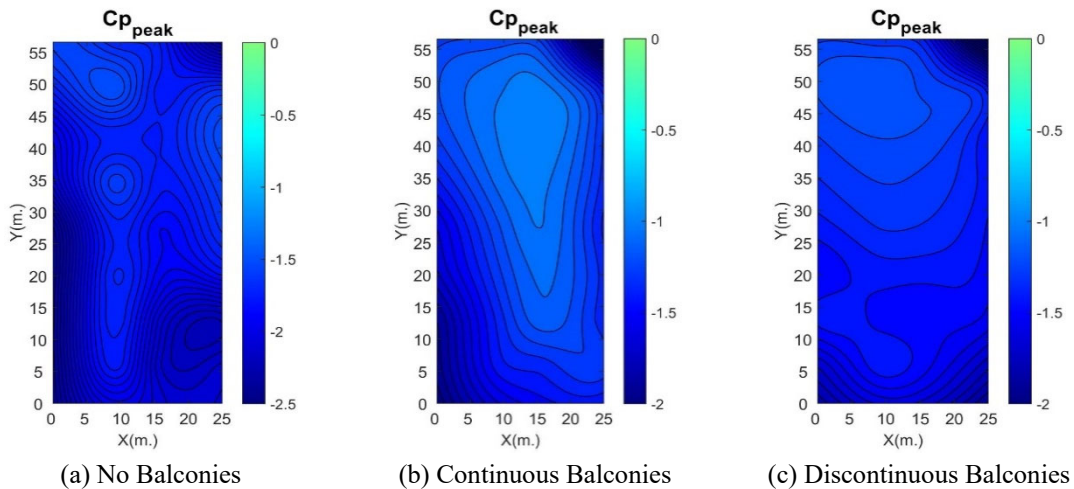


Figure 15 – Envelope of the minimum peak pressure coefficients among all wind directions

#### 4.5.4 Peak Pressure Coefficients on Balcony Handrail Panels

Figure 16 shows the envelope of the minimum and maximum peak net pressure coefficients (Net  $C_{p\ max}$  and Net  $C_{p\ min}$ ) on the balcony handrail panels at the 15<sup>th</sup>, 12<sup>th</sup>, and 9<sup>th</sup> floors by using the largest values (in magnitude) based on all wind directions tested.

Lower floor balcony handrail panels (12<sup>th</sup> and 9<sup>th</sup> floors) show relatively lower net pressures compared to the 15<sup>th</sup> floor balcony handrail panels due to pressure equalization effects. For the 15<sup>th</sup> floor, the effect of pressure equalization is relatively less. For the continuous balconies of 12<sup>th</sup> and 9<sup>th</sup> floors, Net  $C_{p\ max}$  values were in the range of 0.15 to 0.42 at the interior panels, 0.33 to 0.87 near the corners and up to 2.15 at the corners. For discontinuous balconies, slightly higher values are observed, with values up to 2.40 at the corners. For the 15<sup>th</sup> floor continuous balconies, the Net  $C_{p\ max}$  values are in the range of 0.73 to 1.38 at the interior panels, and from 1.08 to 1.81 near the corners. For discontinuous balconies, values ranging from 0.41 to 1.42 are observed at the interior panels, and values from 0.69 to 1.68 are found at the corners.

For the Net  $C_{p\ min}$ , it is also observed that lower floor balcony handrail panels (12<sup>th</sup> and 9<sup>th</sup> floors) show lower (in magnitude) net pressures compared to the 15<sup>th</sup> floor balcony handrail panels due to the pressure equalization effects. For the continuous balconies of 12<sup>th</sup> and 9<sup>th</sup> floors, the Net  $C_{p\ min}$  values are in the range of -0.29 to -0.46 at the interior panels and -0.79 to -2.52 at the corners. For discontinuous balconies, smaller values (in magnitude) are seen near corners compared to the continuous balconies with values ranging from -0.52 to -1.76 at the corners. The 15<sup>th</sup> floor continuous balconies show Net  $C_{p\ min}$  values ranging from -0.95 to -1.09 at the interior panels and -1.03 to -2.17 near the corners. The 15<sup>th</sup> floor discontinuous balconies show values ranging from -0.34 to -1.17 at the interior panels and values ranging from -0.69 to -1.15 at the corners.

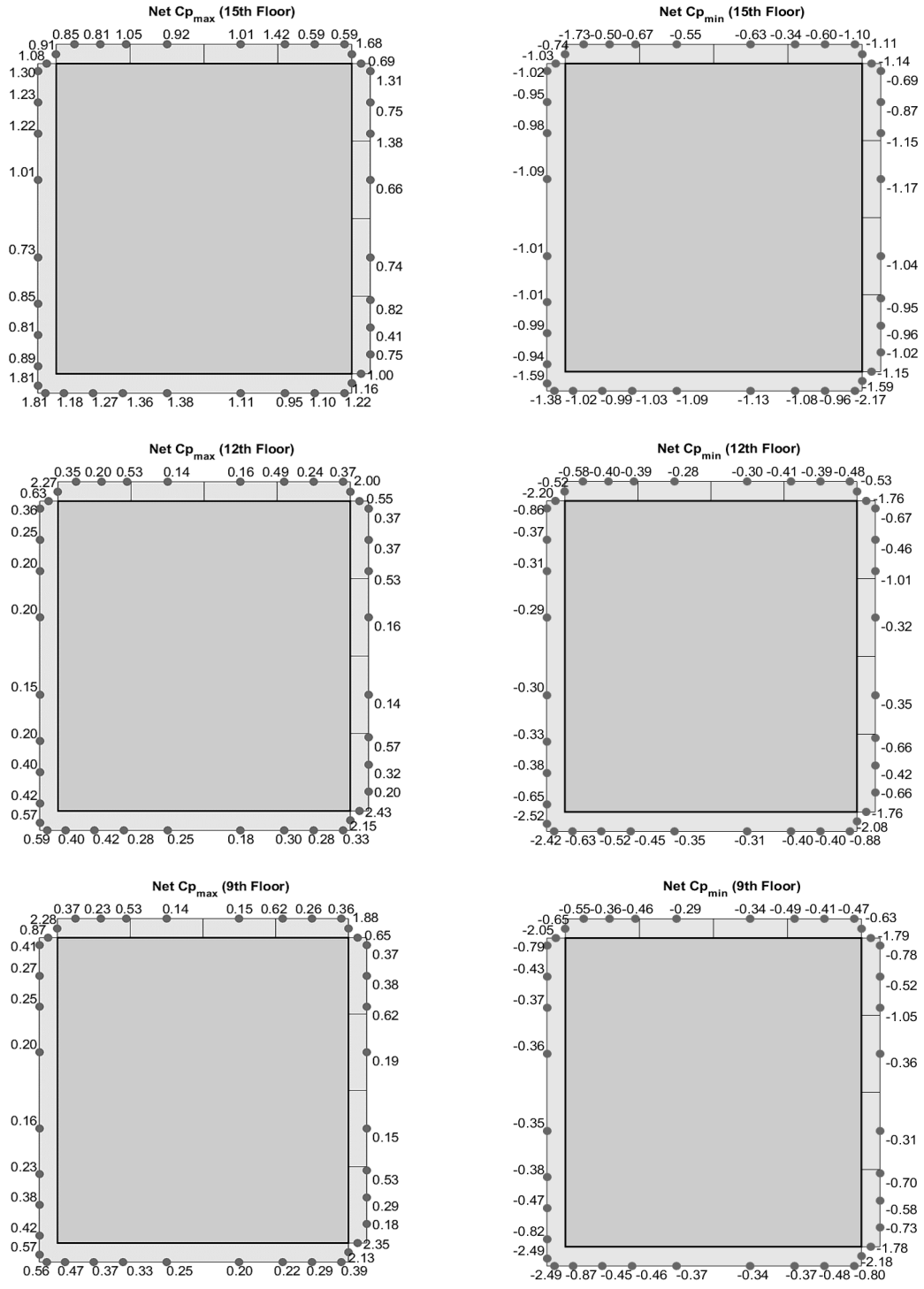


Figure 16 – Envelope of peak pressure coefficients on the balconies among all wind directions (figure shows the plan view of the building and the balconies)

#### 4.5.5 Comparison with Codes and Standards

Building codes and standards such as the American Society of Civil Engineers (ASCE 7-16) do not provide information on the balconies' impact on building cladding or structural wind loads. Therefore, if and how to include the effect of balconies on wind load calculations is decided based on the interpretation of the engineer. Usually, the effects of balconies on the building wall pressures are ignored. In the previous sections of this paper, the effect of balconies on the wind loads on building walls was discussed. Additionally, ASCE 7-16 does not provide any provisions for the wind loads on the balcony handrail panels. Therefore, for designing the balcony handrail panels, different approaches are followed by designers which can affect the overall efficiency of the design. NBCC 2015 provides some provisions for wind loads on the balcony handrail panels. In this section, wind loads obtained on the balcony handrail panels from experiments are compared with the provisions provided in NBCC 2015 and the ASCE 7-16 external pressure coefficients provided for designing components and claddings on building walls which is the most common approach that designers use to approximate the design of balcony handrail panels.

#### Comparison with ASCE 7-16

ASCE 7-16 defines two zones on building walls. Zone 5 is the edge zone, and Zone 4 is the middle zone (Figure 17).

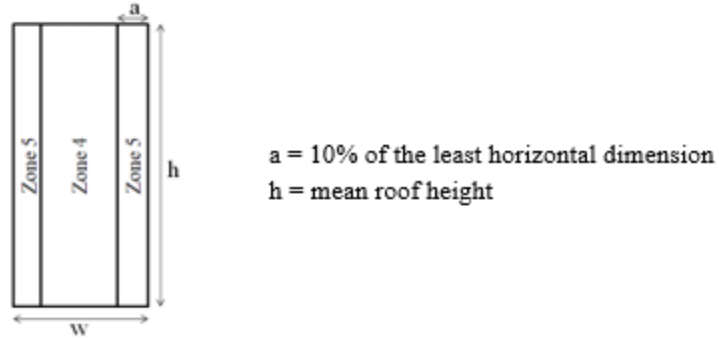


Figure 17 – Definition of Zone 4 and Zone 5 in ASCE 7-16

Table 3 shows the external pressure coefficients for components and claddings from ASCE 7-16 Figure 30.5-1 for different zones. These values are area averaged values within a zone. For ASCE, a  $10\text{ft}^2$  cladding area was considered.

Table 3 – External pressure coefficients from ASCE 7-16

Zone	Zone 4 (Middle Zone)	Zone 5 (Edge Zone)
Positive $C_p$	0.8	0.8
Negative $C_p$	-0.9	-1.6

The results from experiments are area averaged over zones as defined in Figure 18. On each side, Edge Zone I and Edge Zone II correspond to Zone 5 in ASCE 7-16, and Middle Zone I and Middle Zone II correspond to Zone 4 in ASCE 7-16.

Please refer to the next page for Figure 18 regarding the zones for area-averaging of pressures on the balconies.

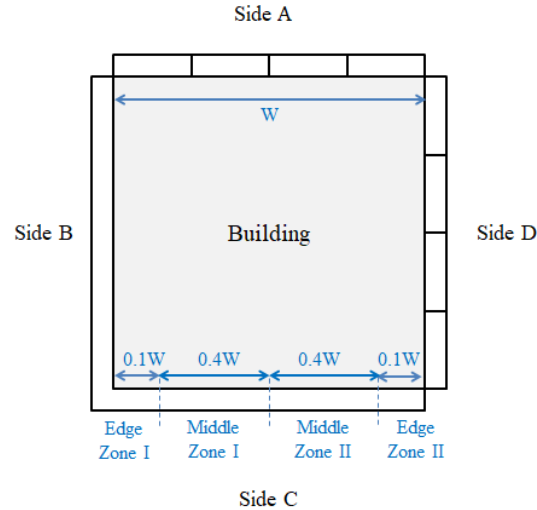


Figure 18 – Zones defined for area averaging of pressures on the balconies (figure shows the plan view of the building and balconies)

Table 4 shows the area averaged pressures on the balcony’s handrail panels from experiments on zones defined in Figure 18. Two different cases of continuous and discontinuous balconies are provided. For the continuous balconies, for each zone, the maximum of the values obtained for Sides B and C is reported. For the discontinuous balconies, for each zone, the maximum of the values obtained for Sides A and D is reported.

Table 4 – Area-averaged net maximum and minimum pressure coefficients on the balcony handrail panels from the envelope of all wind directions

Zone	Floor	Discontinuous Balconies		Continuous Balconies	
		Net $C_{p\max}$	Net $C_{p\min}$	Net $C_{p\max}$	Net $C_{p\min}$
Middle Zone I	15	0.78	-0.96	0.93	-1.02
	12	0.19	-0.34	0.17	-0.29
	9	0.17	-0.37	0.16	-0.34
Middle Zone II	15	0.76	-1.09	0.74	-1.06
	12	0.14	-0.33	0.13	-0.32
	9	0.17	-0.41	0.13	-0.34
Edge Zone I	15	0.75	-1.09	1.00	-0.97
	12	0.36	-0.67	0.36	-0.87
	9	0.36	-0.74	0.41	-1.09
Edge Zone II	15	1.29	-1.70	1.22	-2.19
	12	0.38	-0.69	0.36	-0.93
	9	0.37	-0.80	0.40	-1.05

The area averaged maximum pressure coefficients are lower on the 12<sup>th</sup> and 9<sup>th</sup> floors (in magnitude) compared to those observed on the 15<sup>th</sup> floor. For the continuous balconies on the 12<sup>th</sup> and 9<sup>th</sup> floors, the Net  $C_{p\max}$  values are in the range of 0.13 to 0.17 in the middle zone and 0.36 to 0.41 in the edge zone. For discontinuous balconies, values are relatively similar in the middle zone and 0.36 to 0.38 at the edge zone. For the 15<sup>th</sup> floor continuous balconies, the Net  $C_{p\max}$  values were in the range of 0.74 to 0.93 in the middle zone and 1.00 to 1.22 in the edge zone. For the 15<sup>th</sup> floor discontinuous balconies, most of the area averaged pressure coefficients are smaller compared to the continuous balconies at the middle zone (0.76 to 0.78) and edge zone (0.75 to 1.29). Results from the experiments show that the edge zone area averaged positive pressure coefficients on the 15<sup>th</sup> floor with discontinuous balconies are 60% higher than using ASCE 7-16 values in the edge zone. For the 15<sup>th</sup> floor with continuous balconies, the area average positive pressures are 52% higher in the edge zone than the ASCE 7-16 values.

For the Net  $C_{p\min}$ , it is also observed that lower floor balcony handrail panels (12<sup>th</sup> and 9<sup>th</sup> floors) show lower net pressures (in magnitude) compared to the 15<sup>th</sup> floor. For the continuous balconies of 12<sup>th</sup> and 9<sup>th</sup> floors, Net  $C_{p\min}$  values were in the range of -0.29 to -0.34 in the middle zone and -0.87 to -1.09 in the edge zone. For discontinuous balconies, smaller values compared to continuous balconies are seen in the edge zone with values ranging from -0.67 to -0.80 in the 12<sup>th</sup> and 9<sup>th</sup> floors. The 15<sup>th</sup> floor continuous balconies show Net  $C_{p\min}$  values ranging from -1.02 to -1.06 in the middle zones and -0.97 to -2.19 in the edge zones. The 15<sup>th</sup> floor continuous balconies have 29% higher results than the discontinuous balconies in the edge zones. The 15<sup>th</sup> floor discontinuous balconies have

similar values to the continuous balconies in the middle zones, and lower results compared to the continuous balconies in the edge zones ranging from -1.09 to -1.70. Results demonstrate that the area average negative pressure coefficients on the 15<sup>th</sup> floor discontinuous balconies are 6% higher than using ASCE 7-16 values in the edge zone. For continuous balconies on the 15<sup>th</sup> floor, area average negative pressure coefficients are 37% higher than using ASCE 7-16 values in the edge zone. These results show the wall pressures determined from the codes/standards should be used carefully for designing balconies since these do not report the accurate net pressures on the balconies handrail systems.

#### Comparison with NBCC 2015

NBCC 2015 section 4.1.7.5 (5) provides pressure coefficients for the design of balcony handrail panels. The value of  $C_p$  is provided as +/- 0.9 (corresponding to Middle zone I and II as defined in Figure 18) and the internal  $C_p$  should be taken as zero. For distances within either 0.1W and 0.1D (whichever is larger, with W and D being widths of the building) from the building corner (corresponding to Edge zone I and Edge zone II as defined in Figure 18),  $C_p$  shall be taken a +/- 1.2. Figure 19 and Figure 20 show net maximum and minimum pressure coefficients on the balconies from the envelope of all wind directions (for discontinuous and continuous balconies respectively) compared to the values proposed in NBCC. It can be seen that the pressure coefficients proposed by NBCC are generally conservative except for balconies located on the 15<sup>th</sup> floor which experience higher wind loads compared to the balconies on lower floors.

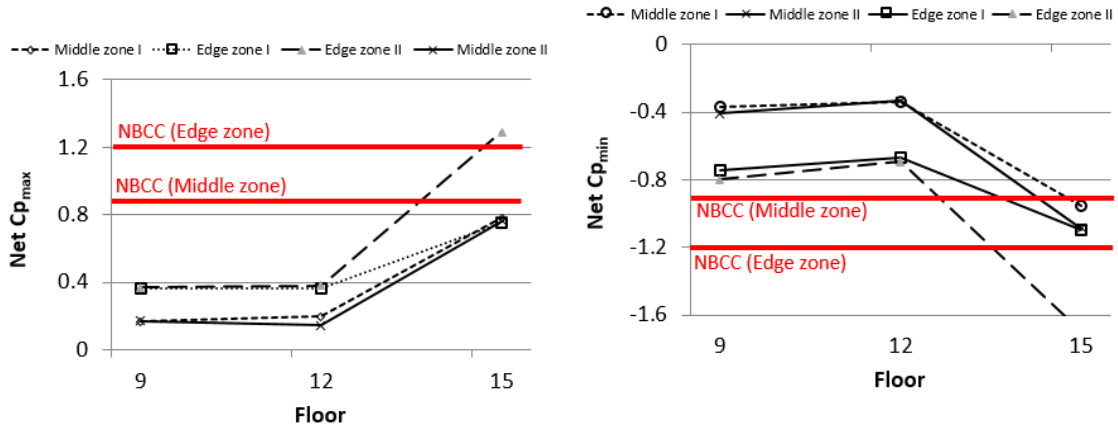


Figure 19 – Area-averaged net maximum and minimum pressure coefficients on the balconies’ handrail panels from the envelope of all wind directions; Discontinuous Balcony (Maximum of Sides A and D)

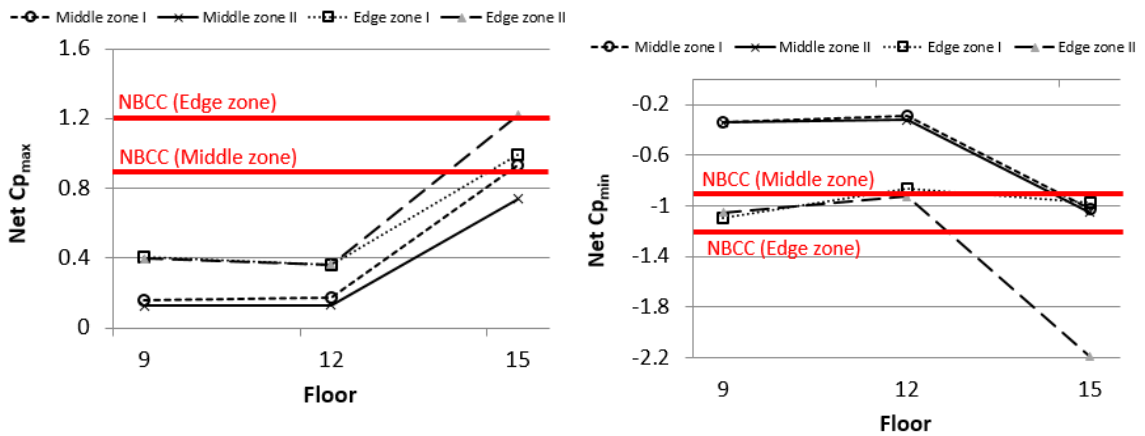


Figure 20 – Area-averaged net maximum and minimum pressure coefficients on the balconies’ handrail panels from the envelope of all wind directions; Continuous Balcony (Maximum of Sides B and C)

#### 4.6 Major Findings

Results of this research show that the pressure distributions along the building walls are impacted by the presence of the balcony handrail systems. For the envelope of results among all wind directions, the peak negative pressure coefficients (corresponding to suction on the walls) for the building with balconies are smaller (in magnitude) than the building without balconies. The balcony glass handrail systems studied in this paper are found to reduce peak suctions of up to 40% of the magnitude of the external peak negative pressure coefficients for the building walls. On another note, the existence of the balconies

does not significantly impact on the peak positive pressure coefficients (corresponding to positive pressure on the walls) except on the top of the building where higher peak positive pressure coefficients are seen for the case of building with balconies.

In absence of specific wind design guidelines, ASCE 7-16 external pressure coefficients for Components & Cladding (C&C) are sometimes used by designers to inform wind design of balcony handrail systems. Regarding the wind pressure on the balcony handrail vertical glass panels, the envelope of positive and negative net pressure coefficients among all wind directions obtained from the experiments, Net  $C_{p\ max}$  and Net  $C_{p\ min}$ , are summarized in Table 5 for the balconies on the top floor. It is noted that the area-averaged positive and negative pressure coefficients from the experiments show higher values (in magnitude) than those based on the C&C external pressure coefficients given by ASCE 7-16 for the Edge and Middle zones. Thus, special attention should be given for designing balcony handrail systems for edge zones.

Table 5 – C&C external pressure coefficients from ASCE 7-16 and the area-averaged net maximum and minimum pressure coefficients on the balcony handrail panels from the experiments

ASCE 7-16		Experiments (Building with Balconies)	
Middle Zone (Zone 4)	Edge Zone (Zone 5)	Middle Zone	Edge Zone
Positive $C_p$ : 0.8	Positive $C_p$ : 0.8	Worst area-averaged positive $C_p$ : 0.93	Worst area-averaged positive $C_p$ : 1.29
Negative $C_p$ : -0.9	Negative $C_p$ : -1.6	Worst area-averaged negative $C_p$ : -1.09	Worst area-averaged negative $C_p$ : -2.19

Similarly, in the NBCC comparison, it is seen that the pressure coefficients proposed by NBCC are not conservative for balconies located on the top floor which experiences higher wind loads compared to the balconies on lower floors.

From this study, it is concluded that the pressure equalization that affects the net pressures acting on vertical glass panels of handrail systems considerably vary depending on the floor location. Significant pressure equalization occurs across balcony handrail glass panels for most floors. However, pressure equalization is minimal across balcony handrail vertical glass panels on top floors. Therefore, using provisions of NBCC for wind design of balcony handrail systems may be appropriate for most floors except the top floors. The corner zone effects should be carefully considered for design because this study showed that the edge zones have net pressures higher than those for the middle zones (for both net inward and outward pressures on vertical panels). Future studies concerning the effect of distinct building configuration and balcony geometry on the wind loads on buildings and their balcony handrail systems are recommended.

#### **4.7 Acknowledgments**

We gratefully acknowledge the financial contributions of The State of Florida Division of Emergency Management and the National Science Foundation for supporting the NHERI Wall of Wind Experimental Facility (Award# 1520853) for this project. We appreciate the help received from Krishna Vutukuru in editing the paper.

#### **4.8 References**

- [1] ASCE 7-16, (2016). Minimum Design Loads for Buildings and Other Structures. American Society of Civil Engineers, ASCE, US.
- [2] NBCC, 2015. User's Guide-NBC 2015, Structural Commentaries (Part 4), National Research Council of Canada, Ottawa, Canada.
- [3] Letchford, C.W., and Mehta, K.C., (1993). The distribution and correlation of fluctuating pressure on the Texas Tech Building. Journal of Wind Engineering and Industrial Aerodynamics, 50, 225-234.

- [4] Kim, Y.C., Yoshida, A., Tamura, Y., (2012). Influence of upstream surrounding buildings on wind pressures acting on low-rise building. *Journal of Structural and Construction Engineering*, 77(680), 1485-1492.
- [5] Uematsu, Y., and Isyumov, N., (1999). Wind pressures acting on low-rise buildings. *Journal of Wind Engineering and Industrial Aerodynamics*, 82(1-3), 1-25.
- [4] Levitan, M.L., Mehta, K.C., Vann, W.P., Holmes, J.D., (1991). Field measurements of pressures on the Texas Tech building. *Journal of Wind Engineering and Industrial Aerodynamics*, Vol 38, 227-234.
- [5] Stathopoulos, T., Zhu, X., (1988). Wind pressures on building with appurtenances. *Journal of Wind Engineering and Industrial Aerodynamic*, 31, 265-81.
- [6] Chand, I., Bhargava, P.K., Krishak, N.L.V., (1998). Effect of balconies on ventilation inducing aeromotive force on low-rise buildings. *Building and Environment*, 33 (6), 385-396.
- [7] Cochran, L., Jon, P., (2000). Cladding Loads: The Influence of Balconies and Slab-Edge Storm Shutters. *Structures Congress 2000*, May 8-10, 2000, Pennsylvania, United States.
- [8] Rofail, A.W., Mans, C., (2003). Wind Loads on balustrades. *Windtech Consultants*.
- [9] AS/NZS 1170.2:2002, (2002). *Structural Design Actions, Part 2: Wind actions*. Standards Australia, Homebush.
- [10] BS 6399-1:1996, (2002). *Loading for buildings, Part 1: Code of practice for dead and imposed loads*. British Standards Institution, London.
- [11] *Building Construction Regulations*, (1991). Chapter 123B: Imposed loads, Department of Justice. Hong Kong.
- [12] Kotani, H., Yamanaka, T., (2007). Wind pressure coefficient and wind velocity along building wall of apartment building with balcony. 6th International Conference on Indoor Air Quality, Ventilation & Energy Conservation in Buildings IAQVEC 2007, Oct. 28 - 31 2007, Sendai, Japan.
- [13] Browne, M., Kumar, S., (2005). Effect of corner balconies on wind-induced response of tall buildings. 10th Americas Conference on Wind Engineering, Baton Rouge, Louisiana, USA.

- [14] Montazeri, H., Blocken, B., (2013). CFD simulation of wind-induced pressure coefficients on buildings with and without balconies: validation and sensitivity analysis. *Building and Environment*, 60, 137-149.
- [15] Kumar, A., Rahul, P. S. and Kumar, S., (2013). Performance Optimization of Tall Buildings Subjected To Wind—An Indian Scenario. *The Eighth Asia-Pacific Conference on Wind Engineering*, December 10–14, 2013, Chennai, India.
- [16] Morton, T. J., Mara, T. G., (2017). Effects of Balconies on the Wind Loading of a Tall Building. *AEI 2017: Resilience of the Integrated Building*, April 11–13, 2017, Oklahoma City, Oklahoma.
- [17] Chowdhury, A. G., Zisis, I., Irwin, P., Bitsuamlak, G., Pinelli, J., Hajra, B., and Moravej, M., (2017). Large-Scale Experimentation Using the 12-Fan Wall of Wind to Assess and Mitigate Hurricane Wind and Rain Impacts on Buildings and Infrastructure Systems. *Journal of Structural Engineering*, 143(7): 04017053.
- [18] Ludena, L, Asghari Mooneghi, M., Moravej, M., Chowdhury, A.G., Irwin, P., (2017). Estimation of Wind Loads on the Balcony Glass Handrails of Mid-Rise Buildings. *ASCE Structures Congress*, 2017.
- [19] Irwin, P., Cooper, K., Girard, R., (1979). Correction of distortion effects caused by tubing systems in measurements of fluctuating pressures. *Journal of Wind Engineering and Industrial Aerodynamics*, 5, 93–107.
- [20] ESDU, (1985). Characteristics of atmospheric turbulence near the ground, Part II: Single point data for strong winds (Neutral Atmosphere). *Engineering Sciences Data Unit Item 85020*, London UK.
- [21] Richards, P.J., Hoxey, R.P., Connell, B.D., Lander, D.P., (2007). Wind-tunnel modelling of the Silsoe Cube. *Journal of Wind Engineering and Industrial Aerodynamics*, 95, 1384-1399.
- [22] Asghari Mooneghi, M., Irwin, P., and Chowdhury, A.G., (2016). Partial turbulence simulation method for predicting peak wind loads on small structures and building appurtenances. *Journal of Wind Engineering and Industrial Aerodynamics*, 157, 47–62.
- [23] Asghari Mooneghi, M. (2014). *Experimental and Analytical Methodologies for Predicting Peak Loads on Building Envelopes and Roofing Systems*. FIU Electronic Theses and Dissertations. 1846. <https://digitalcommons.fiu.edu/etd/1846>.
- [24] Moravej, M. (2018). *Investigating Scale Effects on Analytical Methods of Predicting Peak Wind Loads on Buildings*. FIU Electronic Theses and Dissertations. 3799. <https://digitalcommons.fiu.edu/etd/3799>.

**CHAPTER V**  
**EXPERIMENTAL INVESTIGATION OF THE AERODYNAMICS OF**  
**BALCONIES AND SCALING EFFECTS**

## CHAPTER 5

### EXPERIMENTAL INVESTIGATION OF THE AERODYNAMICS OF BALCONIES AND SCALING EFFECTS

#### 5.1 Abstract

This work presents an experimental investigation of the wind loading on balcony handrail panels of a mid-rise building. The experiments were performed at the Wall of Wind (WOW), a large-scale hurricane testing facility at Florida International University. Experiments included pressure measurements on the balcony handrail panels at the 9<sup>th</sup>, 12<sup>th</sup>, and 15<sup>th</sup> floors. The aerodynamics of the balconies, Reynolds number effects, and the pressure tap resolution effects were investigated in this study. The results showed that the top floor balcony handrail panels tend to behave as a roof parapet. Also, results show that increasing the model scale enhances the accuracy of the net pressures. Furthermore, higher pressure equalization at the 9<sup>th</sup> and 12<sup>th</sup> floors, resulting in reduced net loading, were observed for all model scales. Also, results showed that increasing the model scale increased the net pressures on the panels. The resolution of the pressure taps was found to have significant influence on the test results. Too few taps can result in underestimation of the suction that can cause failure at the balcony corners. Net pressure coefficients obtained from pressure measurements across the handrail panels were compared to those based on ASCE 7-16 exterior pressure coefficients.

**Keywords:** Wind Loading, Pressure Coefficients, Component and Cladding, Balcony Handrail Systems, Wind Tunnel Testing, Wall of Wind, Reynolds Number Effects, Tap Resolution Effects.

## 5.2 Introduction

Balcony handrails are important elements of buildings regarding architecture, aesthetics, and safety. The unpredictability of wind forces imposes a major safety concern for the design of balconies, in particular in ensuring the safety of the occupants. Unfortunately, as of now, there is limited research on the aerodynamics and wind loading on buildings with balconies.

For large structures, such as tall buildings, wind tunnel tests have become the norm as they allow taking into account the effect of the building shape and surrounding terrain and other nearby structures. Wind tunnels testing of these large structures is typically done on models with scales in the range 1:200 to 1:500 [1]. At this range of scales, boundary layer wind tunnels can produce an adequate simulation of the turbulent planetary boundary layer, including the correct scaling of full range of eddy sizes and the integral length scales of turbulence. For smaller structures and for building components (i.e. balconies), the use of model scales of 1:200 to 1:500 becomes impractical. The models become too small for (i) adequate instrumentation and therefore resolution, (ii) modeling of the finer details that may affect the aerodynamics, and (iii) simulating high enough Reynolds number ( $Re$ ) to avoid scale effects that make the test results no longer fully representative of the full scale [1]. All these reasons support the need for large-scale testing as this impacts the accuracy of the test results.

Research on wind loading mechanism on balcony handrail systems in high-rise buildings and their effects on the wind loads on the building's façade has been limited. The balcony study of Montazeri and Blocken [2] using Computational Fluid Dynamics (CFD), states that balconies could cause significant changes to the wind pressure distribution on

windward walls, due to flow separation, recirculation, and reattachment generated by the presence of balconies. In addition, corner balconies could help reduce the crosswind response of tall buildings. This is mainly because they can act as general roughness and disrupt the formation of vortices shedding from the building. Morton and Mara [3] investigated the impact of balconies on the overall wind response of a building. Results of the wind tunnel testing showed that balconies located near a sharp-edged corner reduced the peak suctions experienced by the leeward wall. Also, results showed a minimal impact in the peak positive cladding pressure for the case of wind normal to the balconies.

Only few codes and standards address the design of balconies. In the Australian Building Code is proposed that balustrades in private residences should withstand the highest magnitude loading from either the wind loading or a uniform loading of  $1 \text{ kN/m}^2$  [4]. In the British Standard [5] and Hong Kong Building Regulations [6], it is proposed that balconies should be designed for wind loading if the 3-sec gust wind speed exceeds  $30 \text{ m/s}$ ; otherwise, they should be designed for a live load of  $1 \text{ kN/m}^2$ . Other major international codes and standards for wind loads such the International Building Code (IBC), the Florida Building Code (FBC), and the American Society of Civil Engineers (ASCE 7-16) do not provide information on the influence of balcony handrail systems on cladding or structural wind loads. Therefore, the design decision is up to the engineer's interpretation. This decision could be complicated for the cases where there are many balconies in line sheltering the building. Wind testing that fully captures the aerodynamics of flows over balconies provides information for designing safer and more reliable and safer balconies and façade elements.

This paper presents results from an experiment performed at the Wall of Wind (WOW) at Florida International University (FIU), on a fifteen-story building using 1:180, 1:67, and 1:25 scale models. The paper is comprised of the discussion of results of the wind loads on the balconies, Reynolds number effects, and tap resolution. The results of the peak net pressure coefficients are discussed in **Section 5.4.1**, and Reynolds number effects and taps resolution in Sections **5.4.5 and 5.4.6**, respectively.

### 5.3 Data Analysis

Results from the tests are shown as peak surface pressure coefficients which were obtained based on equations proposed by Richards et al. [7]. They suggested expressing the peak pressure coefficient as the ratio of the extreme surface pressures to the peak dynamic pressure, recorded during the tests. The peak pressure coefficient based on 3-second gust dynamic pressure is calculated as shown in Equation 1.

$$C_{p \text{ peak}} = \frac{P_{\text{peak}}}{\frac{1}{2}\rho U_{3 \text{ sec}}^2} \quad (1)$$

where  $P_{\text{peak}}$  is the peak pressure, and  $U_{3 \text{ sec}}$  is the peak 3-s gust at the balcony elevation.

The net pressure coefficient for the balcony handrail panel is the difference between the external and the internal pressure coefficients as defined in Equation 2. The outward force on the panel is considered negative, and an inward force is considered as positive.

$$C_{p_{\text{net}}} = C_{p_{\text{external}}} - C_{p_{\text{internal}}} \quad (2)$$

The methodology used for this study has been described in Chapter II of this Dissertation. In Chapter II, the PTS approach proposed by author Asghari Mooneghi et al., 2015 [8, 9] is extended to include the PTS for cladding components (i.e., balconies) of tall buildings. The method requires a number of tests in a building and balconies at different

wind direction increments. The flow represented a partial turbulence simulation in which only the high frequency end of the turbulence spectrum was simulated and the low frequency fluctuations were missing.

The missing low frequency fluctuation are compensated using PTS which is applicable for the balcony handrail panels as the fluctuations in the high frequency turbulence intensity  $I_H$  will not be significant, and this brings up the possibility of using a single representative value of  $I_H$  for the level at which the component (i.e. balcony) is located. After measuring the load/pressure coefficients at this representative value of  $I_H$ , the missing low frequency fluctuations are compensated using the quasi-steady assumption, by doing PTS. Analysis of the results was undertaken using the proposed approach, and the results were compared among model scales as shown in the following sections.

## **5.4 Results and Discussion**

### ***5.4.1 Envelope External Pressure and Envelope Net Pressures Results***

#### ***Envelope External Pressures***

Figure 1a and 1b shows the maximum and minimum peak pressure coefficients, respectively, on the building walls by using the largest values (in magnitude) based on all wind directions tested. In other words, each value in the plots corresponds to the worst wind direction case.

Figure 1a shows that for the building without balconies, the envelope external maximum peak pressure coefficient on the building wall with highest magnitude is 1.55 occurring at the top right edge of the building. The 1:25 model is showing a max  $C_p = 1.55$  in the top right edge of the wall. Scale models 1:67 and 1:180 show values of maximum  $C_p = 1.47$  at the same location.

Figure 1b shows the highest magnitude of the envelope external minimum peak pressure coefficients in the building without balconies which occurs at the top corner of the building and at the bottom of the building. For the 1:25 model, the envelope minimum is  $C_p = -3.06$  at the top left corner compared to the minimum  $C_p = -2.97$  for scale 1:67 and minimum  $C_p = -1.95$  for scale 1:180 at the same location.

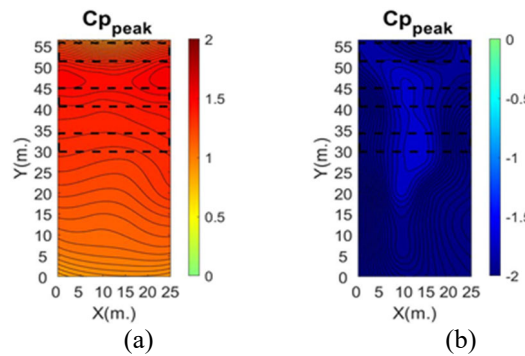


Figure 1 – External Maximum and Minimum Peak Pressures on the Building

### ***Envelope Net Pressures***

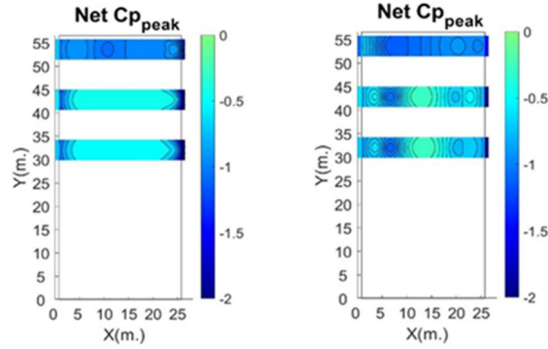
Figures 2A to 2C show the envelope of the minimum peak net pressure coefficients (Net  $C_{p_{min}}$ ) on the balcony handrail panels by using the largest magnitude value based on all wind directions tested.

Across Figures 2A to 2C, the 9<sup>th</sup> and 12<sup>th</sup> floors balcony handrail panels show relatively lower net pressures compared to the 15<sup>th</sup> floor balcony handrail panels (except in corners) due to pressure equalization effects. However, the 12<sup>th</sup> and 9<sup>th</sup> floor balcony handrail panels' corners show higher concentration of suctions in the corners compared to the 15<sup>th</sup> floor balconies.

For example, for continuous balconies, the highest magnitude of the minimum Net  $C_{p_{peak}}$  (Net  $C_{p_{min}}$ ) values at the 15<sup>th</sup> floor (non-corners) are significantly higher than the results of the 12<sup>th</sup> floor balcony handrails. For example, at the 15<sup>th</sup> floor continuous balcony handrail panels (non-corners), the Net  $C_{p_{min}}$  values are -1.28 for scale 1:25, -1.16 for scale 1:67, and -1.04 for scale 1:180 in the same location versus 12<sup>th</sup> floor (non-corners) Net  $C_{p_{min}}$  values of -0.37 for scale 1:25, -0.39 for scale 1:67, and -0.31 for scale 1:180 in the similar location at the 12<sup>th</sup> floor.

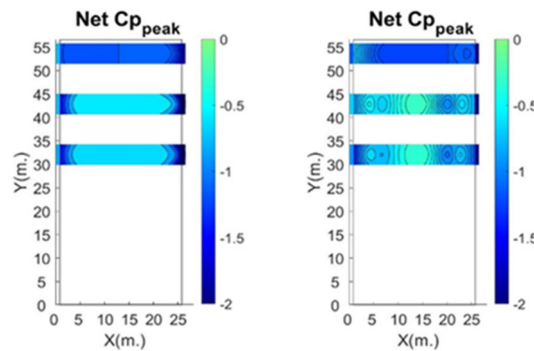
Furthermore, at the 9<sup>th</sup> floor continuous balcony handrail panels corners, the highest magnitude values of the minimum Net  $C_{p_{peak}}$  (Net  $C_{p_{min}}$ ) are observed at which envelope values are -6.25 for scale 1:25, -3.60 for scale 1:67, and -2.70 for scale 1:180 in the same corner location. Additionally, at the 9<sup>th</sup> floor discontinuous balconies, the highest magnitudes of the Net  $C_{p_{min}}$  observed at the balcony handrail panels corners are -3.85 for scale 1:25, -3.28 for scale 1:67, and -2.30 for scale 1:180 in the same corner location.

Overall, when comparing the envelope Net  $C_{p_{min}}$  on the balcony handrail panels with the envelope minimum peak pressure on the building exterior wall, it is seen that the net balconies suctions are higher than the external wall suctions of the base building.



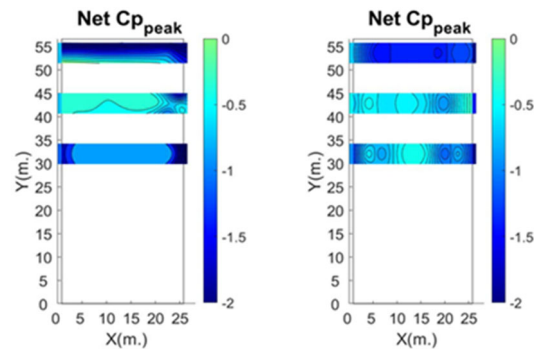
(1) Continuous Balconies (2) Discontinuous Balconies

Figure 2A – Envelope Net Min Peak Pressures ( $Net\ C_{p_{min}}$ ) – Scale 1:180



(1) Continuous Balconies (2) Discontinuous Balconies

Figure 2B – Envelope Net Min Peak Pressures ( $Net\ C_{p_{min}}$ ) – Scale 1:67



(1) Continuous Balconies (2) Discontinuous Balconies

Figure 2C – Envelope Net Min Peak Pressures ( $Net\ C_{p_{min}}$ ) – Scale 1:25

Figures 3A to 3C show the envelope of the maximum peak net pressure coefficients ( $Net\ C_{p_{max}}$ ) on the balcony handrail panels by using the largest magnitude value based on all wind directions tested.

Lower floor balcony handrail panels (9<sup>th</sup> and 12<sup>th</sup> floors) show relatively lower net pressures compared to the 15<sup>th</sup> floor balcony handrail panels (except in corners) due to pressure equalization effects. However, in the corners, the 12<sup>th</sup> and 9<sup>th</sup> floor balcony handrail panels show higher magnitude of Net  $C_{p_{max}}$  compared to the 15<sup>th</sup> floor balconies' corners.

For example, in the 12<sup>th</sup> floor continuous balcony handrail panels' corner, the envelope Net  $C_{p_{max}}$  values are 3.77 for scale 1:25, 2.62 for scale 1:67, and 2.53 for scale 1:180 in the same corner location at 12<sup>th</sup> floor. For discontinuous balconies, the envelope Net  $C_{p_{max}}$  values in the 12<sup>th</sup> floor balcony handrail panels' corner are 3.09 for scale 1:25, 2.47 for scale 1:67, and 2.24 for scale 1:180 in the same corner location.

Overall, comparing the envelope Net  $C_{p_{max}}$  on the balcony handrail panels and the  $C_{p_{peak}}$  on the building exterior wall, it is seen that the balconies envelope of the Net  $C_{p_{max}}$  is higher than the base building wall envelope max  $C_{p_{peak}}$ .

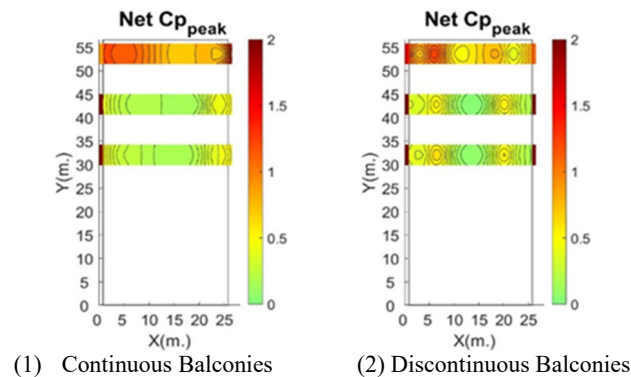
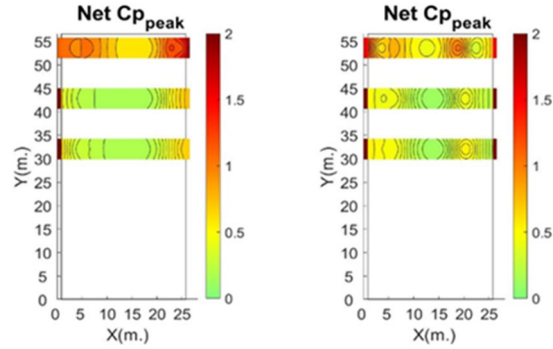
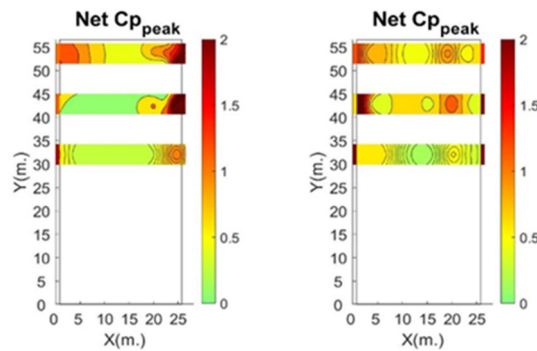


Figure 3A – Envelope Net Max Peak Pressures (Net  $C_{p_{max}}$ ) – Scale 1:180



[1] Continuous Balconies (2) Discontinuous Balconies

Figure 3B – Envelope Net Max Peak Pressures (Net  $C_{p_{max}}$ ) – Scale 1:67



(1) Continuous Balconies (2) Discontinuous Balconies

Figure 3C – Envelope Net Max Peak Pressures (Net  $C_{p_{max}}$ ) – Scale 1:25

#### 5.4.2 Net Peak Pressure Coefficients at Main Wind Directions

##### **Minimum Peak Pressure**

Figure 5 shows the net minimum values of the peak pressure coefficients (Net  $C_{p_{min}}$ ) on balconies' vertical panels for 0 degrees wind direction. Figure 6 shows the external minimum peak pressure coefficients on the building without balconies at 0 degrees wind direction.

Lower floor balcony handrail panels (12<sup>th</sup> and 9<sup>th</sup> floors) show relatively lower net pressures compared to the 15<sup>th</sup> floor balcony handrail panels due to pressure equalization effects (except in corners).

At 0 degrees wind direction, the highest magnitude of minimum external  $C_{p_{peak}}$  results on the building occurs on Sides A and C. At 0 degrees wind direction, the Net  $C_{p_{min}}$  results on balconies' vertical panels at the top floor shows a different behavior than the minimum exterior  $C_{p_{peak}}$  in the building walls. For example, on the 15<sup>th</sup> floor, the highest magnitude of the Net  $C_{p_{min}}$  results on balconies' vertical panels at 0 degrees wind direction occurs on Side B, with a magnitude value of -1.65 for scale 1.67. This shows that the balcony handrail panels suction behavior at the top floor is not predictable compared to the exterior minimum  $C_{p_{peak}}$  result in the building exterior building wall where the highest magnitude occurs on Side C as shown in Figure 6.

Additionally, the balconies' handrail panels are showing high concentration of suction at the corners of the 9<sup>th</sup> and 12<sup>th</sup> floors of Side A and Side C with Net  $C_{p_{min}}$  corners values of -3.60 for scale 1:67 in the left corner of Side C.

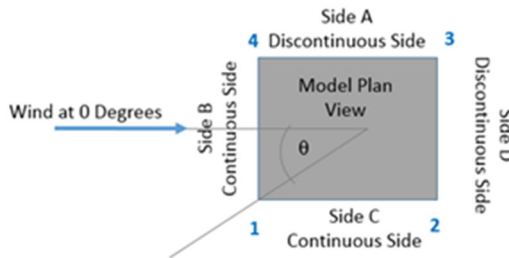


Figure 4 – Convention for the Wind Direction at 0 Degrees. Side walls corners are numbered from 1 to 4

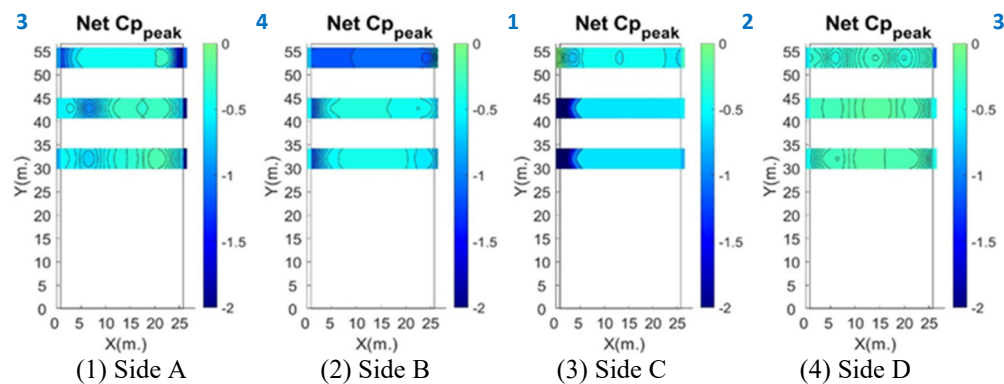


Figure 5 – Net Min Peak Pressures (Net  $C_{p_{min}}$ ) for 0 degrees – Scale 1:67

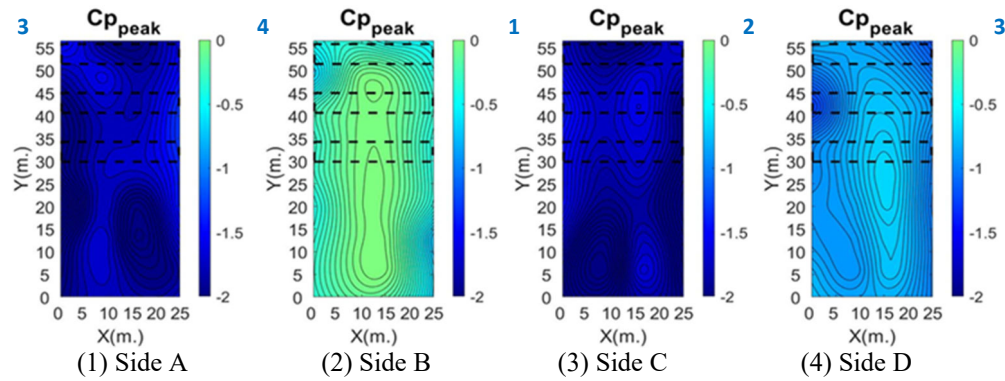


Figure 6 – External Min Peak Pressures for 0 degrees – Scale 1:67

### ***Maximum Peak Pressure***

Figure 8 shows the net maximum values of the peak pressure coefficients (Net  $C_{p_{max}}$ ) on balconies' vertical panels for 180 degrees wind direction. Figure 9 shows the external maximum peak pressure coefficients on the building without balconies at 180 degrees wind direction.

At 180 degrees wind direction, the highest magnitude of maximum external  $C_{p_{peak}}$  results on the building occurs on Side D. At 180 degrees wind direction, the Net  $C_{p_{max}}$  results on balconies' vertical panels show a different behavior than the maximum exterior  $C_{p_{peak}}$  in the building walls.

At the 15<sup>th</sup> floor, the highest magnitude of the Net  $C_{p_{max}}$  results on balconies' vertical panels at 180 degrees wind direction occurs on Side C's corner with a magnitude value of 1.91 for scale 1:25. The balcony handrail behavior is not predictable compared to the building exterior walls behavior for maximum  $C_{p_{peak}}$  results.

Additionally, the balconies' vertical panels are showing maximum magnitude pressure results at the corners of the 9<sup>th</sup> and 12<sup>th</sup> floors of Side D with Net  $C_{p_{max}}$  corresponding values of 2.18 and 2.67 respectively for scale 1:25 at the right-side corner.

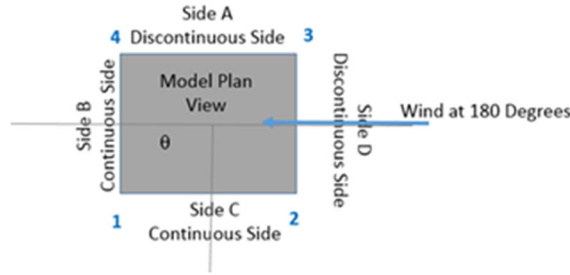
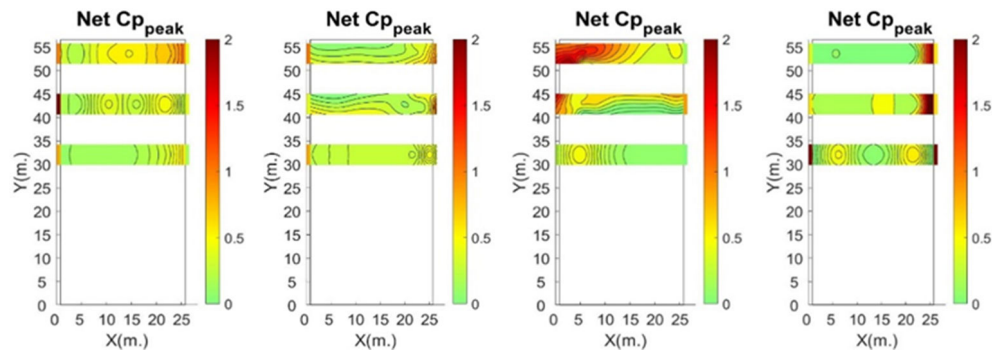


Figure 7 – Convention for the Wind Direction at 180 Degrees. Side walls corners are numbered from 1 to 4

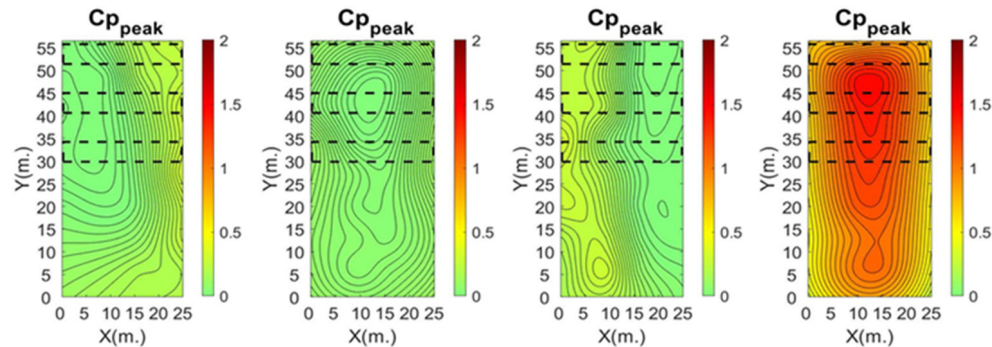
Figure 8 shows the net maximum peak pressure coefficients on the balconies' vertical panels.



(1) Side A (2) Side B (3) Side C (4) Side D

Figure 8 – Net Max Peak Pressures for 180 degrees (Net  $C_{p_{max}}$ ) – Scale 1:25

Figure 9 shows the external maximum peak pressure coefficients on the building walls.



(1) Side A (2) Side B (3) Side C (4) Side D

Figure 9 – External Max Peak Pressures for 180 degrees – Scale 1:25

### 5.4.3 Comparison with Codes and Standards

Building codes and standards such as the American Society of Civil Engineers (ASCE 7-16) do not provide information on the balconies' impact on building cladding or

structural wind loads. Additionally, ASCE 7-16 does not provide any provisions for the wind loads on the balcony handrail panels. Therefore, for designing the balcony handrail panels, different approaches are followed by designers which can affect the overall efficiency of the design. NBCC 2015 provides some provisions for wind loads on the balcony handrail panels. In this section, wind loads obtained on the balcony handrail panels from scale 1:25 experiments are compared with the provisions provided in NBCC 2015 and the ASCE 7-16 external pressure coefficients provided for designing components and claddings on building walls which is the most common approach that designers use to approximate the design of balcony handrail panels.

Comparison with ASCE 7-16

ASCE 7-16 defines two zones on building walls. Zone 5 is the edge zone, and Zone 4 is the middle zone (Figure 10).

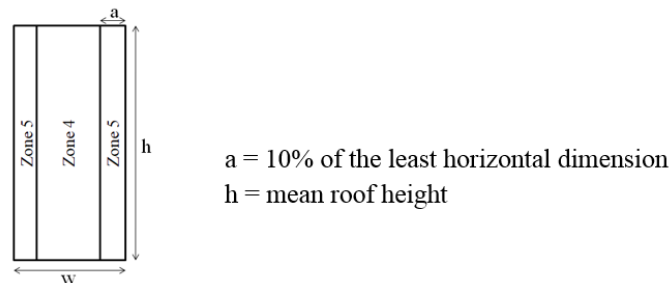


Figure 10 – Definition of Zone 4 and Zone 5 in ASCE 7-16

Table 1 shows the external pressure coefficients for components and claddings from ASCE 7-16 Figure 30.5-1 for different zones. These values are area-averaged values within a zone. For ASCE, a 10 ft<sup>2</sup> cladding area was considered.

Table 1 – External pressure coefficients from ASCE 7-16

Zone	Zone 4 (Middle Zone)	Zone 5 (Edge Zone)
Positive $C_p$	0.9	0.9
Negative $C_p$	-0.9	-1.8

The results from experiments are area-averaged over zones as defined in Figure 11. On each side, Edge Zone I and Edge Zone II correspond to Zone 5 in ASCE 7-16, and Middle Zone I and Middle Zone II correspond to Zone 4 in ASCE 7-16.

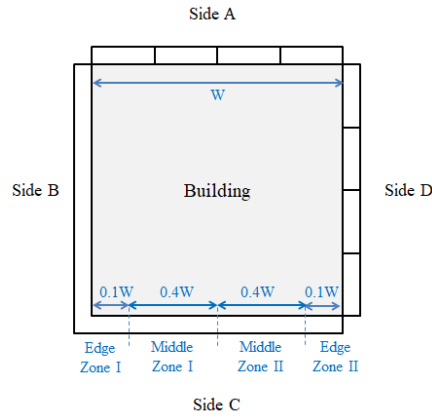


Figure 11 – Zones defined for area-averaging of pressures on the balconies (figure shows the plan view of the building and balconies).

Table 2 shows the area-averaged pressures on the balcony’s handrail panels from experiments on zones defined in Figure 11. Two different cases of continuous and discontinuous balconies are provided. For the continuous balconies, for each zone, the maximum of the values obtained for Sides B and C is reported. For the discontinuous balconies, for each zone, the maximum of the values obtained for Sides A and D is reported.

Table 2 – Area-averaged net maximum and minimum pressure coefficients on the balcony handrail panels from the envelope of all wind directions

Zone	Floor	Discontinuous Balconies		Continuous Balconies	
		Net $C_{p\ max}$	Net $C_{p\ min}$	Net $C_{p\ max}$	Net $C_{p\ min}$
Middle Zone I	15	0.71	-1.16	0.59	-1.15
	12	0.52	-0.41	0.33	-0.27
	9	0.24	-0.50	0.17	-0.53
Middle Zone II	15	0.63	-1.24	0.70	-1.11
	12	0.42	-0.31	0.48	-0.21
	9	0.32	-0.43	0.25	-0.52
Edge Zone I	15	0.61	-1.23	1.30	-1.13
	12	0.50	-0.50	0.66	-0.60
	9	0.32	-1.13	0.52	-2.00
Edge Zone II	15	1.36	-1.20	1.36	-2.40
	12	2.67	-0.65	2.51	-1.30
	9	0.60	-1.10	0.57	-2.99

The maximum area-averaged pressure coefficients  $\text{Net } C_{p_{\max}}$  are lower on the 12<sup>th</sup> and 9<sup>th</sup> floors (in magnitude) compared to those observed on the 15<sup>th</sup> floor in the Middle Zone I and Zone II. However, in the Edge Zone II, the 12<sup>th</sup> floor balcony handrail panels show higher magnitude of  $\text{Net } C_{p_{\max}}$  compared to the 15<sup>th</sup> floor balconies corners.

For the continuous balconies on the 12<sup>th</sup> and 9<sup>th</sup> floors, the  $\text{Net } C_{p_{\max}}$  values are in the range of 0.17 to 0.48 in the middle zone and 0.52 to 2.51 in the edge zone. For discontinuous balconies, the 12<sup>th</sup> and 9<sup>th</sup> floors have larger magnitude results of  $\text{Net } C_{p_{\max}}$  values ranging from 0.24 to 0.52 in the middle zone and 0.32 to 2.67 in the edge zone.

For the 15<sup>th</sup> floor continuous balconies, the  $\text{Net } C_{p_{\max}}$  values were in the range of 0.59 to 0.70 in the middle zones and 1.30 to 1.36 in the edge zone. For the 15<sup>th</sup> floor discontinuous balconies, the area-averaged pressure coefficients are similar to the continuous balconies at the middle zone (0.63 to 0.71) and with smaller magnitude range at the edge zone (0.61 to 1.36).

Results from the experiments show that the edge zone area-averaged positive pressure coefficients on the 12<sup>th</sup> floor with discontinuous balconies are higher than using ASCE 7-16 values in the edge zone ( $\text{Net } C_{p_{\max}}$  2.67 versus ASCE 7-16  $C_{p_{\max}}$  0.90). Similarly, for the 12<sup>th</sup> floor with continuous balconies, the area-averaged positive pressures are higher in the edge zone than the ASCE 7-16 values. ( $\text{Net } C_{p_{\max}}$  2.51 versus ASCE 7-16  $C_{p_{\max}}$  0.90)

For the  $\text{Net } C_{p_{\min}}$ , it is also observed that lower floor balcony handrail panels (12<sup>th</sup> and 9<sup>th</sup> floors) show lower net pressures (in magnitude) compared to the 15<sup>th</sup> floor at the

middle zones. However, in the Edge Zones I and II, the 9<sup>th</sup> floor balcony handrail panels show higher magnitude of Net  $C_{p_{min}}$  compared to the 15<sup>th</sup> floor balconies' corners.

For the continuous balconies of 12<sup>th</sup> and 9<sup>th</sup> floors, Net  $C_{p_{min}}$  values were in the range of -0.21 to -0.53 in the middle zone and -0.60 to -2.99 in the edge zone. For discontinuous balconies, smaller magnitude values compared to continuous balconies are seen in the edge zone with values ranging from -0.50 to -1.13 in the 12<sup>th</sup> and 9<sup>th</sup> floors.

The 15<sup>th</sup> floor continuous balconies show Net  $C_{p_{min}}$  values ranging from -1.11 to -1.15 in the middle zones and -1.13 to -2.40 in the edge zones. The 15<sup>th</sup> floor continuous balconies are double in magnitude than the discontinuous balconies in the edge zone II. The 15<sup>th</sup> floor discontinuous balconies have similar values to the continuous balconies in the middle zones, and lower magnitude results compared to the continuous balconies in the edge zones ranging from -1.20 to -1.23.

Results demonstrate that the area average negative pressure coefficients on the 15<sup>th</sup> floor continuous balconies are higher than using ASCE 7-16 values in the edge zone (Net  $C_{p_{min}}$  -2.40 versus ASCE 7-16  $C_{p_{min}}$  -1.80). These results show the wall pressures determined from the codes/standards should be used carefully for designing balconies since these do not report the accurate net pressures on the balconies handrail systems.

Furthermore, the envelope of positive and negative net pressure coefficients among all wind directions and all floors obtained from the experiments, Net  $C_{p_{max}}$  and Net  $C_{p_{min}}$ , are summarized in Table 3 for the balconies. It is noted that the area-averaged positive and negative pressure coefficients from the experiments show higher values (in magnitude) than those based on the C&C external pressure coefficients given by ASCE 7-16 for the

Edge and Middle zones. Special attention should be given for designing balcony handrail systems for edge zones.

Table 3 – ASCE and area-averaged net maximum and minimum pressure coefficients from the envelope of all wind directions across all floors

ASCE Zone 4 (Middle Zone)	ASCE Zone 5 (Edge Zone)	Balconies - Middle Zone (Wind Tunnel)	Balconies - Edge Zone (Wind Tunnel)
Positive Cp: 0.9	Positive Cp: 0.9	Worst Area Averaged Positive Cp: 0.71	Worst Area Averaged Positive Cp: 2.67
Negative Cp: -0.9	Negative Cp: -1.8	Worst Area Averaged Negative Cp: -1.24	Worst Area Averaged Negative Cp: -2.99

Finally, the positive and negative exterior pressure coefficients for the building walls with balconies versus ASCE were compared, and the summary results are shown in Table 4 below. It is noted that the area-averaged positive pressure coefficients from PTS show slightly higher values (in magnitude) than those based on the C&C external positive pressure coefficients given by ASCE 7-16 at the middle zone. The rest of the external pressure coefficients provided by ASCE have higher magnitude than the external pressure coefficients of PTS for the case of building walls with balconies.

Table 4 – ASCE and area-averaged exterior maximum and minimum pressure coefficients from the envelope of all wind directions across all floors

ASCE Zone 4 (Middle Zone)	ASCE Zone 5 (Edge Zone)	Building with Balconies - Middle Zone (Wind Tunnel)	Building with Balconies - Edge Zone (Wind Tunnel)
Positive Cp: 0.9	Positive Cp: 0.9	Worst Area Averaged Positive Cp: 1.36	Worst Area Averaged Positive Cp: 0.84
Negative Cp: -0.9	Negative Cp: -1.8	Worst Area Averaged Negative Cp: -1.27	Worst Area Averaged Negative Cp: --1.29

### Comparison with NBCC 2015

NBCC 2015 section 4.1.7.5 (5) provides pressure coefficients for the design of balcony handrail panels. The value of Cp is provided as +/- 0.9 (corresponding to Middle zone I and II as defined in Figure 11) and the internal Cp should be taken as zero. For distances within either 0.1W and 0.1D (whichever is larger, with W and D being widths of the building) from the building corner (corresponding to Edge zone I and Edge zone II as defined in Figure 18), Cp shall be taken a +/- 1.2. Figure 12 and Figure 13 show net

maximum and minimum pressure coefficients on the balconies from the envelope of all wind directions (for discontinuous and continuous balconies respectively) compared to the values proposed in NBCC.

It can be seen that the pressure coefficients proposed by NBCC are generally conservative for the maximum pressure coefficients on the balcony handrail panels at the middle zone. However, it is seen that for the majority of floors at the edge zones, the maximum pressure coefficients and minimum pressure coefficients on the balconies have higher magnitude of pressure coefficients compared to the pressure coefficients proposed by NBCC.

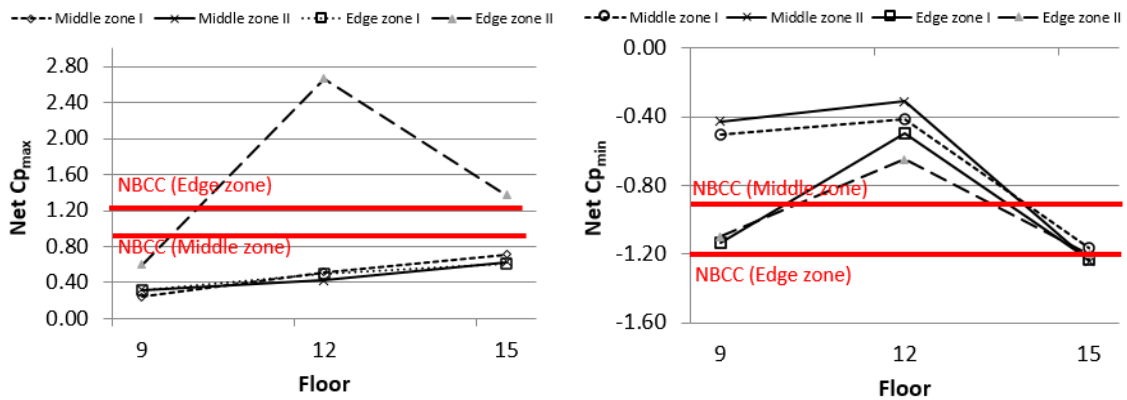


Figure 12 – Area-averaged net maximum and minimum pressure coefficients on the balconies’ handrail panels from the envelope of all wind directions; Discontinuous Balcony

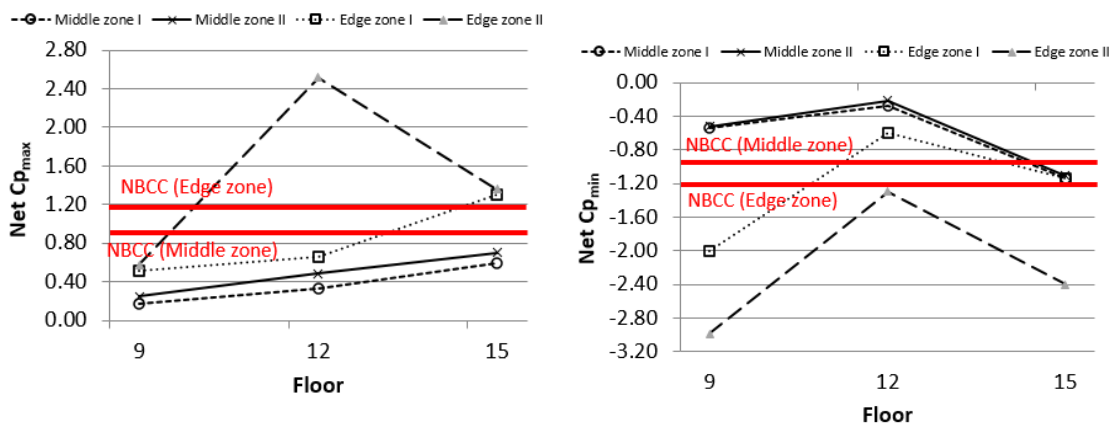


Figure 13 – Area-averaged net maximum and minimum pressure coefficients on the balconies’ handrail panels from the envelope of all wind directions; Continuous Balcony

#### 5.4.4 Major Findings on Balcony Handrail Panels

Lower floor balcony handrail panels (9<sup>th</sup> and 12<sup>th</sup> floors) show relatively lower net pressure coefficients compared to the 15<sup>th</sup> floor balcony handrail panels due to pressure equalization effects at the middle zone only (non-corners).

The balconies' vertical panels show a different behavior than the building walls. The top floor balconies' handrail panels (15<sup>th</sup> floor) show high net peak minimum pressure coefficients. It is noted that the balcony handrail walls do not become identical to a parapet wall until the balcony floor is at the roof level, and this behavior experiences gradation at lower floors.

Wind flowing inside the balcony arrives to a stagnation point at the end of the building in where once it hits on the return section it creates a high concentration area of positive Net  $C_{p_{max}}$  on the corner of the internal side of the balcony which creates a high net pressure on the balcony at the 12<sup>th</sup> and 9<sup>th</sup> floors. Therefore, balcony handrail corners should be carefully designed.

Furthermore, it is noted that the area-averaged positive and negative pressure coefficients from this study show higher values (in magnitude) than those based on the C&C external pressure coefficients given by ASCE 7-16 for the Edge and Middle zones. Special attention should be given for designing balcony handrail systems for edge zones. Therefore, engineers should not use external  $C_{p_{peak}}$  of a building to design balconies as results show that the maximum and minimum Net  $C_{p_{peak}}$  in the balcony handrails are higher than the external envelope  $C_{p_{peak}}$  of a building without balconies.

#### 5.4.5 Scaling and Reynolds Number Effects

Figure 15 shows the net maximum values of the peak pressure (Net  $C_{p_{max}}$ ) on balconies' vertical handrail at different balconies' elevations (y-axis in Fig 15) and corresponding Reynolds number for the scale models 1:180, 1:67, and 1:25 at 40% throttle force and 1:25 at 70% throttle force (x-axis in Fig 15) at 0 and 90 degrees. To further study the Reynolds number effect, the scale 1:25 was run at maximum available throttle at the testing facility (70% throttle). There are two scenarios studied: (1) taps located at the middle zone of the balcony handrail panels which include the non-corners taps and (2) taps located at the corners.

It is observed in Figure 15, as the Reynolds number increases, there is an increase in the Net  $C_{p_{max}}$  results for both analyzed locations at the middle zone and corners of the balcony handrail panels. For example, Figure 15A (Tap 161) shows the Reynolds number at the 1:180 model scale was calculated to be  $Re=2.E+05$  with corresponding Net  $C_{p_{max}}$  of 0.15 compared to the Reynolds number at the 1:25 model scale with  $Re=2.E+06$  and corresponding Net  $C_{p_{max}}$  of 0.27 in the middle zone (non-corner). Similarly, Figure 15C (Tap 163) shows the Reynolds number at the 1:67 model scale was calculated to be  $Re=6.E+05$  with corresponding Net  $C_{p_{max}}$  of 0.40 compared to the Reynolds number at the 1:25 model scale with  $Re=2.E+06$  and corresponding Net  $C_{p_{max}}$  of 0.59 in the corner of the balcony handrail panels.

Although the scale model dimensions are different, the blockage ratio is minimal (7% for the 1:25 model), and the Reynolds number should still be the key factor contributing to the difference in the results between these models.

Please refer to the next page for Figure 14 that shows building elevation view and wind direction at 0 degrees and for Figure 15 that shows Reynolds number effect for 0 and 90 degrees.

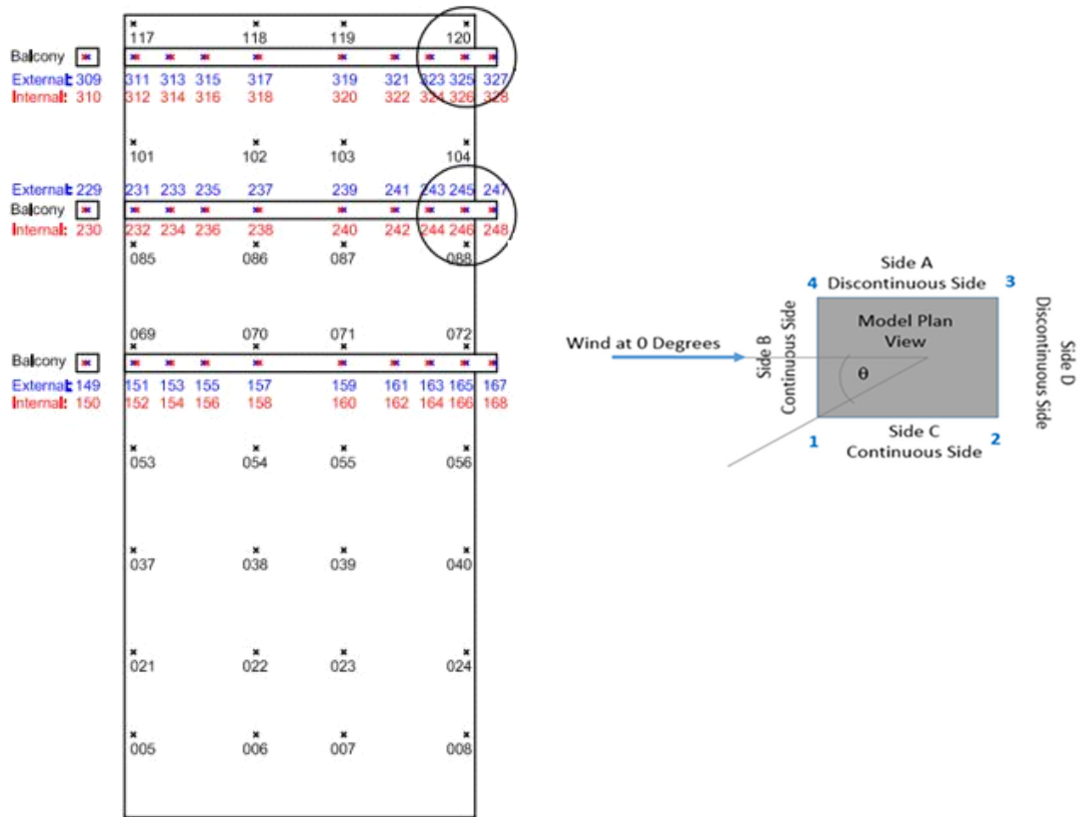


Figure 14 – Building Elevation View and Wind Direction at 0 Degrees

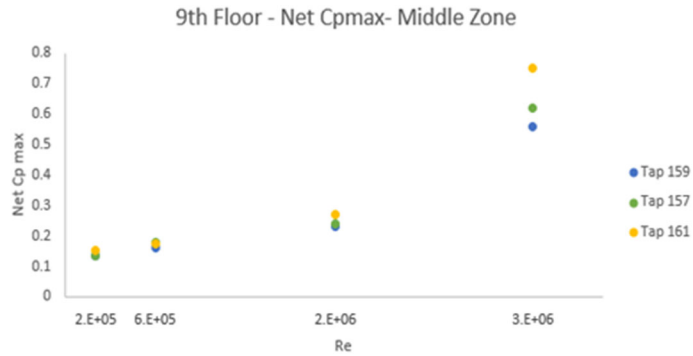


Figure 15A – Reynolds number effect, Net Cp<sub>max</sub> at 0 Degrees

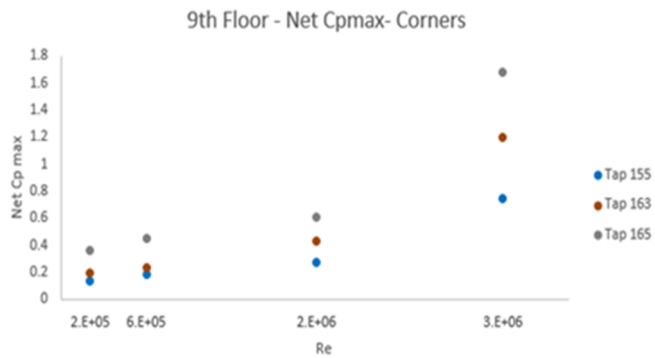


Figure 15B – Reynolds number effect, Net Cp<sub>max</sub> at 0 Degrees

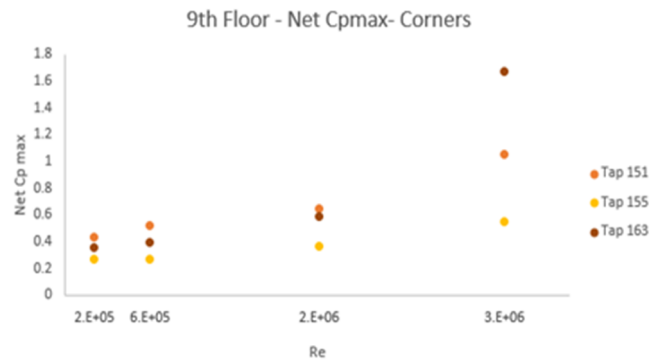


Figure 15C – Reynolds number effect, Net Cp<sub>max</sub> at 90 Degrees

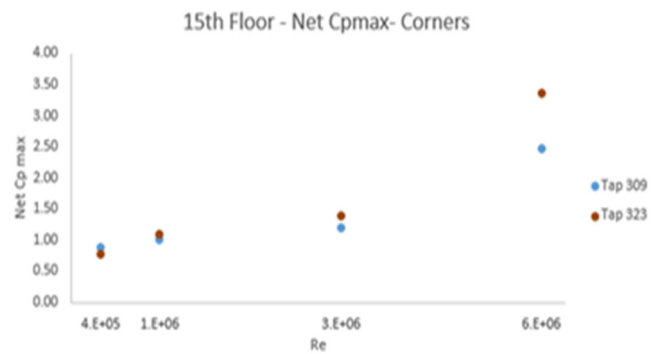


Figure 15D – Reynolds number effect, Net Cp<sub>max</sub> at 90 Degrees

Figure 15 – Reynolds number effect corresponding to Scales 1:180, 1:67, 1:25 @ 40% & 70% Throttle

Figure 16 shows the net minimum values of the peak pressure (Net  $C_{p_{min}}$ ) on balconies' vertical handrails at 0 degrees and corresponding Reynolds number for the different scale models.

As observed in Figure 16, the increase of the Reynolds number has led to an increase the Net  $C_{p_{min}}$  results on the middle zone of the balconies. For the corners, it is seen a slight increase in the Net  $C_{p_{min}}$  among model scales. Furthermore, it is observed a significant increase in Net  $C_{p_{min}}$  for scale 1:25 at 70% throttle for the middle zone and corners. For example, Figure 16C (Tap 161) shows the Reynolds number at the 1:67 model scale was calculated to be  $Re=6.E+05$  with corresponding Net  $C_{p_{min}}$  of -0.42 compared to the Reynolds number at the 1:25 model scale with  $Re=2.E+06$  and corresponding Net  $C_{p_{min}}$  of -0.56 in the middle zone (non-corner). Similarly Figure 16D (Tap 151) shows the Reynolds number at the 1:25 model scale at 40% throttle was calculated to be  $Re=2.E+06$  with corresponding Net  $C_{p_{min}}$  of -1.22 compared to the Reynolds number at the 1:25 model scale at 70% throttle with  $Re=3.E+06$  and corresponding Net  $C_{p_{min}}$  of -3.14 in the corner of the balcony handrail panels.

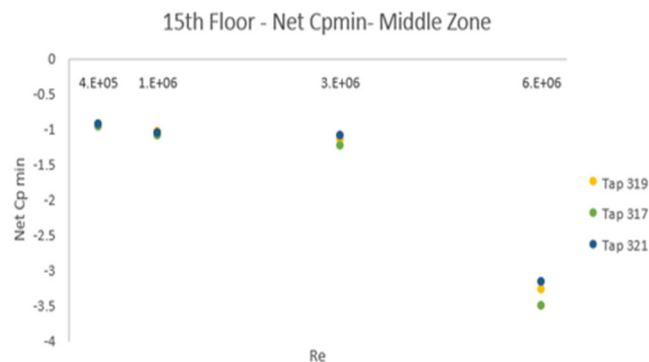


Figure 16A – Reynolds number effect, Net  $C_{p_{min}}$  at 0 Degrees

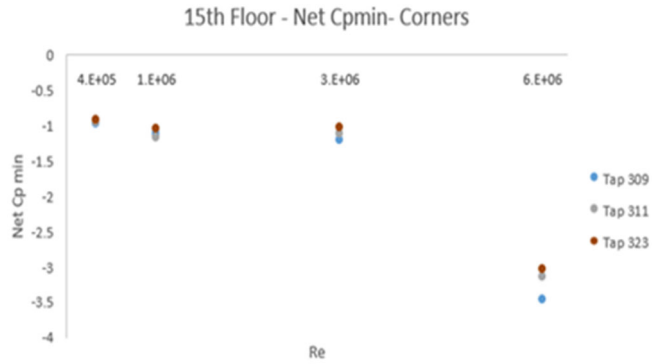


Figure 16B – Reynolds number effect, Net  $C_{p_{min}}$  at 0 Degrees

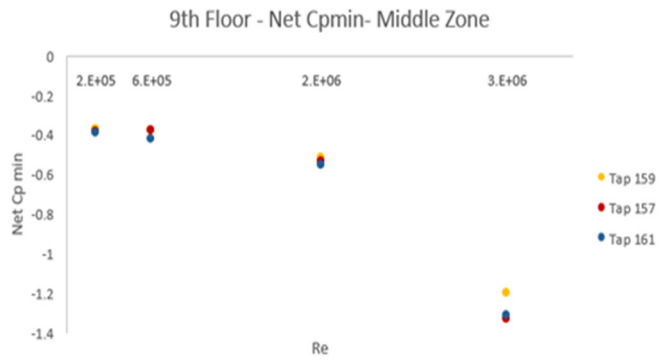


Figure 16C – Reynolds number effect, Net  $C_{p_{min}}$  at 0 Degrees

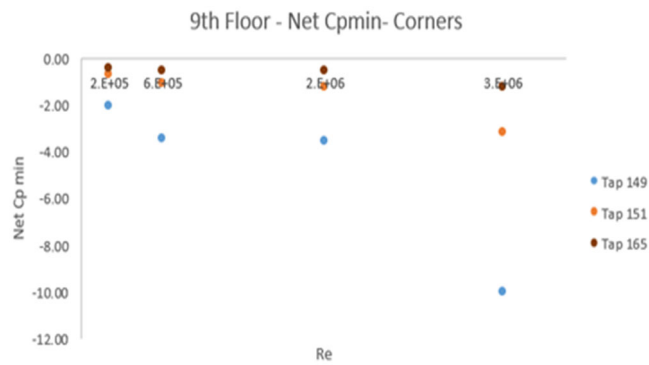


Figure 16D – Reynolds number effect, Net  $C_{p_{min}}$  at 0 Degrees

Figure 16 – Reynolds number effect corresponding to scales 1:180, 1:67, 1:25 @ 40% Throttle and 1:25 @ 70% Throttle

#### 5.4.6 Effect of Pressure Tap Resolution

To find the effect of the tap arrangement and required resolution for pressure taps on the balcony panel handrail corners, four different tap layouts were evaluated in scale 1:25, which results are plotted in Figures 18 and 19. The results show that having the pressure taps near the edges is necessary for capturing an accurate measurement of high suction and positive net pressures.

To study the resolution for pressure taps on the balcony handrail panels, four different tap layouts were analyzed and corresponding Net  $C_{p_{min}}$  at the 15<sup>th</sup> and 12<sup>th</sup> floors are shown in Figures 18A and 18B. Case (d) tap layout shows the tap layout used in the model scales of this study (3 tap layer at the corners of the 12<sup>th</sup> and 15<sup>th</sup> floor balconies). The results show that inaccuracies can occur when having low resolution pressure taps. High suction areas are missed in the case of Tap layout case (a). The results of this study show that to obtain accurate results in the critical areas of a balcony handrail panel, it is necessary to have pressure tap at the edges to capture the high suction at the corners. For this study, the tap layout case (c) provides accurate results similar to the tap layout case (d).

Please refer to the next page for Figure 17 that shows building elevation of Sides B and C and for Figure 18 that shows effect of pressure tap layout.

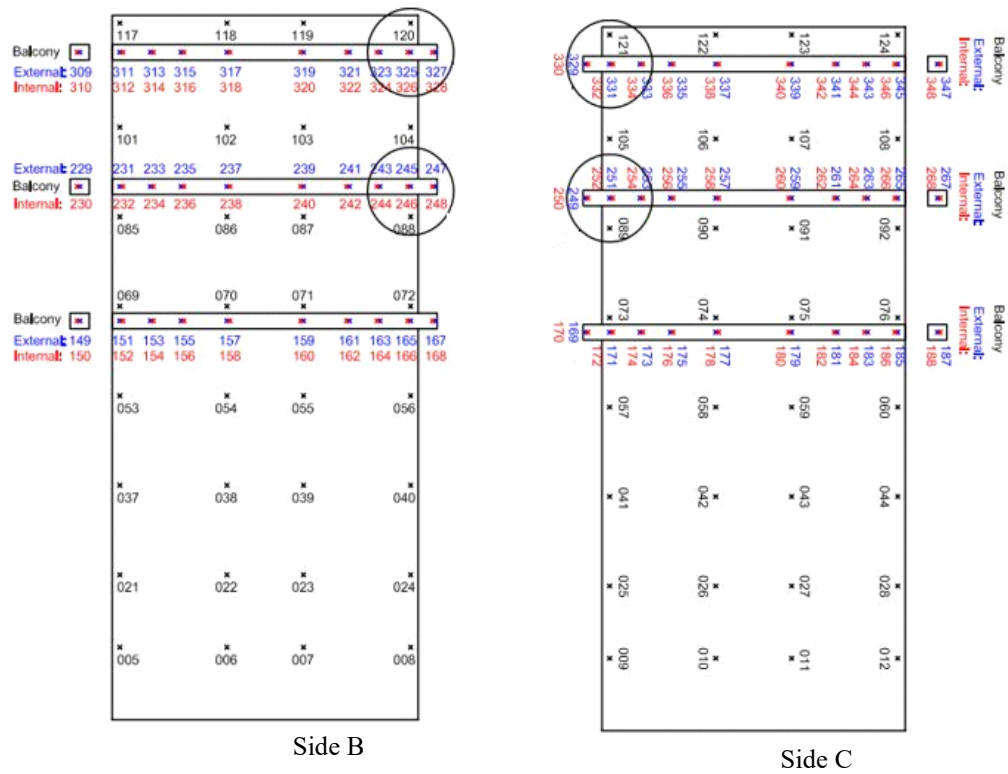


Figure 17 – Building Elevation of Side B and Side C

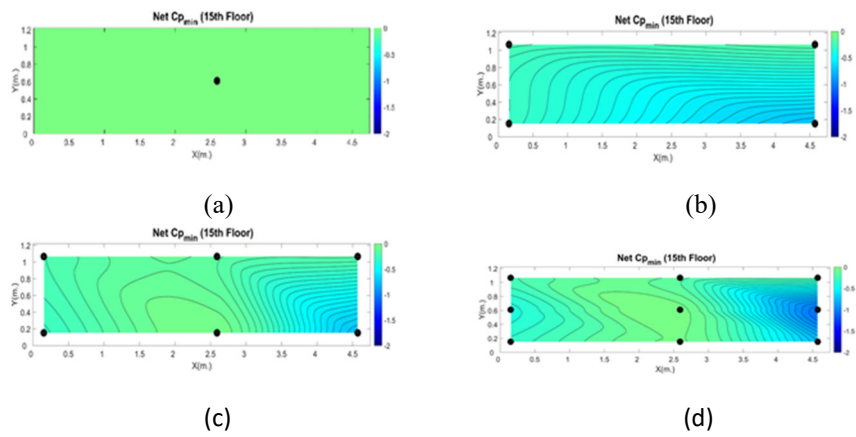


Figure 18A – Effect of pressure tap layout on Net  $C_{p_{min}}$  at the 15<sup>th</sup> floor  
72 degrees wind direction – Side B

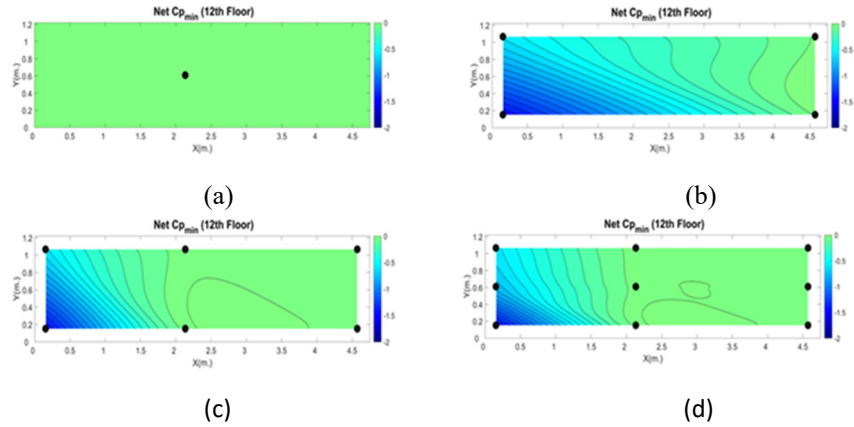


Figure 18B – Effect of pressure tap layout on Net  $C_{p_{min}}$  at the 12<sup>th</sup> floor  
0 degrees wind direction – Side C

Figures 19A and 19B shows four different tap layouts and corresponding Net  $C_{p_{max}}$  at the 15<sup>th</sup> and 12<sup>th</sup> floors. The results show that having the pressure taps near the edges is necessary for capturing an accurate measurement for maximum net peak pressures Net  $C_{p_{max}}$  at the balconies handrail panels. Inaccuracies can occur when having low resolution pressure taps. Critical areas are missed in the case of Tap layout (a). For this study, the tap layout case (c) provides accurate results with Net  $C_{p_{max}}$  results similar to those of the tap layout case (d).

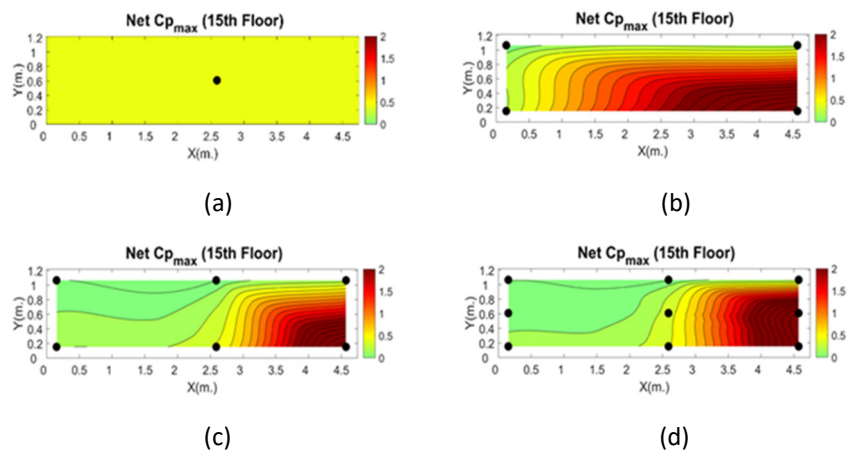


Figure 19A – Effect of pressure tap layout on Net  $C_{p_{max}}$  at the 15<sup>th</sup> floor  
0 degrees wind direction – Side B

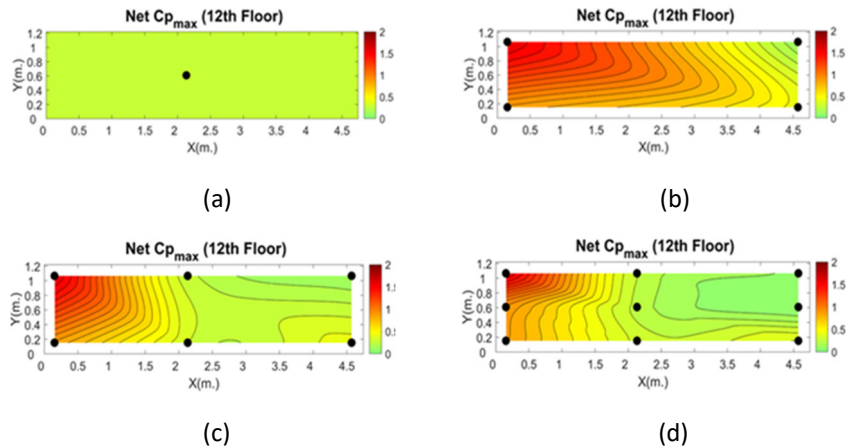


Figure 19B – Effect of pressure tap layout on Net  $Cp_{max}$  at the 12<sup>th</sup> floor  
135 degrees wind direction – Side C

#### 5.4.7 Area Average Pressure

Aside from analyzing at individual taps it is important to consider various combinations of multiple taps. In this study, four tap layout combinations were chosen to capture wind effects on tributary areas (C1, C2, C3, C4) on the 15<sup>th</sup> floor as shown in Figure 20. Furthermore, Table 4 presents the combination of tap cases and corresponding tributary areas.

Figure 22 shows the findings of the tap combination cases on the 15<sup>th</sup> floor. Results show that the largest area of study (C4) has the smallest magnitude values of Net  $Cp_{min}$  and Net  $Cp_{max}$  for the majority of wind orientations from 0 to 90 degrees. On the other hand, the smaller areas (C1, C2) show the maximum magnitude of Net  $Cp_{min}$ , and smaller areas (C1, C2, and C3) show the maximum magnitude of Net  $Cp_{max}$  for majority of angle orientations from 0 to 90 degrees.

The Net  $Cp$  is seen smaller in magnitude when averaged over a larger area, which implies higher pressure equalization. As the tributary area reduces (such as for smaller

areas as C1), the difference between external pressures and internal pressures increases, which leads to limited load reduction.

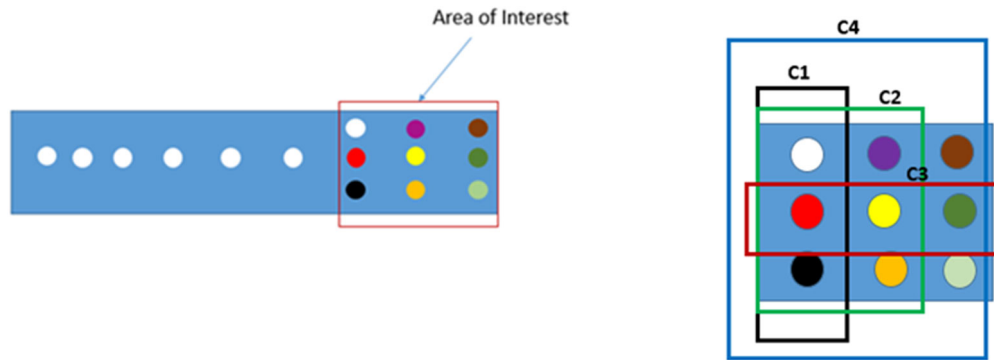


Figure 20 – Tributary Areas

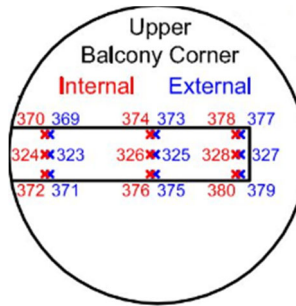
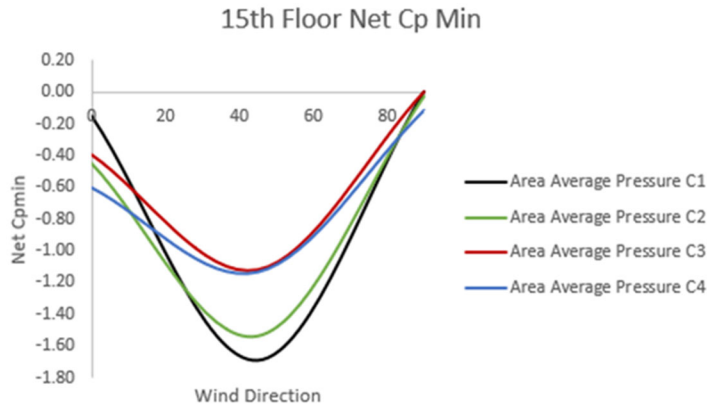


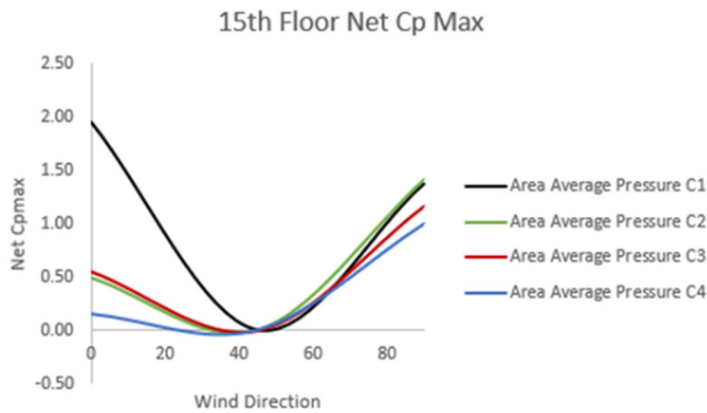
Figure 21 – Notation of tap combinations considered in the study

Table 5 – Area covered by tap combinations in the 15<sup>th</sup> floor

Case No	Included Taps	Tributary Area [m <sup>2</sup> ]
1	Taps 369, 323, 371	2.90
2	Taps 369, 373, 323, 325, 371, 375	5.62
3	Taps 323, 325, 327	2.62
4	Taps 369, 373, 377, 323, 325, 327, 371, 375, 379	7.00



(a)



(b)

Figure 22 – Net  $C_{pmin}$  and Net  $C_{pmax}$  for tap combination cases at the 15<sup>th</sup> floor

Figure 24 shows four tap layout combinations to capture wind effects on tributary areas (C1, C2, C3, C4) at the 12<sup>th</sup> floor. Table 5 presents the combination of taps and corresponding area covered. Findings show that on the 12<sup>th</sup> floor, the larger area of study (C4) shows smallest magnitude values of Net  $C_{pmin}$  and Net  $C_{pmax}$  for majority of wind orientations from 0 to 90 degrees. The Net Cp at the 12<sup>th</sup> floor is seen in smaller magnitude when averaged over a larger area, which implies higher pressure equalization. Similar as the 15<sup>th</sup> floor study, for the 12<sup>th</sup> floor as the tributary area reduces, the correlation between external pressures and internal pressures increases, which leads to limited load reduction.

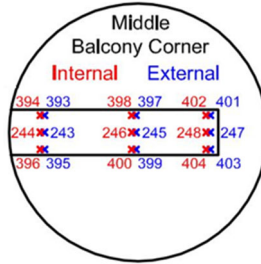


Figure 23 – Notation of tap combinations considered in the study

Table 6 – Area covered by tap combinations in the 12<sup>th</sup> floor

Case No	Included Taps	Tributary Area [m <sup>2</sup> ]
1	Taps 393, 243, 395	2.90
2	Taps 393, 397, 243, 245, 395, 399	5.62
3	Taps 243, 245, 247	2.62
4	Taps 393, 397, 401, 243, 245, 247, 395, 399, 403	7.00

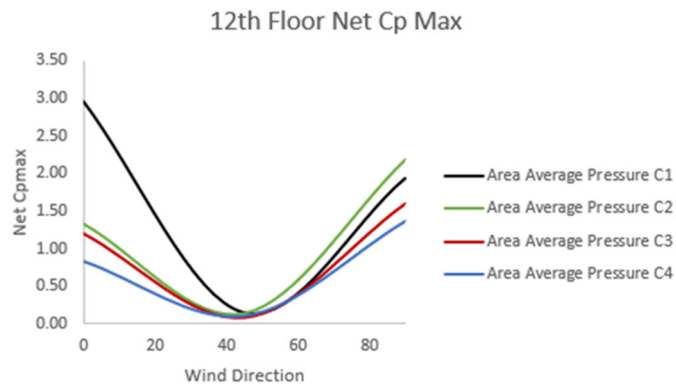
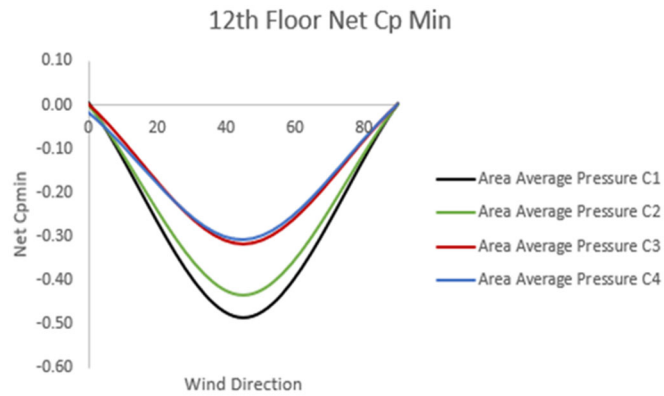


Figure 24 – Net  $C_{p_{min}}$  and Net  $C_{p_{max}}$  for tap combination cases at the 12<sup>th</sup> floor

## 5.5 References

- [1] Moravej, M. (2018). Investigating Scale Effects on Analytical Methods of Predicting Peak Wind Loads on Buildings. Florida International University.
- [2] Montazeri, H., Blocken, B. (2013). CFD simulation of wind-induced pressure coefficients on buildings with and without balconies: validation and sensitivity analysis. *Building and Environment*, 60, 137-149.
- [3] Morton, T.J., Mara, T.G., (2017). Effects of Balconies on the Wind Loading of a Tall Building. AEI 2017: Resilience of the Integrated Building, April 11–13, 2017, Oklahoma City, Oklahoma.
- [4] AS/NZS 1170.2:2002, (2002). Structural Design Actions, Part 2: Wind actions. Standards Australia, Homebush.
- [5] BS 6399-1:1996, (2002). Loading for buildings, Part 1: Code of practice for dead and imposed loads. British Standards Institution, London.
- [6] Building Construction Regulations, (1991). Chapter 123B: Imposed loads, Department of Justice. Hong Kong.
- [7] Richards, P.J., Hoxey, R.P., Connell, B.D., Lander, D.P. (2007). Wind-tunnel modeling of the Silsoe Cube. *Journal of Wind Engineering and Industrial Aerodynamics*, 95, 1384-1399.
- [8] Asghari Mooneghi, M. (2014). Experimental and Analytical Methodologies for Predicting Peak Loads on Building Envelopes and Roofing Systems Dissertation. FIU Electronic Theses and Dissertations. Florida International University, December 2014.
- [9] Asghari Mooneghi, M., Chowdhury, A.G., Irwin, P. (2015). Partial Turbulence Simulation Method for Small Structures. Conference Paper, June 2015.

**CHAPTER VI**  
**CONCLUSIONS**

## CHAPTER 6

### CONCLUSIONS

#### 6.1 Conclusions and Future Work

This chapter summarizes the conclusions of this dissertation. The dissertation conclusions and future work needed are summarized into four parts: 1. Summary. 2. Effects of balconies on the wind loading on buildings. 3. An extension of the partial turbulence simulation methodology to address the peak wind loads on balcony handrail panels in tall buildings. 4. Future work needed. The details are described in the following sections.

##### 6.1.1 *Summary*

In this dissertation, an extension of the Partial Turbulence Simulation (PTS) method for balcony handrail panels was presented to include the effects of missing low frequency turbulence intensity at each balcony handrail panel elevation. In a flow with PTS, only the high frequency end of the turbulence spectrum was simulated, and the effects of the missing low frequency turbulence were included theoretically with the methodology proposed in this dissertation. Scale effects were studied with scale models at 1:180, 1:67, and 1:25 scales. Two series of tests were conducted per scale; one on model building with no balconies and then on the model building with continuous balconies on two adjacent sides and discontinuous balconies on the remaining two sides.

Regarding the wind pressure on the balcony handrail vertical glass panels, the envelope values of positive and negative net pressure coefficients among all wind directions were obtained from the experiments, Net  $C_{p_{max}}$  and Net  $C_{p_{min}}$ . These results obtained from a scale 1:180 model were compared with the ASCE 7-16 external pressure

coefficients for Components & Cladding (C&C) as the ASCE guideline is sometimes used by designers to be informed of wind design of balcony handrail systems.

Furthermore, the pressure distributions along the building walls are analyzed to see the impact of the balcony handrail systems. For the envelope of results among all wind directions, the peak negative pressure coefficients for the building with balconies are smaller (in magnitude) than the building without balconies.

### 6.1.2 Effects of Balconies on the Wind Loading on Buildings

The balcony glass handrail systems studied in this dissertation are found to reduce peak suction by up to 40% of the magnitude of the external peak negative pressure coefficients for the building walls at scale 1:180.

Furthermore, the area-averaged net positive and negative pressure coefficients from PTS show higher values (in magnitude) than those based on the C&C external pressure coefficients given by ASCE 7-16 for the edge and middle zones. Thus, special attention should be given for designing balcony handrail systems for edge zones. Additionally, pressure equalization occurs between external and internal surfaces of the balconies, which causes reductions in the net pressures (Net  $C_{p_{max}}$  and Net  $C_{p_{min}}$ ). From this study, it is seen that top floors have minimum pressure equalization compared to the lower floors (9<sup>th</sup> and 12<sup>th</sup> floors). Therefore, it is concluded that the floor height impacts Net Cps (both max and min Net Cps) on balcony handrail panels.

### 6.1.3 Experimental Investigations of Aerodynamics & Wind Loading on Balconies

The extension of the PTS method was applied to the largest scale 1:25 which shows that Net  $C_{p_{max}}$  and Net  $C_{p_{min}}$  results at lower floor balcony handrail panels (12<sup>th</sup> and 9<sup>th</sup> floors) have relatively lower net pressures compared to the 15<sup>th</sup> floor balcony handrail

panels (except in corners). It is concluded that pressure equalization effects impact results at the 12<sup>th</sup> and 9<sup>th</sup> floors.

Furthermore, it is concluded that balcony handrail systems show a different behavior from the building walls. Results show that the 9<sup>th</sup> and 12<sup>th</sup> floor high suction in the corners at the balcony handrail panels are driven due to the effect of the wind flow inside the balcony arriving to a stagnation point at the end of the building. Once it hits the return section, it creates a high concentration area of positive Net  $C_{p_{max}}$  on the corner of the internal side of the balcony. This behavior creates an additional net negative pressure with high suction areas around the balcony handrail corners. Therefore, it is suggested that special attention should be given for designing balcony handrail systems at the corners.

Additionally, there are differences between building walls and balcony handrail panels for cases where the wind loads are normal to the wall. For this case, the behavior of balconies is driven by the wind flowing backwards against the rear face of the 15<sup>th</sup> floor balcony where it creates a positive pressure on the inner face of the balcony and induces negative net pressures at the top floor balcony at the middle zone.

Furthermore, overall results show that when increasing the model scale, higher net pressure coefficients Net  $C_{p_{min}}$  and Net  $C_{p_{max}}$  are obtained compared to smaller scale. Such accurate estimation is imperative for reliable wind design of handrail systems. This shows the scale effects and justifies the need for large-scale models and PTS.

When studying the Reynolds number effects, it is observed that as the Reynolds number increases, there is an increase in the magnitude of Net  $C_{p_{max}}$  and Net  $C_{p_{min}}$  results for both analyzed locations at the middle zone and corners of the balconies handrail panels. Furthermore, it is observed a significant increase in Net  $C_{p_{min}}$  for scale 1:25 at 70% throttle

for the middle zone and corners. This concludes that the magnitude of the PTS results increases as the Reynolds number increases. This is an important Reynolds number effect and justifies the importance of large-scale model testing with high wind speed.

The effects of resolution and layout of pressure taps on the pressure investigation concludes that to obtain accurate results in the critical areas of a balcony handrail panel, it is necessary to have pressure taps at the edges to capture the high suction at the corners. The results seen from this dissertation show the importance that having high resolution of pressure taps enables improved accuracy for the Net  $C_{p_{min}}$  and Net  $C_{p_{max}}$  results.

It is concluded that large-scale testing allows modeling the details more accurately so that accurate wind pressures can be obtained. A large-scale test with moderate pressure taps at the edges of the balconies followed by PTS peak estimation method, taking into account the turbulence at the balcony elevation, is deemed to be the desirable approach for balcony handrail panels.

#### *6.1.4 Limitations and Future Work*

The balcony handrail panels in tall buildings were examined, and it was proposed that for components it can be acceptable to use the method described in this dissertation. However, there is a limitation of not having a full-scale prototype of the building of study for further validating the method proposed in this dissertation and finding out its limitations. To address this limitation, future full-scale studies should be planned to verify the current study and advance the state of the art of the aerodynamics and wind loading for balconies on high-rise buildings. Also, to further explore the range of adequacy for the Reynolds number, it will be useful to study different model scales from 1:180 to 1:25 at

different higher speeds. Finally, future studies pertaining to the effect of different balcony geometries (i.e. different depth and length) and terrain exposures on the wind loads on buildings are desirable.

## **VITA**

## VITA

### LISSETTE LUDENA

2003-2007	B.Sc., Civil Engineering Florida International University Miami, Florida
2008-2008	M.Sc., Civil Engineering (Structural) Florida International University Miami, Florida
2009-2012	Structural Engineer Avart Ammann & Whitney Miami, Florida
2012-2014	Structural Engineer T.Y. Lin International Group Miami, Florida
2014-2016	Master's in Business Administration Massachusetts Institute of Technology Cambridge, Massachusetts
2016-Current	Manager Microsoft Fort Lauderdale, Florida
2014-2021	PhD, Civil Engineering Florida International University Miami, Florida

### PUBLICATIONS AND PRESENTATIONS

Ludena, L., Chowdhury, A.G., Hajra, B., Moravej, M., Asghari Mooneghi, M., Irwin, P., Zisis, I. *The effect of Balconies on the Wind Induced Loads on a Fifteen Story Building*. 4<sup>th</sup> American Association for Wind Engineering Workshop. Miami, Florida. August 2016.

Ludena, L., Chowdhury, A.G., Hajra, B., Moravej, M., Irwin, P., Zisis, I. *Experimental assessment of the effect of balconies on the wind load distribution on a high-rise building*. 13<sup>th</sup> Americas Conference on Wind Engineering. Gainesville, Florida. May 2017.

Ludena, L., Chowdhury, A.G., Asghari Mooneghi, M., Irwin, P., Moravej, M. *Estimation of Wind Loads on the Balcony Glass Handrail of Mid-Rise Buildings*. Structures Congress 2017.

Ludena, L., Chowdhury, A.G., Asghari Mooneghi, M., Irwin, P., Moravej, M. *The Effect of Balconies on the Wind Loading on Buildings*. Engineering Structures Journal, under review.